Desalination 500 (2021) 114883

Contents lists available at ScienceDirect

Desalination

journal homepage: www.elsevier.com/locate/desal

A review on lithium recovery using electrochemical capturing systems

Sifani Zavahir [a], Tasneem Elmakki [a], Mona Gulied [a], Zubair Ahmad [a], Leena Al-Sulaiti [b], Ho Kyong Shon [c], Yuan Chen [d], Hyunwoong Park [e], Bill Batchelor [f], Dong Suk Han [a,*]

[a] Center for Advanced Materials, Qatar University, Doha, Qatar
[b] Department of Math., Stat. and Physics, College of Arts and Sciences, Qatar University, Doha, Qatar
[c] Center for Technology in Water and Wastewater, School of Civil and Environmental Engineering, University of Technology Sydney, Sydney, NSW 2007, Australia
[d] School of Chemical and Biomolecular Engineering, The University of Sydney, NSW 2006, Australia
[e] School of Energy Engineering, Kyungpook National University, Daegu 41566, Republic of Korea
[f] Zachry Department of Civil and Environmental Engineering, Texas A&M University, College Station, TX 77840, USA

HIGHLIGHTS

- SED and BMED are the most appropriate methods for high recovery of Li^+ at low SEC.
- ESIX technology for Li recovery considered extracting Li from other liquid Li resources.
- CDI is an advancement of ESIX since it utilizes intercalating electrodes with IEMs.
- ELiCSs need to be studied at pilot-scale using continuous processes.
- Future ELiCSs research needs to focus on using natural Li liquid resources.

GRAPHICAL ABSTRACT

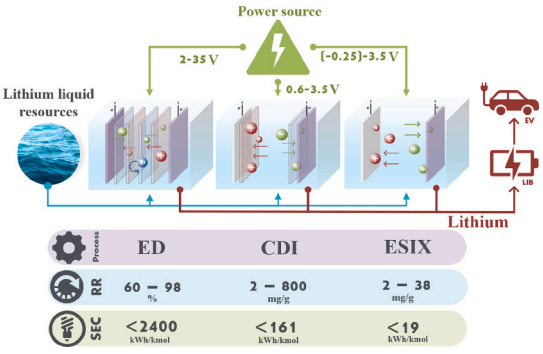

ARTICLE INFO

Keywords:
Lithium
Resource recovery
Electrodialysis
Capacitive deionization
Electrochemically switchable ion exchange

ABSTRACT

Resource recovery from natural reserves is appealing and Li extraction from different brines is in the forefront. Li extraction by membranes is reviewed in the literature much more than electrochemical processes. However, a very recent review thoroughly discussed Li recovery by electrochemically switchable ion exchange (ESIX). This paper reviews Li recovery by both charge transfer processes, namely electrodialysis (ED), and electro-sorption processes, namely capacitive deionization (CDI). It also reviews ESIX with a focus on performance matrices and includes comments on the technology readiness of each separation technique. These processes exhibit promising perspectives on the separation and recovery of Li both selectively and non-selectively from simulated brine solutions and Li salt solutions. Readers are provided with guidelines to choose between the processes,

Abbreviations: AEM, anion exchange membrane; BM, bipolar membrane; BMED, bipolar membrane electrodialysis; BDD, boron doped diamond; CDI, capacitive deionization; CEM, cation exchange membrane; CE, current efficiency; EIONS, electrochemical ion separation processes; ELiCSs, electrochemical lithium capturing systems; ED, electrodialysis; IEM, ion exchange membrane; IIM, ion imprinted membrane; ILM, ion liquid membrane; ISM, ion sieve membrane; LIBs, Li-ion batteries; Li, lithium; MDC, membrane distillation crystallization; MCEM, monovalent cation exchange membrane; MAEM, monovalent anion exchange membrane; NF, nanofiltration; PSMCDI, permselective exchange membrane capacitive deionization; RR, recovery rate; SED, selective electrodialysis; SEC, specific energy consumption; SLM, supported liquid membrane.

* Corresponding author.
E-mail address: dhan@qu.edu.qa (D.S. Han).

https://doi.org/10.1016/j.desal.2020.114883
Received 5 August 2020; Received in revised form 28 October 2020; Accepted 22 November 2020
Available online 4 December 2020

depending on the applied voltage, current density, specific energy consumption and purity of recovered Li. Most electrochemical lithium capturing systems (ELiCSs) have been tested at the lab scale. Therefore, future research should be directed toward pilot-scale development and parameter optimization. Furthermore, we urge the ELiCSs research community to report information in a standard form that allows meaningful comparisons and insights into the systems.

1. Introduction

The global demand for clean, cheap and sustainable energy resources is tremendously escalating and is driven by technological advancements [1]. The most prominent sources of renewable and clean energy are solar and wind power. In fact, by 2030, solar and renewable wind energy will cost only two-thirds as much as fossil fuels [2]. However, these energy resources are seasonal, which reduces their reliability at all timings and locations of need. This demonstrates that the flexibility of power systems to quickly adapt to changes in power supply and demand is key. Storage technologies will therefore be the cornerstone for energy security during low production and high demand times. In this context, electrochemical energy storage emerges as one of the fastest-growing segments that is able to provide an uninterrupted power supply and load-shifting capability [3]. Fig. 1 shows the accumulated global electrochemical energy storage market power capacity at the end of 2019. It shows an operational installed battery storage capacity of about 9520.5 MW, with Li-ion batteries (LIBs) accounting for the largest portion (88.8%) of this capacity [4]. This huge share taken by LIB poses a lithium supply risk since Li is increasingly used in grid storage, electronic devices, and next-generation electric vehicles (EV) [5].

Lithium (Li), the 25th most abundant metal on earth [1], is considered a critically important element in energy systems. The small ionic radius of Li makes it an electrochemically active metal, which has become an important building block for the construction of the increasingly demanded LIBs [6]. According to the consumption and production status of Li, utilization of Li by the LIB industry by 2025 is expected to account for almost 66% of the current Li production worldwide [7,8]. This rapidly growing demand for rechargeable LIBs is due to their unique characteristics, such as high operating voltages, energy densities, long life cycles at low self-discharge rates, and environmental friendliness [9]. The former properties make the LIBs an essentially valuable material that derives our modernized world today. The use of LIBs is expanding every day in various applications, from small cellular phones to large power generation systems. In this context, the biggest future consumer of LIBs will be the EV industry. Demand for LIBs for electric (EV), hybrid electric (HEV), and plug-in hybrid electric (PHEV) vehicles are expected to reach about $221 billion by 2024 [10].

Besides the use of Li and its compounds in fundamental batteries and energy storage devices, they are tremendously attractive as vital elements in numerous industries. Fig. 2 shows the distribution of the global Li end-use market share in 2019 [11]. Li is used in various fields in the form of lithium carbonate (60%), lithium hydroxide (23%), lithium metal (5%), lithium chloride (3%), and butyl lithium (4%) [12]. Lithium carbonate is mainly used in batteries, ceramics, special glass, and continuous casting mold-flex powders industry [11]. Lithium hydroxide is primarily used to produce synthetic rubber, dyes, and lubricating greases that can function in high temperatures and loads. Around 70% of the lubricating greases used in the world contain Li [13]. Industrial drying and air conditioning/treatment applications use Li in the form of lithium chloride due to its distinctive hygroscopic properties. Additionally, highly purified Li compounds are increasingly used in pharmaceuticals, biomedical applications, and the synthesis of vitamins and organic compounds. Furthermore, Li metal is used in the primary aluminum production industry and the manufacture of strong and lightweight alloys of manganese and Li [5,7,10]. As a consequence of the accelerating global demand for Li in numerous important applications, the global annual Li consumption rate is expected to continue to increase from 2015 to 2050. During this time, 5.11 million tons of Li will be consumed, which may account for one-third of the total Li reserves on

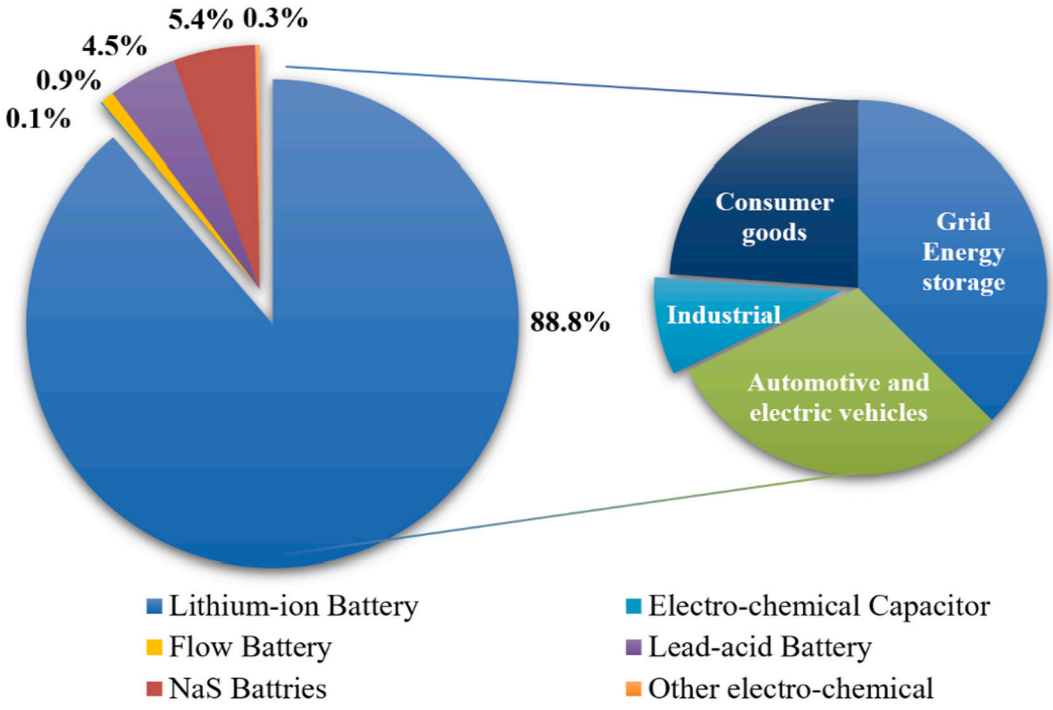

Fig. 1. Electrochemical energy storage market capacity till the end of 2019 (modified from [4]).

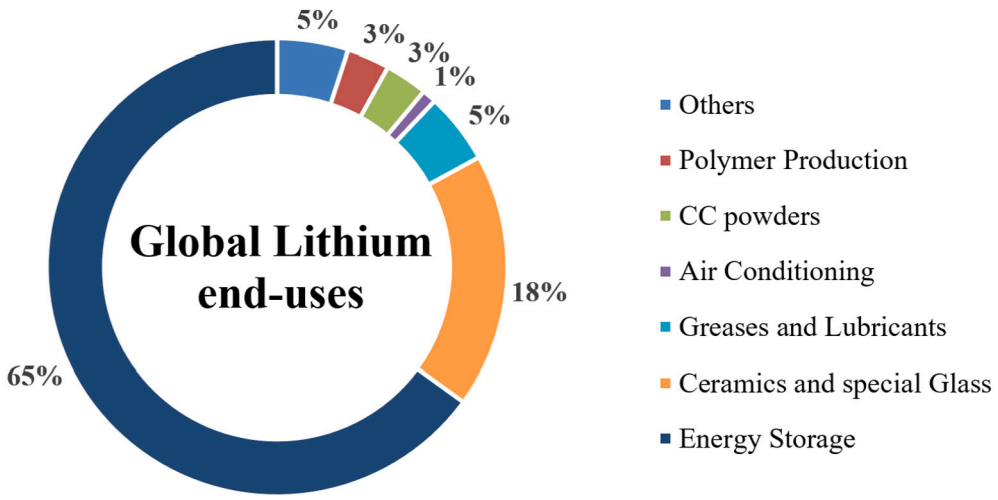

Fig. 2. Distribution of global Li end-uses in various applications in 2019 (modified from [11]).

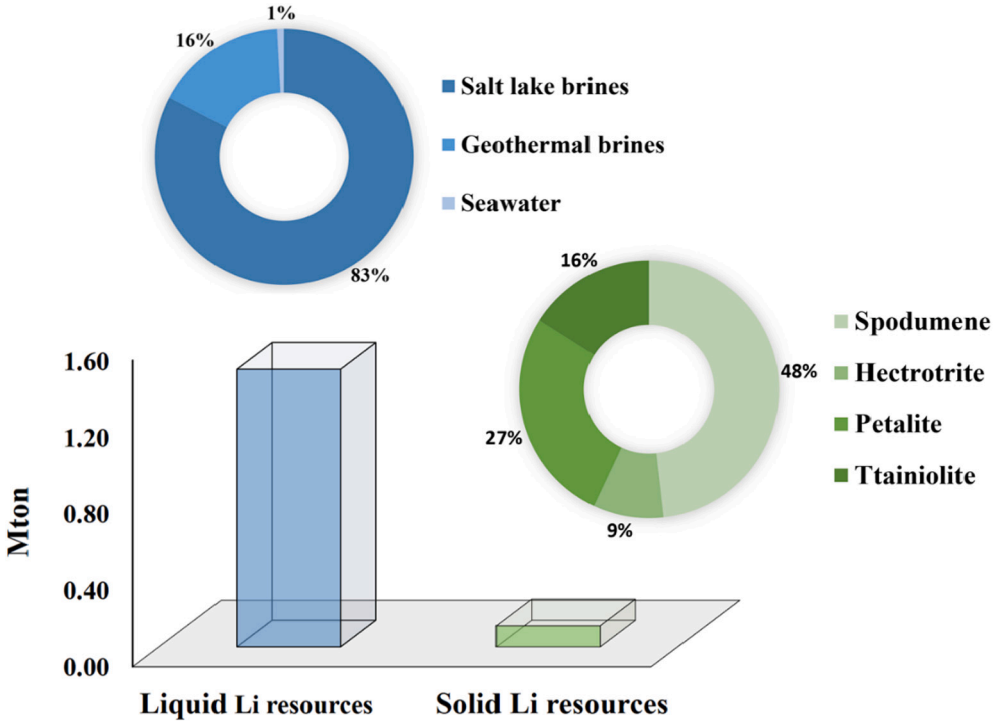

Fig. 3. Graphical representation of the amount and type and of lithium resources based on their physical state (generated from [16]).

land today [10]. If the consumption continues to increase at such an accelerating rate, efforts should be conveyed and directed toward the allocation and processing methods for the separation, purification, and recovery of Li from all potential resources [14].

With the increased utilization of Li in various fields, the demand for accessible lithium is increasing [1]. Li resources can be classified according to their physical state [15], as illustrated in Fig. 3. Salt lake brine, geothermal brine, seawater, and spent Li electrolyte are the most common liquid resources of Li [1,9]. Minerals ores such as spodumene, petalite and lepidolite as well as spent Li batteries and electronic waste make up the solid lithium reserves [9]. In 2020, the US Geological Survey (USGS) reported that the total Li resource is about 80 million tons; however, it demonstrates an uneven geographic distribution worldwide, with the majority of the Li resource concentrated in Bolivia (31%), followed by Argentina (25%),), Chile (13%), Australia (9%), and China (7%).

Brine is defined as a high saline solution with average total dissolved solids (TDS) concentrations in the range of 170–330 g/L, which are much higher in value than that for seawater (about 35 g/L) [16]. The cations other than Li^+ present in most brines are sodium (Na^+), magnesium (Mg^{2+}) and calcium (Ca^{2+}) [17]. Important anions in brines are chloride (Cl^-), carbonate (CO_3^{2-}) and sulfate (SO_4^{2-}) [17]. Geothermal brines persist deep underground with Li concentrations in the range of 10–20 mg/L, while salt lake brines exist on the surface and exhibit much higher Li concentrations in the range of 100–1000 mg/L [16,18]. Seawater contains an enormous amount of Li, 230 billion tons [17]. However, the concentration of Li^+ is too low (0.17 mg/L) to be used in direct Li recovery [19].

A secondary Li resource is spent Li-ion batteries. Currently, the industry favors the extraction of Li from aqueous resources because they contain more than 85% of recoverable Li and it can be recovered cost-effectively [20]. The largest resource for commercial Li production is

continental brine with a production capacity of 120.5 ktons/year (59% of the total), followed by hard rock (25%), clay (hectorite) (7%) and geothermal brine (3%) [15]. However, it is very challenging to achieve high selectivity of Li^+ relative to other dissolved cations present in brine [18]. In particular, the high Mg^{2+}/Li^+ mass ratio is a limiting factor that restricts the development of processes for recovering Li from brine [18]. Despite the predominance of brine as a source of Li, the depletion of high-quality brine continues to increase, which can lead to the loss of the primary source of Li [15]. Moreover, the total Li content in hard rock (0.11 Mton) is much lower than that in brine (1.45 Mton) and the cost of extracting Li from hard rocks is estimated to be US$ 6–8 kg^{-1}, which is twice the price of Li extraction from brine (US$ 2–3 kg^{-1}). However, the extraction of Li from hard rocks persists, and according to the USGS in 2018, the production of Li from brines is still not enough to meet market demand [16]. This is mainly due to the presence of excessively high concentrations of interfering ions, especially Mg^{2+}, which hinder the extraction of Li from salt lake brines. The alternative of extracting Li from seawater is considered a major challenge due to the complicated technical procedures, high capital costs, and the low concentration of Li, all of which make it economically impractical [5,9,21]. However, the recycling of Li in spent LIBs has gained great interest and is expected to increase as demand for rechargeable LIBs increases [1].

1.1. Existing technologies for Li recovery

Li extraction from the Li containing mineral rocks such as spodumene, petalite and lepidolite generally begins with crushing and heating of the mineral in order to increase the surface area and the mobility of constituent ions. Also, heating shifts the mineral from the alpha to the beta configuration, and then the mineral concentrate is sequentially cooled, powdered, treated with hot sulfuric acid and sent through a thickener filter system. This step separates the liquid containing Li^+ from solids containing impurities like Mg^{2+} and Ca^{2+} that had been precipitated in previous steps. The addition of soda ash (Na_2CO_3) into the Li stream precipitates Li_2CO_3. This solid is purified by dissolution, crystallization, filtration and drying, to yield high purity Li_2CO_3 [22,23].

Brine processing for Li extraction has not one, but many different techniques. Commercial-scale Li production is carried out by a soda evaporation process. Typically, geothermal brine or continental brine is collected in wide, short-walled tanks where it undergoes solar-influenced liquor concentration. Brines carry Li concentrations in the range of 220–3800 mg/L [24], which after partial evaporation increases to the range of 300–5000 ppm. During the solar-induced concentration procedure, other cations tend to precipitate with counter anions once their concentration increase above saturation. Remaining ions in the solution, particularly Mg^{2+} and SO_4^{2-}, are removed by adding a small amount of lime or are removed in a post-treatment stage. Then Li^+ is precipitated as Li_2CO_3 with the addition of soda ash. Impurity removal at the post-treatment stage is performed either by solvent extraction or lime addition, depending on the remaining impurities. Solar drying is a crucial step in the entire process since the sun is a freely available resource. This method renders high profits due to its low cost. The time required for Li extraction is important when there is a huge market with a massive demand for the extracted Li. Solar drying takes 12–18 months in general, and the actual timeline varies depending on the climatic conditions. Therefore, almost all of the Li extraction processes for brines that have been studied to date focus on concentrating Li^+ in the mother liquid more rapidly by reducing the solar evaporation step from months to hours, while at the same time separating Li from coexisting ions to reduce post-treatment costs [16].

Solvent extractions and chemical precipitation are other early methods for recovering Li from brines. Li can be chemically precipitated as lithium aluminate or lithium carbonate with the addition of aluminum chloride or sodium carbonate, respectively. The aluminate process is suitable for high Mg^{2+}/Li^+ brines, while the carbonate process is suitable for low Mg^{2+}/Li^+ brines. Li can also be separated by solvent extraction using chelating reagents that have a particular affinity for Li^+, such as triacyl phosphine and tributyl phosphate. Long-chain alcohols and diols can also be used in solvent extraction. However, chemical precipitation and solvent extraction leave huge volumes of sludge to dispose and are therefore, less environmentally friendly.

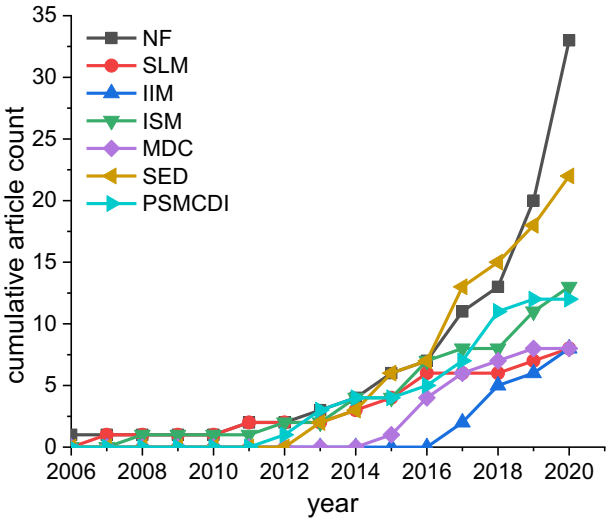

Fig. 4. Year vs a cumulative number of published papers for the membrane-based techniques. Abbreviations in the legend refer to nanofiltration (NF), supported liquid membrane (SLM), ion-imprinted membrane (IIM), ion sieve membrane (ISM), membrane distillation crystallization (MDC), selective electrodialysis (SED), and permselective exchange membrane capacitive deionization (PSMCDI), respectively. Based on data from [15,25–40,44–51].

Li^+ extraction by membrane-based processes has a long history compared to electrochemical techniques. Membrane-based processes are driven by external stimuli such as thermal gradient, pressure, and electric field. Nanofiltration (NF) for Li extraction has been studied at a full scale [25,26]. Commercial NF membranes (Desal 5 DL [26], Desal DK [27], Desal DL-2540 [28], DK 1812 [29], and NF 90 [30]) have been applied in different systems, as have some custom-made membranes. Simulated, dilute brine solutions were used in almost all experiments since the technique is unable to handle a high Mg^{2+}/Li^+ ratio. The best performing system exhibited 85% separation of Li^+ over Mg^{2+}. The separation of Li in these processes is based on steric hindrance and Donnan exclusion. Li^+ has lower steric hindrance along with lower hydration energy. Membrane-based processes are promising in sustainability aspects, because they have a low footprint, yet they suffer from membrane fouling and high operational costs.

Ion imprinted membrane (IIM) [31–33] and ion sieve membrane (ISM) [34–36] demonstrate selective adsorption of Li but are driven by different stimuli. Ion-imprinted membranes that are prepared mainly using crown ether and calixarenes demonstrate lower adsorption capacity despite being highly selective. Adsorption capacity and chemical stability are high in ion sieve membranes, and this is the result of an intercalation mechanism. Furthermore, both of these membrane processes require chemical treatment to facilitate the desorption of Li^+ and to regenerate the membrane.

Employing low-grade heat to create a gradient in vapor pressure on either side of the membrane distillation crystallization (MDC) unit allows the passage of water and volatile components from the feed side to permeate stream across a hydrophobic membrane. Subsequently, the MDC unit crystallizes Li ions from the concentrated brine in the feed side by transporting them through the crystallizer unit [37–39]. At the best-operating conditions, the system renders a 73% recovery of Li^+ [40]. This value is still low and separation of Li^+ from other ions is extremely difficult. Furthermore, membrane fouling and wetting are additional problems.

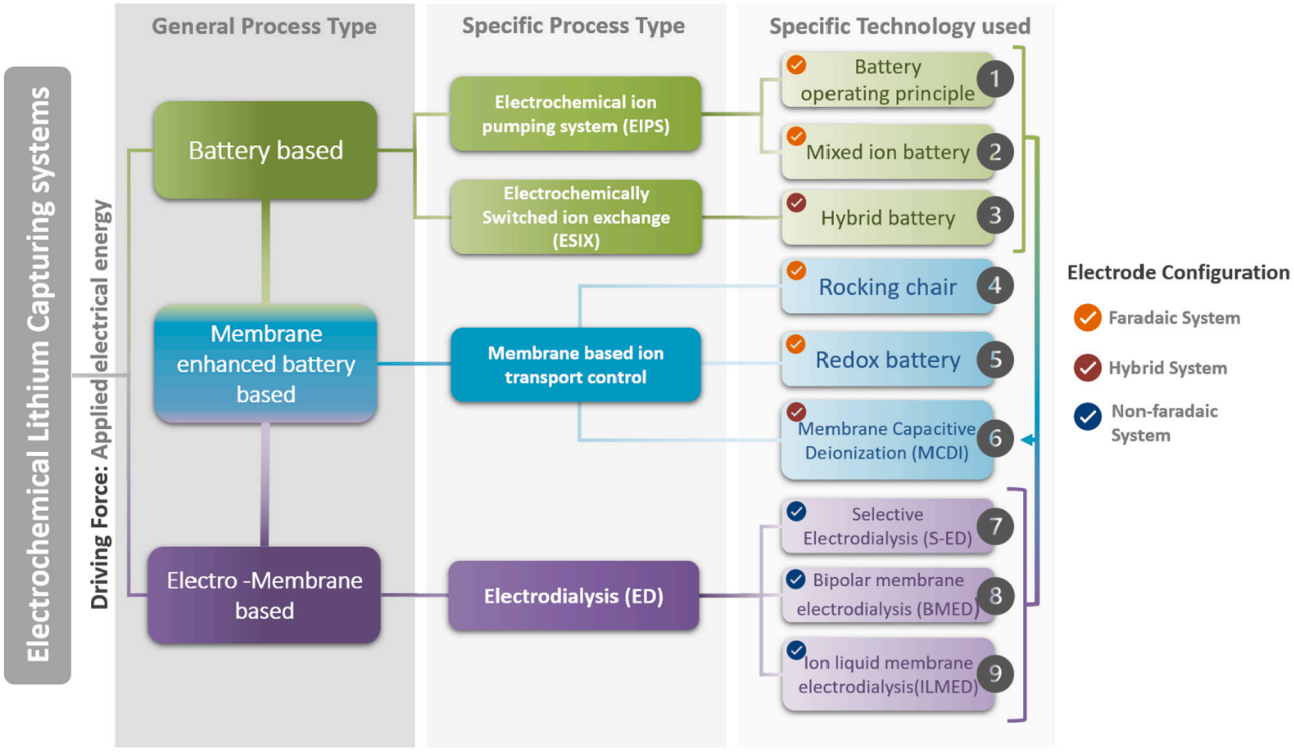

Fig. 5. Classification of electrochemical Li capturing systems.

The cumulative numbers of articles published about different membrane-based techniques for Li recovery from the year 2006 are plotted in Fig. 4. This figure shows that despite concerns over fouling, NF is researched to a greater degree compared to IIM, ISM, and MDC. Research on Li recovery using IIM, MDC and supported liquid membranes (SLM) has shown little growth over the last two years. This could be due to limitations of the process caused by large volumes of organic solvents involved or by the difficulty in reusing waste chemicals. Li extraction utilizing membranes is well reviewed in two papers [15,41]. Although electrodialysis (ED) [42] and capacitive deionization (CDI) [43] employ membranes, ion mobility in the two processes is induced by an applied potential difference. Thus they are within the scope of this research paper and discussed later in Sections 2.2.2 and 2.2.3.

1.2. *Highlighting electrochemical Li capturing systems (ELiCSs)*

High-efficiency methods for production of Li are continually being investigated to meet the demand associated with the accelerating growth of its consumption [52]. It is important to focus not only on technologies for Li recovery that are considered novel and promising, but also to consider technologies that have environmentally friendly [53–56], energy-efficient [53–56] and cost-efficient [53] features. These processes draw tremendous attention toward them, and their attractive characteristics make them strong substitutes for the conventional Li recovery techniques addressed in the previous section. Traditional Li recovery techniques have continuously suffered from their lengthy process times [54], high energy consumption, low utilization of resources and high sludge formation [19], and these characteristics hinder their effective use as reliable Li recovery approaches in the near future. Electrochemical ion-separation processes have emerged as simple and environmentally benign methodologies that can be effectively utilized for the selective capture of Li as well as a vast array of other valuable elemental resources such as nickel [57,58], cesium [59,60], and copper [57]. For Li extraction, electrochemical systems are very promising and exhibit outstanding performance in terms of Li recovery capacities, tunability [53,61], cyclic efficiency, reversibility, and selectivity. Thus, vast research activities were conducted in the past decade to investigate and improve the performance of these electrochemical lithium capturing systems (ELiCSs).

ELiCSs can be categorized into three broad classes depending on their basis of separation: battery-based, electro-membrane-based, or membrane enhanced battery-based. They can be further classified based on their recovery system and configuration, as shown in Fig. 5. Generally, the driving force for capturing Li in all ELiCSs is to apply current [53], where the amount of Li removed (immobilized) from a feed stream depends on the invested charge of the electrode [62].

Battery-based ELiCSs are systems that usually employ at least one faradaic electrode to capture Li-ions using charge transfer across the fluid-solid interface between the electrolyte and the electrode [2,12]. Kanoh and his team first reported this approach in the early 1990s, when they designed an electrochemical system that used λ-MnO_2 as the working electrode and Pt wire as the counter electrode to capture Li ions from a solution of mixed cations. Li ions were captured via the λ-MnO_2 intercalation electrode, while oxygen evolution took place on the counter Pt electrode [7,20,63]. This approach was innovative at the time but suffered from considerable energy consumption during its capture and release steps [53]. Two decades later, inspired by the concept of the desalination battery, La Mantia and Yoon groups proposed the use of silver as a counter electrode to simultaneously capture chloride ions at the counter electrode while Li ions are adsorbed and desorbed at the intercalation electrode, thus requiring much less energy [64,65]. The approach mentioned above is now known as the electrochemical ion-pumping mechanism. Electrochemical ion-pumping systems (EIPS) have two main configurations depending on the operating principle. EIPS with battery operating principle uses Li selective electrodes (intercalation electrode) to capture Li ions and usually metal counter electrodes (like Pt and Ag) to capture cations simultaneously (Fig. 6(1)). On the other hand, EIPS with a mixed ion battery principle uses a Li selective electrode and a Li exclusive electrode, as shown in Fig. 6(2).

The last recovery system under the category of battery-based separation systems is the electrochemically switched ion-exchange recovery system (ESIX). This system has a hybrid electrode configuration since it

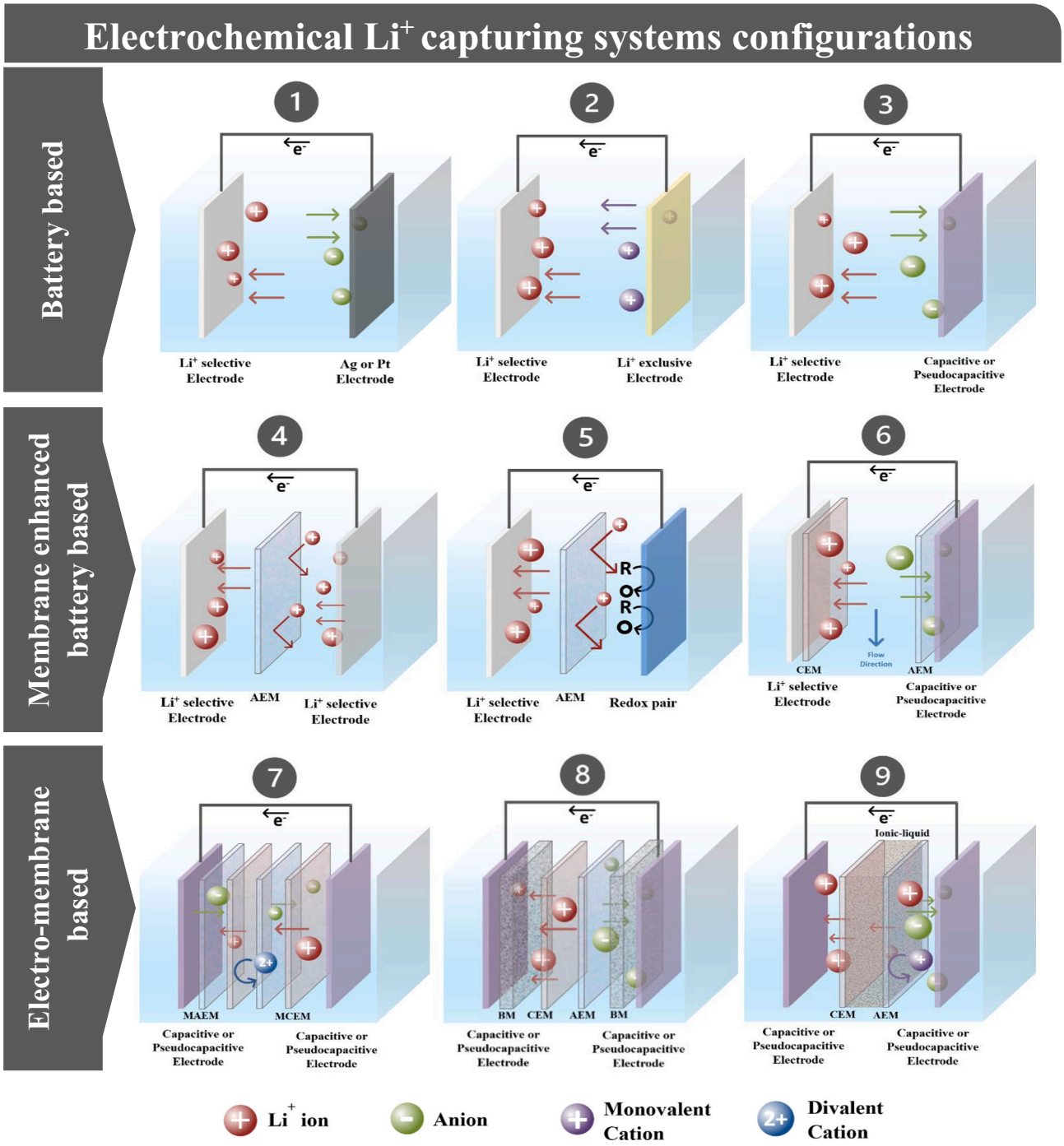

Fig. 6. Different configurations of ELiCSs: (1) Battery operating principle, (2) Mixed-ion battery operating principle, (3) Hybrid battery principle, (4) Rocking chair configuration, (5) Redox battery configuration, (6) HCDI configuration, (7) Selective Electrodialysis (SED), (8) Bipolar membrane electrodialysis (BMED), and (9) Ion liquid membrane electrodialysis (ILMED). The individual panel numbers correspond to the configuration numbers in Fig. 5 [53,54,69–72].

employs a faradaic intercalating electrode against a non-faradaic (capacitive or pseudocapacitive) electrode (Fig. 6(3)). The utilization of the large capacity and low self-discharge characteristics of faradaic electrodes and fast removal rates experienced with the non-faradaic electrodes bridges the performance gap between battery and capacitor-based separation systems [66].

Membrane-enhanced battery-based ELiCSs have a similar configuration to the battery-based ones, but include both membranes and faradaic electrodes to achieve Li capturing. The rocking chair (Fig. 6(4)) system is a faradaic ion separation process where an anion exchange membrane (AEM) divides its cell into two compartments, each having a Li intercalating electrode. By applying an electric potential between the two electrodes, Li is captured from the brine reservoir by the cathode, while it is released into the recovery solution at the anode. Continuous recovery of Li can be achieved through the proper switching of the position of the electrodes. Similar to the rocking chair configuration, the redox battery configuration (Fig. 6(5)) also uses AEM to separate the system into two reservoirs, one capturing and releasing Li from the intercalating electrode, and the other using redox couple reactions such as the I_3^-/I^- [67] and Zn/Zn^{2+} [1,20] redox couples. Traditional capacitive deionization (CDI) is known for its extensive and effective use in low saline desalination applications. With the increased interest in Li

recovery, it has been enhanced by using the battery operating principle to recover Li. Li passes through a cation exchange membrane to be absorbed into an intercalating electrode, while anions pass through an anion exchange membrane to accumulate at a capacitive or pseudocapacitive electrode, as shown in Fig. 6(6). Lastly, electro-membrane-based ELiCSs are applications of the well-known electrodialysis (ED) systems. The ED system for Li recovery is considered membrane-based and consists of a series of anion and cation exchange membranes between two non-faradic electrodes. When the potential is applied to those electrodes, Li selectively migrate through the cation exchange membranes toward concentrating compartments and so, the process is termed selective electrodialysis (SED) (Fig. 6(7)). This SED process is further developed by employing a bipolar membrane or an ionic liquid membrane (Fig. 6(8,9)) that facilitates this lithium recovery process.

Increased global focus on Li research has been best evidenced by the number of exclusive reviews published in 2019–2020 on Li recovery. A total of six reviews have been published with two mainly focusing on membrane-based processes for Li extraction. These two reviews highlight membrane fabrication [15] and nanochannel regulation [41] to enhance the selectivity for Li, while the others focus on the electrochemical aspects [20,61,68], the broad spectrum of charge transfer and ion separation principles, with particular emphasis on material and engineering aspects and reactor design of ESIX systems. However, there has not been a single review comparing electrochemical Li recovery by ESIX, CDI and ED processes. Such a review is much needed since understanding the common and process-specific features of these processes will influence the design of new hybrid processes that will pave the way for highly selective and energy-efficient Li recovery from natural brines. Hence, this review intends to cover the recent research done on ESIX, CDI and ED, starting with the fundamental operation principles, evaluating how process parameters govern the quality of Li output, as well as with their technology readiness level (TRL).

2. Electrochemical Li capturing systems

2.1. Performance parameters

The performance of ELiCSs is assessed by key parameters such as recovery ratio of Li^+, insertion capacity, separation coefficient of Li^+ toward co-existing ions, current efficiency, and specific energy consumption. Those parameters are directly influenced by the ionic strength of feed, solution, which account for the concentration and mass ratio of co-existing ions, and expressed using a mathematical model as addressed below [55,73,74].

Many Electrochemical processes depend on the selectivity of electrodes for capturing desired ions (e.g., Li^+) by intercalation. The Li^+ selectivity of a Li-capturing electrode (α_M^{Li}) in the presence of other ions is determined by the ratio of the molar concentration of Li^+ in the recovery solution (C_{Li}^r) to the molar concentration of coexisting cation in the source solution (C_M^s). This is shown in Eq. (1), where M represents any cation other than Li^+ (e.g., Na^+, K^+, Mg^{2+} or Ca^{2+}) [75]. The separation factor (SF) represents the enhancement of Li concentration by recovery process, as well as a comparison of Li purity in the recovery and in source solution as expressed in Eq. (2) [55]. SF can determine the required run time needed to achieve desired performances, but they are strongly dependent on the characteristics of the brine solution.

$$\alpha_M^{Li} = \frac{C_{Li}^r}{C_M^s} \tag{1}$$

$$SF = \left(\frac{C_{Li}}{C_M}\right)_r \Big/ \left(\frac{C_{Li}}{C_M}\right)_0 \tag{2}$$

The recovery rate of Li^+ (RR_{Li}) determines the amount of Li^+ recovered from the source solution per unit mass of the electrode material [75]. The recovery rate is a critical parameter that is commonly employed to evaluate the overall performance of ELiCSs such as ESIX and CDI process. In Eq. (3), the (RR_{Li}) is found by dividing the concentration difference of the initial (C_{Li}^0) and the final (C_{Li}^f) concentration of Li^+ in source solution and final volume of the source solution ($V_{f,s}$) over the mass of active material of the electrode.

$$RR_{Li} = \frac{V_{f,s}\left(C_{Li}^0 - C_{Li}^f\right)_s}{m} \tag{3}$$

ELiCSs consume electrical energy while recovering Li and the amount used is an important aspect of their performance. The energy required per unit Li recovered by ELiCSs can be calculated using Eq. (4) [76]. This equation calculates the electrical energy consumed as the circular integral of voltage profile with respect to charge (W) and the amount of Li^+ recovered (C_{Li}).

$$W = \frac{\oint \Delta E \, dq}{VC_{Li}} \tag{4}$$

For EISX and CDI technologies, the specific energy consumption (E_{SEC}) can be determined using Eq. (5) at constantly applied voltage (U). Where (M_{Li}) is the molar mass of Li, (I) is the applied current, (w) is the effective mass of electrode, and (E_{Li}) is the extraction capacity of Li [55]. The current efficiency (η_{Li}) determines the percentage of current applied that is effectively employed to extract Li^+. The current efficiency (Eq. (6)) is affected by the selectivity of capturing material. The current efficiency will be low if the electrode intercalates a large amount of cations other than Li^+ or provide a secondary reaction [76]. In Eq. (6), F is the Faraday constant of (96,485 C/mol).

$$E_{SEC} = \frac{M_{Li}\, U \int_0^t I\,(t)dt}{3.6E_{Li}w} \tag{5}$$

$$\eta_{Li} = \frac{F\, E_{Li}\, w}{10\, M_{Li} \int_0^t I\,(t)dt} \times 100 \tag{6}$$

Typical electrodialysis (ED) processes as well as processes based on ED consist of IEM, concentrate and dilute chambers and electrodes. Ideal IEMs are determined by the ease transport of cations to the negatively charged cathode, while the migration of anions toward the positively charged anode [23]. The migration rate of Li^+ (J_{Li}) through IEM is determined by the concentration difference of Li^+ in the concentrate chamber ($C_{Li,c}$) and in the desalinating chamber (C_{Li}^0) with respect to the effective area of IEM (A) and the operating time (t), as expressed in Eq. (7). The percentage of Li recovered (R_{Li}%) is found by the difference of initial ($C^0_{Li,c}$) and final ($C^f_{Li,c}$) concentrations of Li^+ in the concentrate chamber with respect to the initial volume (V_o) and concentration of Li^+ (C_{Li}^0) in dilute chamber, as displayed in Eq. (8) [74,77,78].

$$J_{Li} = \frac{V_c\left(C_{Li,c} - C_{Li}^0\right)}{A\ t} \tag{7}$$

$$R_{Li} = \frac{V_c\left(C_{Li,c}^f - C_{Li,c}^0\right)}{V_o C_{Li}^0} \times 100\% \tag{8}$$

The effectiveness of Li recovery can be evaluated by the separation coefficient (F_{M-Li}) or the separation efficiency (S_{Li}) as expressed in Eqs. (9) and (10), respectively. The separation coefficient refers to the molar concentration of Li^+ relative to the molar concentration of coexisting ions at the dilute chamber. The final total molar concentration of ions in the dilute chamber relative to the initial concentration was divided by the same ratio for molar concentration of Li in the desalinate chamber. The separation efficiency refers to the difference of initial ($C_{Li,d}^0$) and final concentration ($C_{Li,d}^f$) of Li^+ with respect to the initial concentration of Li^+ in the dilute chamber.

$$F_{M-Li} = \frac{C_{M,c}^f / C_M^0}{C_{Li,c}^f / C_{Li}^0} \tag{9}$$

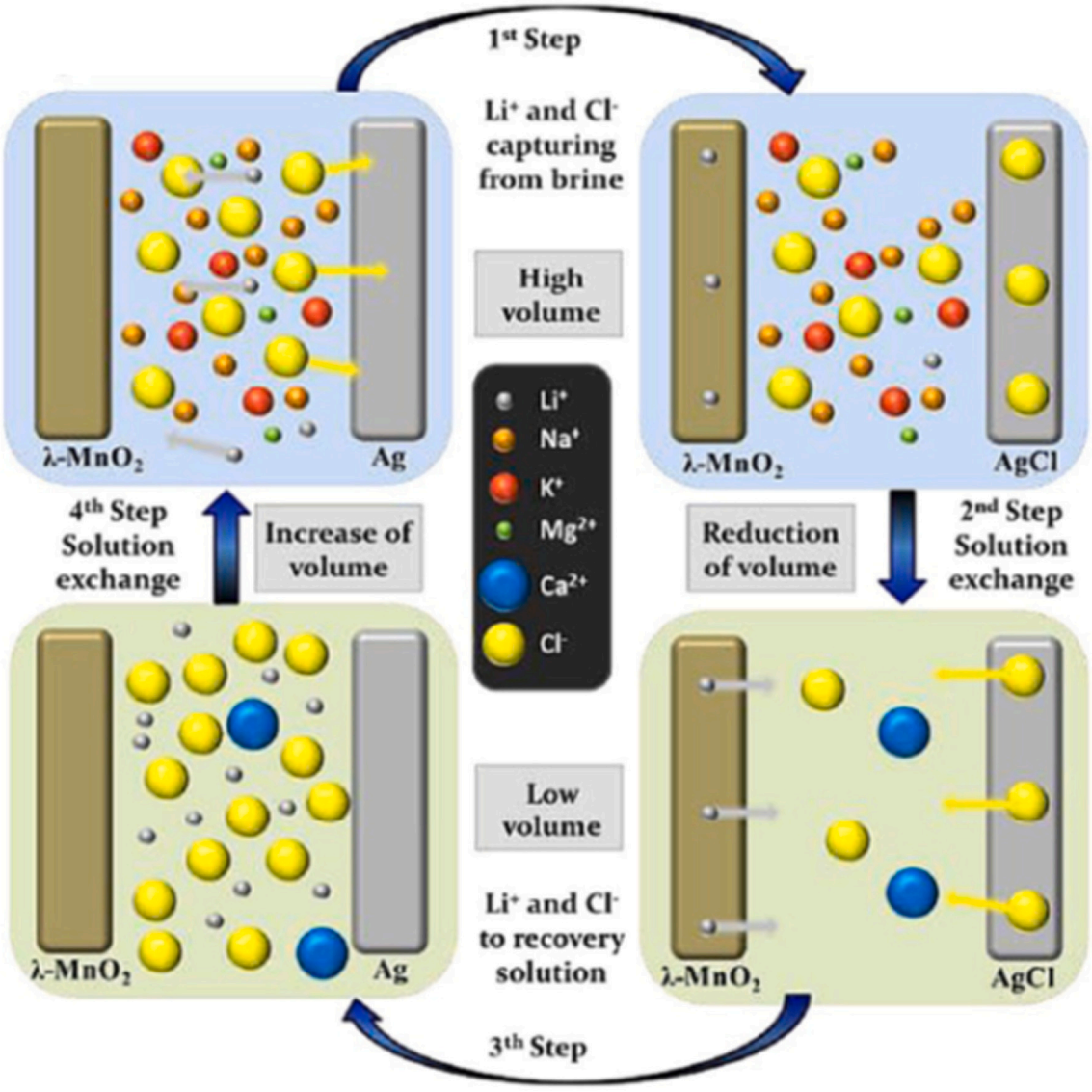

Fig. 7. Schematic of typical Li recovery process in brine using λ-MnO_2 as the Li capturing electrode and Ag as the chloride capturing electrode (obtained from [56]).

$$S_{Li} = \frac{C^0_{Li,d} - C^f_{Li,d}}{C^0_{Li,d}} \times 100\% \quad (10)$$

For ED and ED-based processes, the specific energy consumption (E_{SEC}) and current efficiency (η_{Li}) for Li^+ recovery from brine solution are evaluated as shown in Eqs. (11) and (12), respectively. In Eq. (11), (n_R) refers to the number of moles of Li^+ that migrated from the feed solution. The current efficiency (Eq. (12)) influences by the number of moles Li^+ at the initial time ($n_{0,\,c}$) and at time t ($n_{t,\,c}$) in the concentrate chamber, the valence of other ions that are present (z) and the number of membranes in electrodialysis stack (N) [79].

$$E_{SEC} = \frac{U \int_0^t I\,(t)dt}{n_R} \quad (11)$$

$$\eta_{Li} = \frac{\left(n_{t,c} - n_{0,c}\right) z\,F}{N \int_0^t I\,(t)dt} \times 100 \quad (12)$$

2.2. Types of processes

2.2.1. Electrochemically switched ion exchange (ESIX)

Electrochemically switched ion exchange (ESIX) technology enables intercalation and deintercalation of an element into an appropriate electrode material upon application of an electrical potential. This electrode switches between a cathode and an anode as the electrical potential is switched. The technology has evolved significantly over the years. The entire cycle consists of four steps [56] as shown in Fig. 7. In the first step, the intercalation of Li ions onto the electrode material occurs at negative bias. During this stage, Li^+ adsorbs to the working electrode, which is an energy-generating step analogous to discharge of a battery. The role of the counter electrode varies depending on the nature and type of counter electrodes. After a given period, the Li source solution will be replaced with a recovery solution in the second step. The recovery solution is typically a solution with low or no Li^+. In the third step, a positive bias is applied to the electrode pair, during which all Li^+ captured by the working electrode is transferred to the recovery solution. This step consumes energy and is similar to charging a rechargeable battery. Finally, the recovery solution is replaced again with the source solution, prior to starting another Li^+ capture/release cycle. This technique operates in a mechanism complementary to that of a Li-ion battery, and the corresponding intercalation and deintercalation steps are analogs to discharging and charging a rechargeable battery.

λ-MnO_2, which is an electrode material used in commercially available Li-ion batteries, iron (III) phosphate and Li-deficient lithium

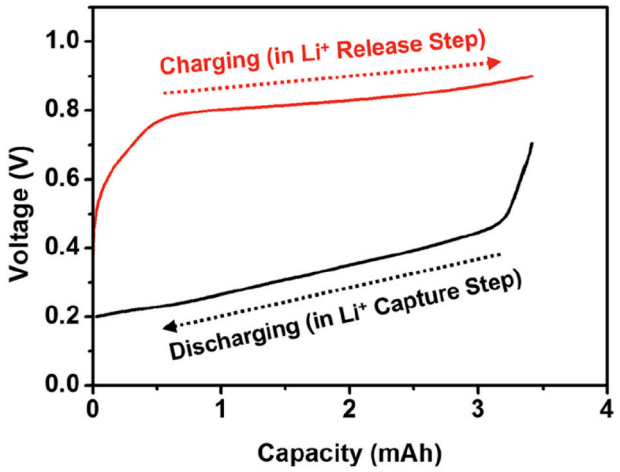

Fig. 8. Plot of voltage vs. capacity curve of λ-MnO_2/Ag system, and energy consumption during operation was calculated by the circular integral of the graph (2.48 Wh·g_{Li}^{-1}) [82].

manganese oxides (LMO), have been frequently used as working electrodes. Pt was the counter electrode used in the early ESIX processes, but energy-intensive water splitting reactions that produce H_2 and O_2 took place at the Pt counter electrode increasing energy consumption [80,81]. However, in later studies, Pt was replaced with Ag, due to its ability to adsorb Cl^-. In this configuration, the cell was simple and was driven by entropy. Energy consumption was further lowered with the introduction of a nickel hexacyanoferrate (II/III) based electrode. These systems no longer entail mixing entropy and are somewhat limited to the solvation of Li^+ ions in the solution. The technique is simple, rapid, easy to operate, and shows low energy consumption with high selectivity.

ESIX, similarly to other electrochemical Li recovery methods, does not yield Li in a form that is directly usable. If Li concentration is high enough in the recovery solution, there would be no need for the time-consuming solar drying steps used in the conventional lime soda evaporation process for Li extraction. This process is mainly being used in the countries of Chile, Bolivia, Argentina, and Australia. Studies show that adopting ESIX reduces the time scale for producing a usable product from years for solar drying to hours [20]. ESIX isolates Li from the coexisting ions in the source solution and concentrates it in the release solution. This technology offers the extended advantages of efficiently removing other coexisting ions. In the conventional process, other ions are removed by precipitation, which requires additional reagent and produces large volumes of sludge that require additional treatment prior to disposal. In the following section, the most recent ESIX systems are critically compared to highlight each system's advantages and disadvantages. The evolution of the working/counter electrode pairs will also be discussed.

The recovery of Li or any other elements from a very low concentration solution is mostly limited by mass transport. However, this can be overcome by having a higher electrode surface area with a stack of smaller electrode pairs of working and counter electrodes arranged in an array, rather than a single electrode with a larger area [17]. In order to obtain a high concentration of Li in the final product, it is important to keep the volume of the recovered solution as low as possible [17]. Li's selectivity to other elements is assessed by evaluating test samples from source and recovery solutions taken before and after the test [82].

Li possesses a smaller ionic radius and hydration energy than other cations that are naturally present in salt lake brines and spent LIBs or discharges. In electrochemical Li recovery, liquid sources of Li are used, where Li^+ coexists with chlorides of Na^+, K^+, Ca^{2+}, and Mg^{2+}. Li migration to suitable sites is based on how compatible the ionic radius of Li^+ is with the interstitial sites of the Li capturing electrode. In this aspect, K^+, Na^+, and Ca^{2+} do not compete with Li because they have higher ionic radii. However, Mg^{2+} has a smaller ionic radius, and it is similar to that of Li^+, so maintaining a satisfactorily higher level of Li/Mg selectivity is crucial but difficult [69]. Hydration energy of Mg^{2+} is four folds higher than that of Li^+. The difference in hydration energy in the aqueous medium is used to separate the two ions. The energy supplied to the system by the applied potential in the test window during the intercalation process is only sufficient for the Li^+ to migrate to the tetrahedral interstitial sites of the λ-MnO_2 electrode. The higher hydration energy of Mg restricts its effective diffusion into the oxygen-rich λ-MnO_2 lattice [82].

Li capture and release are characterized by the capacity vs voltage curves, as shown in Fig. 8. During Li capture, cell capacity decreases along with a drop in cell voltage while the releasing step demonstrates capacity increase with the increase in voltage. The energy consumed in a single cycle is calculated by the circular integral of the capacity vs. voltage plots obtained for charging and discharging half-cycles. It is also the area of the polygon formed by combining the curves of the two half-cycles. To increase its meaningfulness, the energy consumption is usually reported per mole or per gram of Li recovered, which is called the specific energy consumption (SEC).

2.2.1.1. λ-MnO_2/Pt. The concept of Li-ion recovery by the ESIX approach was first proposed by Kanoh et al. in 1991, employing a 0.75 μm film-thick spinel-type MnO_2 (λ-MnO_2) battery material fabricated on a Pt plate [80]. Electrochemical Li insertion and release were characterized by cyclic voltammetry (CV) performed on 0.1 M LiCl solution in the potential region of 0.246 to 1.244 V. During the intercalation step, which corresponds to the discharging cycle of a battery, the insertion of Li resulted in two distinct peaks at 0.69 and 0.52 V (vs. SCE) in the forward sweep of the CV test. The subsequent release of Li from the Li loaded electrode was probed by two oxidation peaks at slightly higher potentials of 0.67 and 0.82 V (vs. SCE) in the anodic curve. The definite peaks at cathodic and anodic sweeps were found to correspond to the reduction and oxidation of Mn (IV)/Mn (III) at two different sites, occurring with the transport of Li into and out of the spinel lattice. The kinetics of the process tended to increase at peak currents as the scan rate increased from 0.1 to 0.5 mV·s^{-1}. However, above 0.5 mV·s^{-1}, the two peaks combined into one, leading to the belief that Li insertion is a slow kinetic process. In this initial demonstration, the Pt counter electrode had no specific role other than maintaining charge balance in the system during intercalation and deintercalation by undergoing a high energy-consuming water-splitting reaction. A subsequent study by the same team found that this λ-MnO_2/Pt system was effective for recovery of Li at concentrations higher than 10 mM, while it was completely ineffective at concentrations below 0.1 mM [81]. Furthermore, inhibition of Li insertion was observed in mixtures containing alkali earth metals. Li ions are inserted into the tetrahedral binding sites of λ-MnO_2 to reduce the valence state from (IV) to (III). It was assumed that the divalent ions adsorb to the outer surface of the electrode by electrostatic interactions and act as a barrier for Li to intercalate into the electrode. However, in the later study, Li selectivity was reduced primarily by Mg^{2+}, which as an ionic radius similar to Li^+ [69,82]. This method rendered good performance results for Li salt solutions with a Li concentration greater than 10 mmol/L, but the sensitivity was poor at 0.1 mmol/L or less. Furthermore, in the early studies, the ionic composition of the aqueous phase was evaluated by AAS, whereas it was evaluated by a more precise method of ion chromatography (IC) later in the study. The Pt counter electrode of this combined system has little contribution to process improvement.

2.2.1.2. λ-MnO_2/Ag. λ-type manganese dioxide is often used as an electrode in battery-based processes. Li is captured and subsequently released by applying potentials in the range of 0.2 to 1.2 V and then reversing the potential. A simulated desalination brine solution having 0.063 mM of Li^+ and 132.7 mM of Mg^{2+} (Mg/Li ratio of 2107) in a

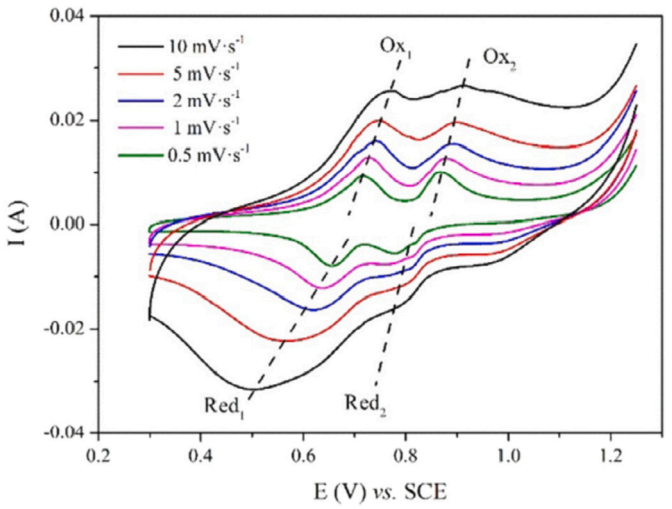

Fig. 9. CV curves of λ-MnO_2 electrode in 1 mol·L^{-1} of LiCl solutions at various scan rates [84].

diverse solution containing Na^+, K^+, Ca^{2+}, and Mg^{2+} was processed by a system using circular-shaped λ-MnO_2 electrode [82]. Compared to seawater, brine from a desalination plant is regarded as a better source of Li due to its high concentration in brine. The Li content in seawater is extremely low at 0.17 ppm, which indicates that developing an efficient and economical method of capturing Li is difficult. On the other hand, the brine from seawater desalination plants has 2–3 times higher concentrations of Li. The utilization of seawater as a source for water and specific elements has been widely studied. Along with Li^+ ions, desalination brine contains all elements present in seawater, yet at a higher concentration.

It was able to produce a concentration of Li in the recovery solution of 190 mM with 99% purity [82]. It is noteworthy that 99% purity was achieved after applying two consecutive recovery processes, with purity averaging 56% after the first recovery process. This demonstrates the value of applying multiple recovery processes. Performance of multiple recovery processes can also be assessed by the enrichment factor, which is the concentration of Li in the recovery solution compared to that in the feed solution. The enrichment factor increased from 249.5 after the first recovery process to an excellent 3019 after the second consecutive recovery process while demonstrating a specific energy consumption of only 3.07 Wh·g_{Li}^{-1}. Li recovery per unit mass of electrode material was high at 10.1 mg/g. Furthermore, this study examined the effect of applied current density on the resultant Li capture process. At a constant current density of −10 μA·cm^{-2}, the Li enrichment factor was 249, whereas it dropped to 135 when the current density doubled to −20 μA·cm^{-2}. This behavior was caused by limited mass transport at high discharging rates. In addition to mass transport limitations, there was some evidence that lower enrichment factors were caused by increased dissolution of Mn at high applied currents [83].

In another study using λ-MnO_2 and Ag electrodes, Liu and coworkers [84] used repetitive half-cycles to increase adsorption capacity. The adsorption half-cycle was repeated five times before proceeding to desorption. The results clearly show a decrease in Li^+ concentration in the source solution after each run, accounting for 2 mmol·g^{-1} of Li adsorbed per cycle. Additionally, in a mixed solution with Na^+, K^+, Ca^{2+} and Mg^{2+}, Li^+ had superior selectivity with selectivity coefficients of 38.8, 35.6, 29, and 120, respectively. The retention of activity after 50 cycles of intercalation/deintercalation was 82.8% of its starting value when adsorption and desorption were performed at a constant current of 50 mA·g^{-1}. This system was tested with a high Li^+ concentration of 1 M, which is far from that in available Li^+ sources.

A study by Xu et al. showed a transformation in cathodic and anodic peak positions when the scan rate was increased from 0.5 to 10 mV·s^{-1} in CV tests using a λ-MnO_2 cathode and an Ag anode [83]. Sweep at 0.5 mV·s^{-1} scan rate, the two reduction peaks appeared at 0.75 and 0.6 V, and conversely, two oxidation peaks at 0.65 and 0.85 V in the respective cathodic and anodic curves, as given in Fig. 9. With the increment of the scan rate, the distinct peaks broadened and shifted toward lower potentials in the cathodic curve, and the shift was toward higher potentials for the two oxidation peaks in the anodic curve [83]. The driving force of the Li intercalation, whether it is diffusion controlled or the adsorption controlled, can be understood by the intensity of the redox peak vs square root value of the scan rate plot. This plot is compiled by processing information in Fig. 9. If the intercalation is driven predominantly by diffusion of Li^+, the plot will exhibit a linear relationship between the intensity and the square root of the scan rate. More precisely, the transfer from Mn (IV) to Mn (III) is faster than Li inclusion and exclusion from the interstitial sites and electrolyte solution. The effect of the morphology and surface area of the MnO_2 electrodes was assessed by employing a MnO_2 powder electrode and a MnO_2 film electrode in otherwise identical reaction systems, authors assuming similar MnO_2 content in both systems. After 100 cycles of operation, concentration of Li^+ in the feed was dropped by 25.4 mM for the MnO_2 film electrode while it decreased by 18.6 mM for MnO_2 powder electrode, corresponding to that Li concentration increase was 25.3 mM and 18.1 mM in the recovery solutions, respectively. Additionally, Li^+ recovery efficiency over 100 cycles declined slightly in the film electrode (<10% drop), but the decline was relatively large in the powder-based electrode (> 20% loss). This could be related to the combined effects of the dissolution of Ag and loss of MnO_2 powder. Notable features in this process include a potential reduction from 0.6 V to 0.3 V during 30 min of intercalation, along with a potential increase from 0.7 V to 1.0 V for 30 min of deintercalation.

Preliminary work on a pilot-scale system is vital in order to take advantage of the progress in developing technologies at smaller scales and use it to develop processes that can deal with commercial quantities of brines. Scaling up comes with an inherent set of problems that require slight modifications of process parameters compared to those used in laboratory-scale systems. The upscaled system that uses λ-MnO_2/Ag electrodes for electrochemical Li ion pumping showed a slight decrease in the purity to 88% with an enrichment factor of 1800 [17]. The process design could support an incoming flow of 250 L·h^{-1} and could produce a flow of 1 L·h^{-1} of brine concentrate. When the system is fed with desalination concentrate from a RO and MD based water desalination plant with an initial Li concentration of 0.035 mM, the Li concentration in the product was 62 mM after being treated by 14 pairs of λ-MnO_2/Ag electrode couples in a parallel configuration. The initial brine contained Na^+, Ca^{2+}, Mg^{2+} and Cl^- ions with a Mg/Li ratio of 2029. Like the lab-scale system, during Li insertion, λ-MnO_2 is converted to $Li_xMn_2O_4$ and Ag to $AgCl_x$, where x is between 0 and 1 ($0 < x < 1$). An additional step of washing the chamber with a fresh stream of deionized water is included in the pilot-scale system as shown in Fig. 10. Its purpose is to wash out the impurity ions before releasing Li ions into the release solution. Having the middle step of washing the chamber alleviates the necessity of costly post-treatment to enrich Li in the recovery solution. In general, these tests were performed at a potential sweep between 0.2 V to 1.2 V with a change of ±0.3 V and a constant current of ±50 μA [17]. Higher selectivity for Li was demonstrated by the purity values. In the initial feed, Li exhibits a purity of 0.0048% due to the massive abundance of coexisting ions. The value increased to 3.0% in the intermediate tank and to 88% in the final recovery solution, and Li capture performance was improved by repeating the Li release step 5 times.

2.2.1.3. λ-MnO_2/activated carbon. Despite Ag's indispensable role in the capture of chloride ions, the dissolution of Ag, which reduces the long-term stability of the anode, is an intractable challenge [64,85]. Replacing Ag with activated carbon showed an increase in the energy consumption for Li recovery by 29.148 Wh·g_{Li}^{-1} [69] when the feed

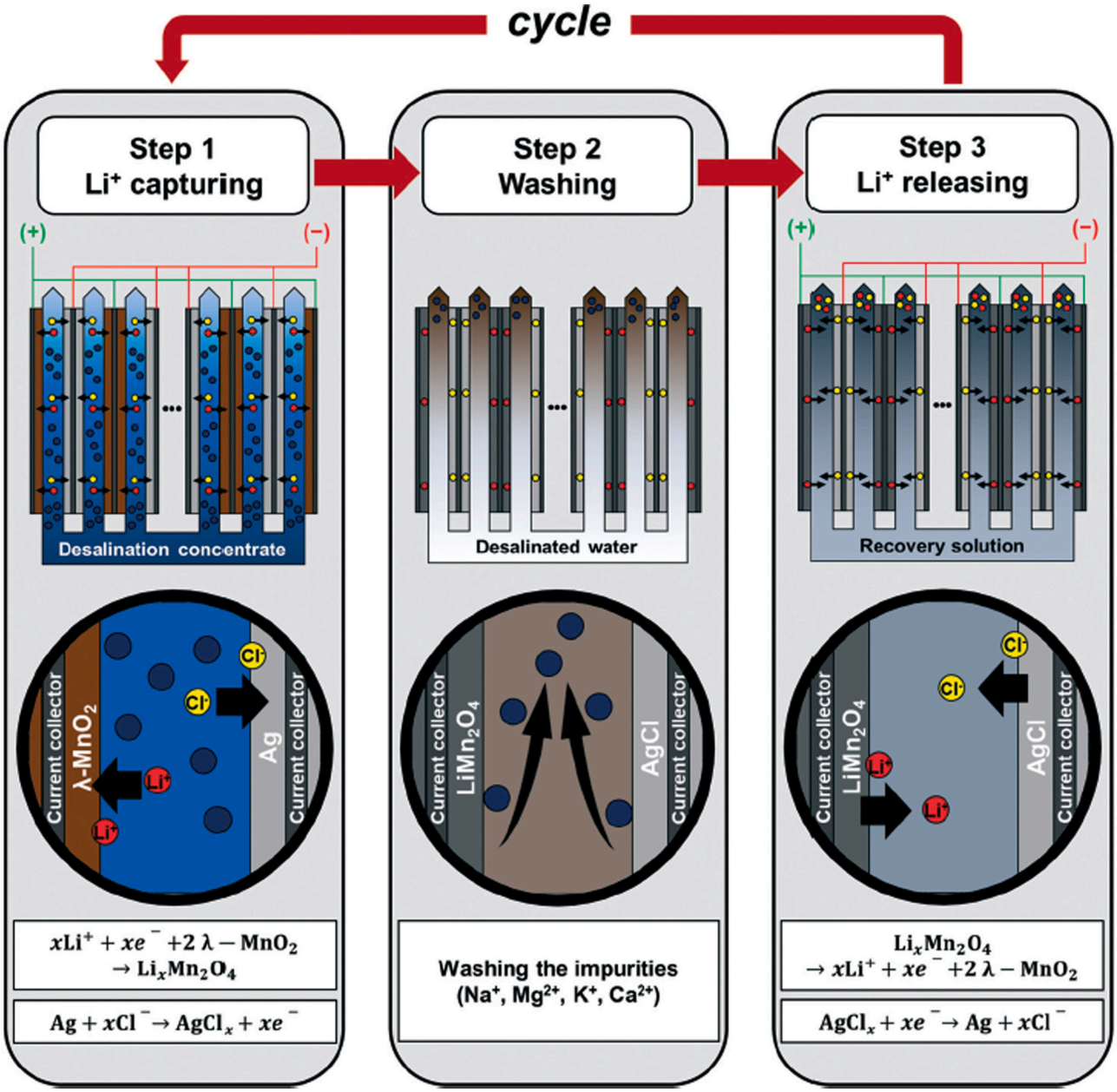

Fig. 10. Schematic of λ-MnO_2/Ag cell design in the pilot-scale [83].

solution is a mixture of chlorides of Na^+, K^+, Ca^{2+} and Mg^{2+} along with 30 mM Li. However, the system rendered a high level of stability, demonstrating no loss in coulombic efficiency with an insignificant drop (3%) in capacity over 50 cycles of charging-discharging in the CV sweep region from 0.0 to 1.1 V. This λ-MnO_2/activated carbon system resembles a hybrid supercapacitor system. The hybrid supercapacitor conceptually consists of a supercapacitor electrode (activated carbon) and a battery electrode (λ-MnO_2), which is advantageous in increasing overall cycle performance by increasing the charge density. Here, an AEM is used in the middle of the spacer and activated carbon to prevent cations from adsorbing onto the pores of activated carbon. The role of AEM in the system is similar to the membrane used in CDI [86]. The amount of Li recovered is enhanced by repeating the release cycle twice.

2.2.1.4. λ-MnO_2/NiHCF. NiHCF is a derivative of Prussian blue and is cheap and earth-abundant material. It is the coordination compound typically found as the sodium or potassium salt of nickel hexacyanoferrate(II) or (III). The affinity of the hexacyanoferrate unit for Na^+ and K^+ offers the advantage of removing coexisting alkali metal ions from brine, given that NiHCF is deployed in a two-electrode system as the counter electrode. NiHCF is already being studied as the positive electrode for Na^+ and K^+ ion batteries and has been found to have good specific charge retention [87]. NiHCF is undeniably cost-effective and durable, compared to Ag or Pt. In the λ-MnO_2/NiHCF system, NiHCF has been shown to act as a Li exclusion electrode with at least a 23.6% improvement in Li^+ selectivity compared to λ-MnO_2/Ag [54] and λ-MnO_2/AC [56,69]. This was based on measurements that were made on the recovery solution by ICP-MS. The function of the NiHCF counter electrode is different from that of Ag. In the case of Ag, at the same time as Li^+ is adsorbed to λ-MnO_2, Cl^- is adsorbed to Ag to form AgCl. On the other hand, in the NiHCF system, adsorption of co-ions occurs in the Li release step, when the system is subjected to a positive bias. As Li is released from $LiMn_2O_4$ to regenerate λ-MnO_2, secondary ions from the solutions are included in NiHCF to form (M-NiHCF) [56].

In an equimolar solution of 100 mM LiCl, NaCl, KCl, and $MgCl_2$, after

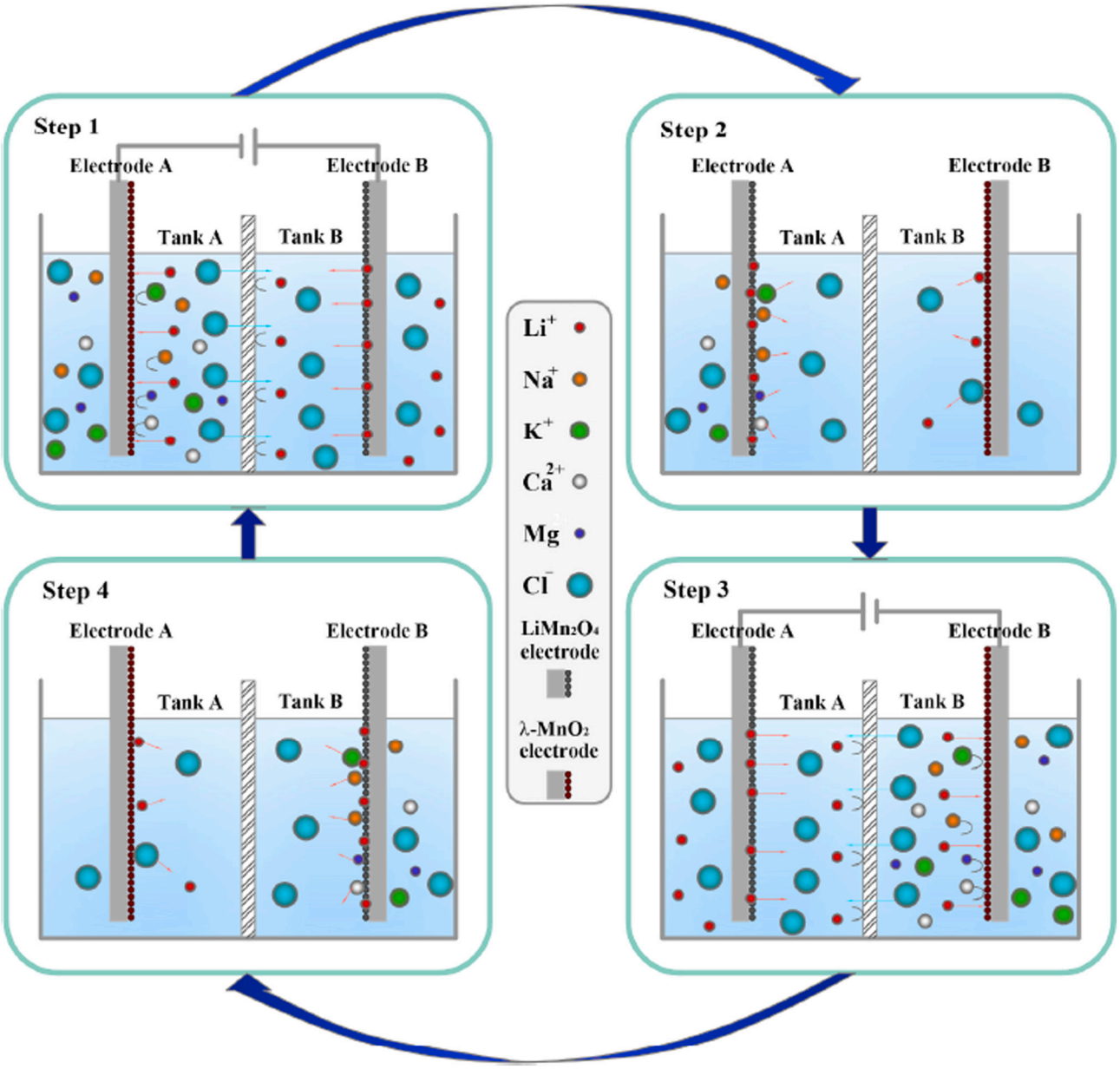

Fig. 11. Schematic of four steps operation in lithiated and delithiated working/counter electrode pair, solutions in tank A and B during step 1 are switched by step 3, and it is represented by relative amounts of ions in each compartment. For instance, tank A is the concentrate in step 1, while tank B is the concentrate in step 3 [89].

an extraction/release cycle, the selectivity coefficient of Li against Mg was 315, when the release step was performed on a 156.3 mM KCl of recovery solution. In the simulated Atacama brine, which has a low Li concentration (42 mM) but has concentrations of K^+ and Mg^{2+} near 100 mM, the selectivity (Li^+/Mg^{2+}) was high at 1700 with an energy consumption of 3.6 $Wh{\cdot}mol^{-1}_{Li+}$. This confirms the possibility of this process being used with real salt lake brine solutions that have high Na^+, K^+ and Mg^{2+}. Another distinct advantage of the NiHCF counter electrode is the ability to use seawater or other brine as a recovery solution, rather than a salt solution prepared in pure water. This is possible because NiHCF attracts cations of alkali metals from solution in order to maintain the charge neutrality in the recovery solution.

Rapid and non-destructive X-ray diffraction (XRD) analysis gives insight into the underlying Li insertion process. The change in lattice constant evaluates Li capture and subsequent changes in the λ-MnO_2 crystal structure during various time intervals along with the capture and the release step. Spinel type $LiMn_2O_4$ belongs to the *Fd3m* space group with a lattice constant of 8.23 Å, while that of completely delithiated λ-MnO_2 is 8.03 Å. During Li capture, Li may intercalate into all of the λ-MnO_2 vacant sites, in which case the XRD pattern of the working electrode after capture is identical to spinel $LiMn_2O_4$ lattice frame [88]. In the second possibility, λ-MnO_2 and $LiMnO_4$ phases coexist after the discharge step [82]. However, the lattice constant corresponding to the $LiMn_2O_4$ phase in the binary mixture was slightly lower at 8.19 Å, but no significant difference in the lattice constant of MnO_2 in pristine and coexisting phases was observed. This is due to Li's partial insertion into the spinel λ-MnO_2 lattice caused by the insufficient mass transfer of Li. In most of the studies employing λ-MnO_2 cathode, regardless of the phase after lithiation, XRD analysis showed that the pristine λ-MnO_2 phase recovered faster during the regeneration step than during the capture step.

2.2.1.5. λ-MnO_2/$LiMn_2O_4$. Another possibility for the Li recovery process is to have working and counter electrodes of the same type. Both electrodes could have an Mn-based framework, with the working

electrode having a lower content of Li (MnO_2) compared to the counter electrode ($LiMn_2O_4$). In such a system, two electrodes are immersed in two different tanks separated by an AEM, and adsorption and desorption take place simultaneously on working and counter electrode, respectively [89]. Unlike the usual four-steps adsorption-desorption approach, the four steps in these systems are defined for one electrode because the working electrode becomes the counter electrode later in the cycle (Fig. 11). The first step of the cycle starts with the adsorption of Li at the working electrode, during which the working electrode compartment is filled with Li^+ source solution and the counter compartment with a recovery solution (30 mM LiCl). The second step includes flushing the solution from both tanks until the outlet stream's conductivity is lower than 10 $\mu S \cdot cm^{-1}$, followed by refilling with the solutions opposite to that in step 1. Then, in the third step, the direction of the current is reversed to that of the first step. The initial Li concentration in the source solution has a positive effect on the resulting adsorption capacity. For example, increasing the Li^+ concentration from 5 to 100 mM enhanced the Li^+ adsorption capacity from 1 $mmol \cdot g^{-1}$ to 4.5 $mmol \cdot g^{-1}$ after 120 min of cycle runtime. Also, the impact of the applied voltage on the adsorption capacity was not as prominent as the Li^+ concentration effect. When the applied voltage varied from 0.25 V to 1.5 V with an increment of 0.25 V, the adsorption capacity was approximately 3.7 $mmol \cdot g^{-1}$ for all applied voltages in the range 0.5 V to 1.5 V. In the case of an applied voltage of 0.25 V, the adsorption capacity was as low as 2.8 $mmol \cdot g^{-1}$, and this drop was related to an applied voltage being lower than the voltage required for the system to reach equilibrium [89]. Manganese loss was found to be minimal (0.01%) during all operating conditions of the system. Although the Mn loss was not significant, the adsorption capacity was 57.1% of the original after 30 cycles.

2.2.1.6. LMO/BDD. Battery recycling wastewater is a rich source of many compounds. If properly designed, the anodic reaction at the counter electrode of an ESIX system could be manipulated to remove organic pollutants. At the same time, Li^+ is captured at the LMO working electrode along with the rapid removal of organic pollutants [88]. Boron doped diamond (BDD) is an oxidant generating electrode, thus reactive oxygen species formed degrade the pollutants partially by fractionation or completely by mineralization. In the case of the LMO/BDD system, 98.6% pure Li^+ was recovered from the process, and 65% of the total organics in the system were decomposed, when the system operation was studied using a battery cycler. The Li recovery rate was proportional to the applied current density, however, the applied current density had a negative impact on the LMO's adsorption capacity. Therefore, it is important to select an appropriate current density depending on the amount of Li^+ expected to be captured over a given period of time. The findings of this study are important because wastewater from battery recycling plants could potentially be a large source of Li^+ to meet the high demand for this element in the future.

2.2.1.7. LMO/Ppy. Polypyrrole (Ppy) was also studied as a replacement for the Ag electrode in a system with a Li deficient LMO acting as the working electrode [90]. The Li_xMnO_2 fabricated by pulse layer deposited thin film was evaluated to have 1:2 Mn/O and 1:1 Mn(IV)/Mn(III). Detailed analysis of the bulk chemistry of the LMO material showed that Li insertion in the MnO_2 happens by a topotactic Li insertion mechanism, whereas Li^+ is removed from $LiMn_2O_4$ by maintaining the cubic symmetry in isotopical expansion. Additionally, Mn(III) depletion and recovery take place at 1.1 V and 0.4 V, respectively. At low intercalation rates, Na^+ was found to interfere with Li^+, but XRD showed no evidence that Na^+ is intercalated in the MnO_2 structure.

2.2.1.8. LMO/Ppy/Al_2O_3. Most recently, a Ppy/Al_2O_3 hybrid was immobilized on a LMO electrode to produce a working electrode with a versatile 3D nanostructure that was used in combination with an activated carbon counter electrode [7] in a LMO-based ESIX system. The system had promising stability in a complex simulated brine solution (23.5 mM Li^+, 120.8 mM Mg^{2+}, 256.4 mM Na^+, 47.8 mM K^+ and 0.57 mM Ca^{2+}). It showed an activity retention of 91.7% after 30 cycles of continuous operation with 97.4% pure Li^+ at a constant current of 0.75 mA. SEC was as low as 1.41 $Wh \cdot mol^{-1} \cdot L^{-1}$ with an adsorption capacity of 1.85 $mmol \cdot g^{-1}$. The importance of Ppy/Al_2O_3 on LMO was assessed to have a higher diffusion coefficient of Li^+ compared to other systems, which affirms the enhanced Li^+ capture/release kinetics with Ppy/Al_2O_3 on the LMO surface.

2.2.1.9. LiFePO$_4$/Ag. Mantia and coworkers employed iron(III) phosphate in a 4-step Li intercalation deintercalation cell [55]. When the system resembled the actual extraction process taking place at Salar de Atacama, observations suggest that the ESIX process operating at a current density of 0.5 $mA \cdot cm^{-2}$ could yield within eight days the same amount of Li extracted over a year at Salar de Atacama. With a low energy consumption of 2.8 $Wh \cdot mol^{-1}$, the selectivity of Li^+ with respect to Na^+ and K^+ was very high at 29,000 and 36,000 respectively, but moderately high for Mg^{2+} (9000). Increasing the current density from 0.05 to 0.5 $mA \cdot cm^{-2}$ increased Li adsorption from 74 to 99 mM, but further increasing to 5 $mA \cdot cm^{-2}$ reduced it to 52 mM. The corresponding Li recovery efficiencies were 69.4, 92.9, and 48.8% as the current density increased. This shows that at a high current density, such as 5 $mA \cdot cm^{-2}$, mass transport is hindered, resulting in lower Li recovery. Concentrations of secondary ions generally increased as the current density increased, except for potassium. Thus, a current density as high as 5 $mA \cdot cm^{-2}$ is not appropriate for Li recovery in some solutions. The purity (99.98%) and adsorption (74 mM) is excellent at 0.05 $mA \cdot cm^{-2}$, while Li recovery efficiency (97.86%) adsorption (99 mM) is high at 0.5 $mA \cdot cm^{-2}$. These values are important in industrial processes to decide on which system parameters are economical for an expected production outcome.

2.2.1.10. FePO$_4$/NiHCF. Iron (III) phosphate ($FePO_4$) in olivine structure and NiHCF(II) both have iron in the matrix, but with iron in different oxidation states. Iron phosphate serves as the Li-capturing electrode and NiHCF is the Li exclusion counter electrode. The pair showed similar energy consumption to systems with Ag as the chloride capturing counter electrode [64,73]. During Li capture, Fe (III) is reduced to Fe(II) as Li enters the matrix of iron phosphate, and Fe(II) is oxidized to Fe(III) in NiHCF as a cation is released into solution. During the Li release step, the cation returns to the NiHCF matrix. In this study, Atacama brine, seawater, and 90 mM KCl solutions were studied as recovery solutions to evaluate the selectivity and Li release characteristics in the LFP/NiHCF system. Results showed that the use of Atacama brine dramatically increased the Li content in the recovery solution from an initial 4.3% to 106%. At the same time, concentrations of Na^+ and K^+ were reduced in the brine solution by 18% and 56%, respectively, due to their inclusion in the NiHCF matrix. Similarly, when seawater was used as a recovery solution, concentrations of Na^+ and K^+ were reduced by 31% and 62%, respectively, while Li content increased by 20.4%. These observations shed light on the importance of research on counter electrode materials that can operate well using natural salt resources as recovery solutions if the technology is to be viable on an industrial scale. Observed SEC with different recovery solutions was in the order of Atacama < seawater < 90 mM KCl, showing that Li content has a positive influence on the specific energy consumption. The initial Li concentration was high in Atacama brine, which yields a lower specific energy consumption of 8.7 $Whmol^{-1}$. On the other hand, seawater with the lowest Li concentration had the highest SEC at 12 $Whmol^{-1}$. Li purity in systems where real brines are used is well below 99%, but this is to be expected because the source solution contains many other cations and anions at different proportions. Therefore, assessing the percentage increment or decrement of a specific ion of interest in the recovery solution is a fair approach to evaluating the process validity.

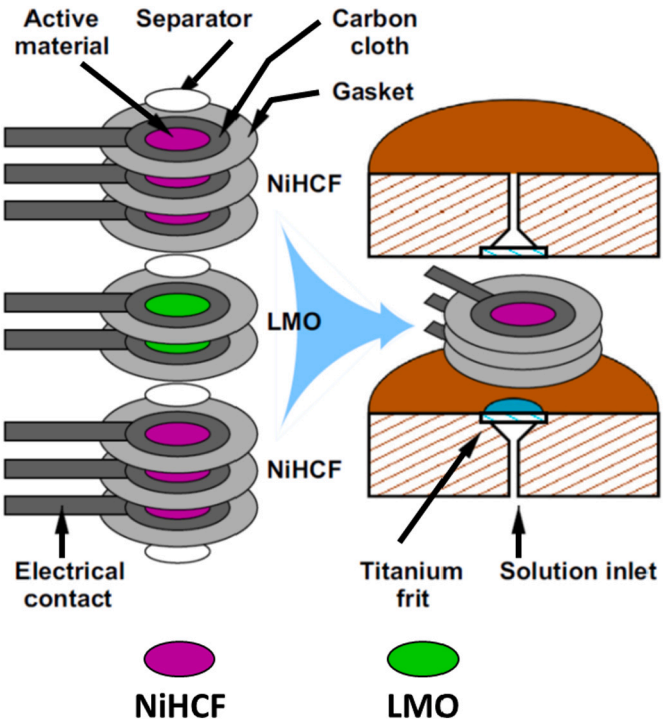

Fig. 12. Representation of electrode stacks (left) and plates (right) in a flow-through ion pumping system [92].

The specific energy consumption, purity, and Li content of the recovery solution of the LFP/NiHCF system are comparable to MnO_2/Ag or MnO_2/NiHCF systems. The theoretical specific charges calculated by Mantia et al. were found to be 148 and 170 mAh·g^{-1} for LMO and LFP, respectively, which were about 20 units higher than the actual values [56]. When it comes to ESIX systems, studies mainly focus on developing new working and counter electrodes. Additionally, studies also focus on different scan rates and current densities to deduce the mechanism involved and gain insight into the kinetics. MnO_2 is sometimes found to have high energy consumption with insufficient purity after one recovery cycle [54,81].

2.2.1.11. Flow-through ESIX. ESIX systems have rarely been studied in flow-through operations. In industrial operation, continuous flow-through processes are more reliable than batch processes. An important aspect of the flow-through process is that when changing the solution from the source solution to the recovery solution, no contaminants from the source solution should be carried over to the recovery solution. On the research scale, flushing is usually done with pure water until the outlet stream has a minimum conductivity of 10 μS·cm^{-1} or less. It is questionable how practical this is in an industrial process, as the use of large quantities of the scarce resource of fresh water must be avoided to ensure sustainability.

Palagnia et al. studied a flow-through ESIX system, which incorporates a LMO electrode sandwiched between two NiHCF electrodes [91]. The cell boundary was defined by two circulating plates that pressed the electrode stack as shown in Fig. 12, which was an improvement to previously reported designs [92,93]. The system was initially tested with a source solution containing only LiCl (1 mM) and NaCl (1 M). The inlet stream was maintained at a flow rate of 15 mL/min, and the recovery solution of 120 mM KCl was pumped at a rate of 5 mL/min. Adsorption was carried out at 0.5 mA constant current, while desorption was at 1 mA. Between the cycles, the system was flushed with 50 mL of 120 mM KCl, which is the same composition as the recovery solution. The reactor design was optimized to reduce the dead volume, which was found to be 0.82 mL, much less than the recovery solution's volume. The system yielded 5 mL of 100 mM LiCl with 94% purity after 9 consecutive operation cycles, showing a greener prospect for industrial utilization. Nevertheless, the system was estimated to concentrate 800 mM LiCl after 200 cycles, given that the electrodes exert good stability over time.

ESIX technology for Li recovery, in brief, has employed simulated brine, natural brine or multi-ion solution as source solution instead of solutions made from only the lithium salt. SEC showed a variation in the range 1.4 kWh/kmol to 18.5 kW kWh/kmol. Low SEC for simulated brine source solutions with moderately high Mg/Li value of 18 is appreciable since this can be improved to industrial scale. With an AC counter electrode, SEC of 1.4 kWh/kmol was achieved with Mn-based working electrodes modified with either rGO [70] or Ppy/Al_2O_3 [7]. A very high SEC of 60 kWh/kmol was reported when a LMO/BDD-based system examined the capability of recovering Li along with organic pollutant degradation simultaneously [88]. This study focused on more proof of concept for the dual role, rather than the process improvement with regards to Li recovery. Furthermore, Li recovery was carried out in a phosphate buffer solution, a media suitable for pollutant degradation and Li recovery. On the other hand, traditional Li recovery solutions are KCl, LiCl or $CaCl_2$ solutions in the range of 10–100 mM, and the solutions ensure sufficient conductivity in the medium to enable the charge transfer. The time to complete the discharge/charge cycle varied between 25 min to 18 h. Compared to 1–2 years to complete a conventional solar evaporation process that also has a high level of uncertainty, 18 h is highly regarded. Energy consumption and recovery rate values were 7.9 kWh/kmol and 14.4 mg/g for the system with a short cycle time (25 min) [9] as opposed to the 3.07 kWh/kmol and 7.34 mg/g for the system with a long cycle time (18 h) [82]. The two afore regarded systems employed different working/counter electrode pairs and source solutions with different initial Li concentrations. Higher Li recovery of 14.4 mg/g with AC counter electrode in the short cycle system recommends the use of AC counter electrode in ESIX systems since the recovery is nearly half at 7.34 mg/g in the long cycle system which employed Ag counter electrode. With Salar de Atacama brine [73,94] (real or simulated), the specific energy consumption was in the range of 6–8 kWh/kmol, regardless of the working/counter electrode pair. Interestingly highest Li recovery rate was observed with $Li_{(1-x)}Mn_2O_4$/$LiMn_2O_4$ system [76]. The majority of λ-MnO_2 working electrodes exhibit adsorption capacity around 10 mg/g, while it is slightly higher around 30 mg/g for LMO working electrode systems [76,84,90,95].

In ESIX, within a single cycle of Li capture/release, several repetitive recovery steps are performed to increase the amount of Li recovered. Energy consumption is generally calculated with reference only to the first cycle, resulting in lower calculated energy consumption than actually occurs over all cycles. Also, the recovery solution volume is usually maintained at low values in order to increase the concentration of recovered Li. If extraction to the μL volume requires several cycles (about 5 concentrating cycles), then the large volumes that are expected at an industrial scale will require ≥1000 cycles of concentrating during the Li release half cycles. The pumping energy related to the multiple steps within a cycle, together with the time-inclusive release process, must endure a considerable amount of energy that needs a full understanding before being implemented on a large scale.

Source and recovery solutions in ESIX systems are kept either in two separate tanks or in the same tank, which requires that it be flushed between the two solutions. Flushing is done with pure water or the recovery solution, but since the recovery solution is made with pure water, a scarce resource is being consumed. In this regard, very few studies with NiHCF counter electrode have utilized brine as a recovery solution, which is unfortunate in light of the need for sustainability.

2.2.2. Capacitive deionization (CDI)

Besides ED and ESIX, capacitive deionization (CDI) is another promising electrochemical process that is considered to be simple in configuration and environmentally benign, and that can be utilized as a

Table 1
Summary of previous research on CDI processes for Li recovery.

Research focus	Source of Li	Source solution		Applied voltage [V]	Recovery ratio (RR_{Li}) [mg/g]	Stability [cycles] [duration]	Efficiency	Specific energy consumption (SEC) [Wh/mol]	Ref.
		Concentration [ppm]	Flowrate [mL/min]						
Process enhancement	LiCl + $MgCl_2$	152.6 $_{LiCl}$	10–30	0.6–1.4	–	2–30 min	–	1.8	[99]
Membrane development	LiCl	848 $_{LiCl}$	67	1.23	30	3 cycles 1 h	96% desorption eff.	–	[101]
Electrode development	Lithium based binary solution	1457 $_{Li}$	20	1.0	2.415	5 Cycles 40 min	–	160.77	[103]
Electrode development	LiOH	60 $_{LiOH}$	40	3.5	8.7	3 days	45% desorption eff.	–	[104]
Electrode development	LiOH	50 $_{LiOH}$	20	0.1–2.0	1.36	5 Cycles 2 h	–	–	[105]
Electrode development	LiCl	424 $_{LiCl}$	67	1.23	98	30 min	76% faradaic eff.	–	[107]
Process evaluation	Geothermal brine	16 $_{Li}$	67	2	800	3 cycles 1 h	73% faradic eff.	1.26	[108,109]
Process development (flow process)	LiCl	100 $_{LiCl}$	3–9	1.2	215.06 $\mu mol \cdot m^{-2} \cdot s^{-1}$	2 h	91.7% salt removal eff.	–	[111]

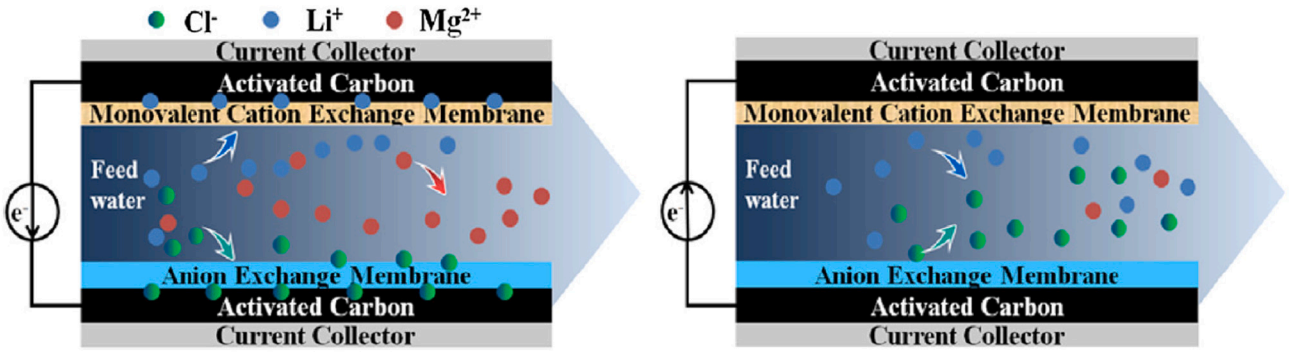

Fig. 13. Adsorption and desorption processes of membrane capacitive deionization (MCDI) system [99].

potential Li recovery method [15]. CDI has long been extensively investigated and gained a huge interest as an advanced water treatment technology that can be employed in various applications ranging from desalination of brackish water and seawater to water softening and removal of weak acids [96]. The basic operation of CDI is based on creating an electrostatic field between two porous electrode materials characterized by a high specific surface area. Applying the voltage forces cations and anions to migrate toward the oppositely charged electrodes and the ions enter the electrical double layer created between the electrode surface and the bulk solution. Then, when a reverse charge is applied, the ions are released to the solution, thus regenerating the electrodes for the next cycle [71,97]. With the growing exploration and advancements of CDI cell architectures and designs [98], CDI is widely investigated as a tool for the selective removal of specific ions from a multicomponent electrolyte. In this context, new and limited references have discussed and explored the application of the CDI process for the selective capture of Li. These studies are summarized in Table 1 and briefly reviewed below.

To enhance the selective capture of certain ions and the deionization efficiency of the process, membrane capacitive deionization (MCDI) was introduced. Here, conventional CDI processes were adapted by adding anion and cation exchange membranes (AEM and CEM) between the two electrodes. To promote specific recovery of Li^+, the MCDI process was further modified by using a monovalent cation exchange membrane that is selective for Li ions. This process is called monovalent selective membrane CDI (MSMCDI). Shi et al. [99] demonstrated the use of this MSMCDI approach for the selective capture of Li ions from a mixed solution containing lithium and magnesium ions. Here, the MSMCDI process combined two activated carbon (AC) capacitive electrodes, which are usually employed in conventional CDI processes. The process differed from conventional CDI by the addition of a monovalent selective cation exchange membrane (MSCEM) between the solution and the cathode and a conventional AEM between the solution and the anode. The MSCEM allowed for the selective capture of monovalent Li^+ over Mg^{2+}. This system was applied to a LiCl/$MgCl_2$ simulated brine feed mixture containing 5.0 mg/L of Li^+. Fig. 13 shows a schematic diagram of this MSMCDI process. When voltage is applied to the MSMCDI cell, Li^+ migrates through the MSCEM to accumulate in the double layer near the cathode surface, while Mg^{2+} is blocked by the membrane and retained in the feed. This process demonstrated a superior Li selectivity of 2.95 when operating conditions such as cell voltage, feed concentration, and operating time were optimized to 1.0 V, 30 mL/min, and 10 min, respectively. Fig. 14(a) compares the corresponding selectivity coefficients and removal rates of Li^+ and Mg^{2+} using conventional CDI, MCDI, and MSMCDI. It was evident from these results that the MSMCDI demonstrated the highest selectivity and removal percentage for Li^+ ions, reaching a removal rate of 38%. Additionally, the process demonstrated a lower specific energy consumption of around 0.0018 kWh/mol, which is much lower than that of a conventional ED process (0.04–0.27 kWh/mol). Therefore, this increases the feasibility of using MSMCDI for Li recovery.

The application of Li recovery using CDI and MCDI processes is

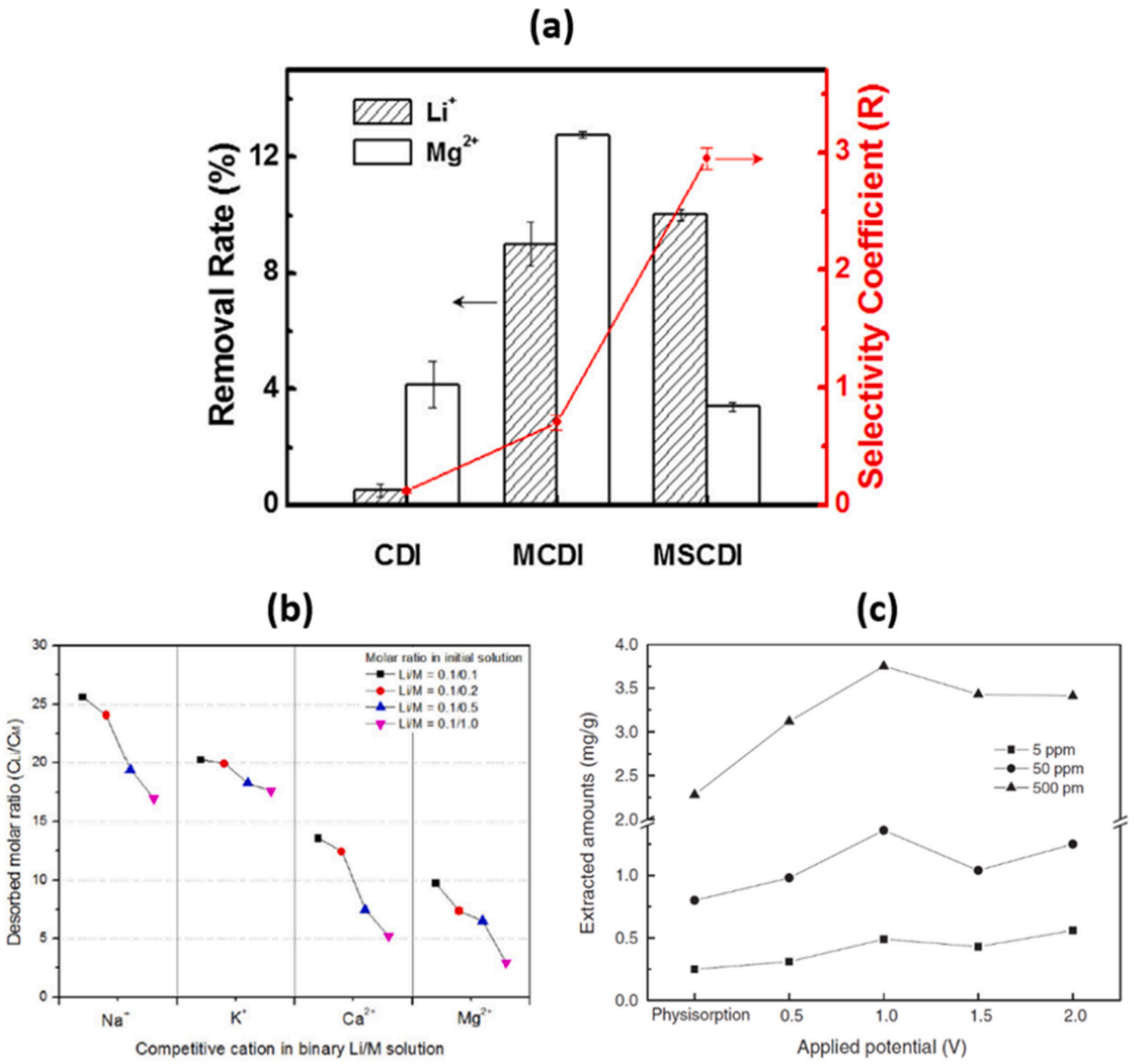

Fig. 14. (a) Selectivity coefficients and removal rates of Li^+ and Mg^{2+} using CDI, MCDI, and MSMCDI [99,103,104]. (b) Li-ion selectivity with respect to competitive cations with various feed concentrations of Li^+/M (M = Na^+, K^+, Ca^{2+}, and Mg^{2+}) [99,103,104]. (c) Amounts of extracted Li obtained with various initial Li^+ concentrations, with and without an applied cell potential in the adsorption process [99,103,104].

considered new and somewhat limited. Thus, hybrid capacitive deionization (HCDI) is gaining much interest as an emerging electro-membrane assisted process for the selective capture of ions such as Li from mixed ion solutions [100,101]. HCDI is a modified CDI process designed specifically for the targeted recovery of ions of interest. This aim is typically achieved by replacing one of the capacitive electrodes with a faradaic intercalating electrode that can selectively capture and retain an ion of interest during the adsorption process and successfully release it during the desorption process. Furthermore, the counter capacitive electrode is usually wrapped with an AEM to prevent the capture of targeted ions by these electrodes during the desorption process and to reduce the effects of co-ions, thereby controlling the ion recovery efficiency [102]. A λ-LMO/AC HCDI cell was examined for the selective recovery of lithium from an aqueous solution containing (Li^+, Na^+, K^+, Ca^{2+}, and Mg^{2+}) [103]. This process had a specific recovery of 0.35 μmol Li/g-adsorbent, which was 7 times higher than the amount recovered by a physical adsorption process under the same experimental conditions. This study has shed light on the effects of competitive ions and the concentration of Li^+ on the selective recovery of Li^+ ions. The selectivity order obtained was $Li^+ > > Mg^{2+} > Ca^{2+} > K^+ > Na^+$, which indicated the primary influence of ionic radii and the extent of charge of these cations on Li-ion selectivity (Fig. 14(b)). It was observed that the higher the concentrations of coexisting cations in a solution, the lower the recovery of Li^+. Also, considerable Li-ion selectivity was observed when the solution contained sodium as a competitive cation, and this behavior was attributed to the narrow void space of the intercalation electrode that may not allow the intercalation of sodium ions. On the other hand, a reduction in Li^+ selectivity was noted when the feed solution contained divalent cations. When an electrical potential is applied to the electrode surface, divalent ions exhibit a stronger electrical force,

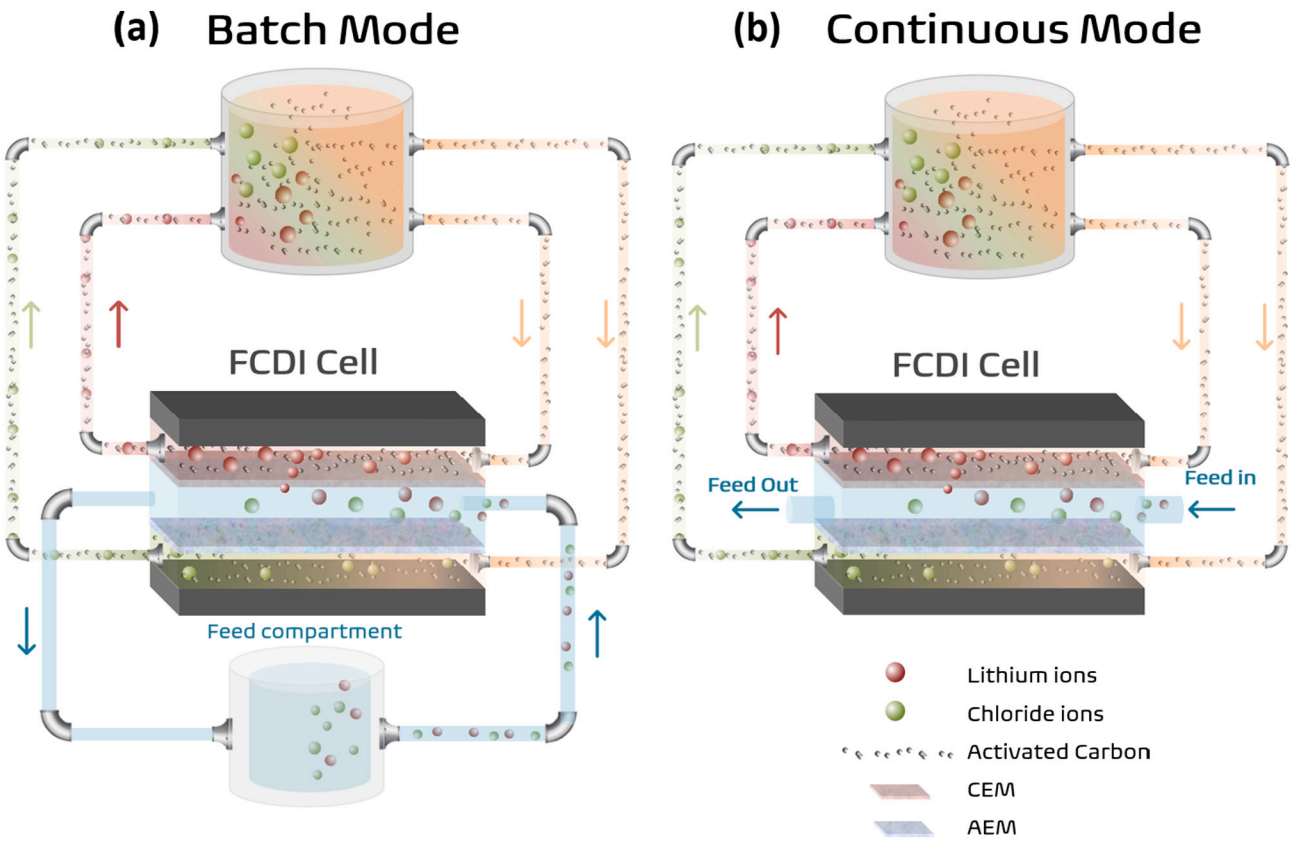

Fig. 15. Schematic of FCDI with (a) batch and (b) continuous mode of operation for Li^+ removal (modified from [111]).

move faster, and form a thicker diffusion layer on the electrode surface than monovalent ions, thereby hindering the migration of Li^+. Nevertheless, one of the shortcomings of this study was the high specific energy consumption of the process, which was 23.3 Wh/g of Li.

Early studies done by Ryu et al. focused on electrode enhancement for a better HCDI process. They were the first to suggest using electrostatic field assistance (EFA) to improve the desorption and absorption of Li ions in the LMO/AC HCDI process [104]. They tested the desorption of Li by coating the current controller with a Li selective adsorbent rather than the carbon/CEM layer. They observed a lower desorption efficiency of 45%, compared to the conventional desorption process that uses an acidic solution. In their later study [105], they focused on studying the effects of varying initial Li concentration and applied potential on Li adsorption in the adsorption step. Fig. 14(c) illustrates the main results of this study that show that Li adsorption increased with increasing feed concentration and applied voltage up to 1.0 V. This effect was due to these parameters increasing the diffusivity of Li when they are higher. It is important to note that in general, the CDI or HCDI process needs to apply voltages less than 1.0 V to avoid water splitting and the occurrence of other undesirable electrode reactions [106].

Due to its simple and straightforward setup, the HCDI process offers an easy and fast approach to evaluating fabricated membranes for such applications as lithium recovery. For instance, an HCDI setup was used to study the effectiveness of a novel polyvinylidene fluoride (PVDF-EDA) based AEM that was thought to efficiently block the co-ion effect and improve the desorption step in the HCDI process [101]. In this study, the effectiveness of a series of fabricated membranes was evaluated based on effective Li adsorption and desorption efficiencies, and the membrane with the best overall performance in the HCDI process was selected. The chosen membrane was characterized by a high salt adsorption capacity (SAC) that reached over 30 mg/g with a desorption efficiency of 96%. The HCDI process also demonstrated its stability over more than 20 repetitions of the process by showing current efficiencies reaching above 0.9 with a current density of 10 A/m^2. In another work, Siekierka [106,107] used a novel spinel-type material based on lithium-manganese and iron compounds as a Li adsorptive material in an HCDI process for Li recovery from a multicomponent solution. The material was used to build a negatively polarized electrode that provided an adsorption capacity of 32 mg/g-salt, 16 mg/g-salt, and 0 mg/g-salt for LiCl, NaCl, and KCl, respectively. One of the main aims of this study, which is of great interest here, was the determination of the working electric mode that optimized Li capture. The study analyzed an array of various electrical sequences, including constant current (CC), constant voltage (CV), zero current (ZC), zero voltage (ZV), reversed constant current (RCC), zero charge voltage (ZVC), and reversed constant voltage (RCV). The results show that the successful application of CC-ZC-RCC mode allowed the system to extract Li ions from the multicomponent solution with the highest observed efficiency of more than 76.

For ELiCSs, an important aspect to consider is their performance when using real brine solutions, because using real brines provides information on the influence of existing impurities on process performance. One of the few research papers that utilized real brine solutions to test and evaluate the performance of HCDI was by Siekierka et al. [108]. In this work, geothermal brine was used to evaluate the performance of a HCDI system consisting of a lithium-titanium-manganese-oxide (LMTO) and an AC electrode coated with a poly(vinyl chloride)/ethylene diamine AEM. Two sets of process parameters were compared and evaluated. The first sequence started with adsorption of Li at constant voltage (CV), followed by its desorption at reversed constant voltage (RCV) and final desorption with zero voltage (ZVC), hence resulting in a CV-RCV-ZVC mode. The other mode reversed the sequence of the desorption processes, giving a CV-ZVC-RCV mode. This study shows that by applying 2 V of external voltage in both modes during the CV and RCV operations, the CV-RCV-ZVC system exhibited slightly less energy-intensive behavior and consumed about 0.059 kW/m^3 of energy.

Table 2
Summary of previous research on ED-based technology for the recovery of Li at optimum conditions.

Source of Li	Method	Operating parameters					Results					Ref.
		Li^+ concentration (M)	Ratio (M/Li^+)	Acid and base concentration (M)	Flowrate (LPM)	Applied voltage (V)	Recovery percentage (R_{Li} %)	Separation coefficient ($F_{M\text{-}Li}$)	Separation efficiency (S_{Li}) %	Current efficiency (η %)	Specific energy consumption (kWh/m^3)	
Li_2SO_4 (aq)	SED	0.3	n.m.	n.a.	25.2	6	75.8	n.m.	n.m.	n.m.	40.5	[148]
Na- LiBr (aq)		2	n.m.	n.a.	n.m.	7	20	n.m.	45	180	n.m.	[119]
		2	n.m.	n.a.	n.m.	5	n.m.	n.m.	32.2	n.m.	n.m.	[125]
$LiCl.H_2O$ and		1	150[b]	n.a.	1000	6	70	27.5	n.m.	n.m.	n.m.	[124]
$MgCl_{2\cdot6}H_2O$		0.7	18.9[b]	n.a.	1000	20	90.5	10.4	n.m.	8.68	0.01	[124]
Salt lake		0.8	21.4[b]	n.a.	1000	20	n.m.	9.9	n.m.	n.m.	22.3	[124]
Brine solution[a]		1	60[b]	n.a.	n.m.	5	72.5	12.5	7	n.m.	0.2[e]	[121]
Brine solution[a]		0.02	3[c]	n.a.	n.m.	5	77.5	65	n.m.	51.5	0.05	[122]
		0.02	1[d]	n.a.	n.m.	5	76	7.8	n.m.	41.5	0.03[e]	
		0.02	20[b]	n.a.	n.m.	6	67.7	6.4	n.m.	n.m.	0.2	[123]
Concentrated seawater		0.02	16[b]	n.a.	n.m.	7	n.m.	n.m.	n.m.	≈1.2	≈2.3[e]	[19]
Salt lake brine		5	36[b]	n.a.	n.m.	10	76.5	n.m.	n.m.	≈4.7	0.7[e]	[19]
$Li_2B_4O_7{\cdot}5H_2O$	BMED	0.05	n.m.	n.m.	n.m.	30	97.8	n.m.	n.m.	20	18.7	[134]
		0.04	n.m.	0.003	n.m.	15	83.7	n.m.	99.9	n.m.	n.m.	[132]
		0.05	n.m.	0.05	n.m.	30	62	n.m.	94.7	n.m.	7.9	[135]
		0.04	n.m.	0.003	50	25	73	n.m.	n.m.	n.m.	3.2	[136]
Seawater	ILM-ED	4.9E−5	n.m.	n.a.	n.m.	2	22.2	n.m.	n.m.	n.m.	n.m.	[144]
			n.m.	n.a.	n.m.	2–3	n.m.	n.m.	63	n.m.	n.m.	[145]
Simulated brine		0.14	50[b]	n.a.	n.m.	2	n.m.	n.m.	n.m.	65	0.11[e]	[18]
Salt lack			100[b]	n.a.	n.m.	3	n.m.	n.m.	n.m.	n.m.	0.13[e]	[146]

Not applicable (n.a.) and not measured (n.m.).
[a] Simulated solution.
[b] Mass ratio (Mg/Li).
[c] Mole ratio (Mg/Li).
[d] Mole ratio (Na/Li).
[e] Specific energy consumption (kWh/mol of Li).

However, the CV-ZVC-RCV mode was chosen as the preferable mode for this application, because it provided an extremely high SAC value of 800 mg/g of salt. This was due to the RVC mode allowing the formation of a thin and highly packed layer of ions on the surface of the electrode, namely a solid electrolyte interface (SEI). This interface exhibits high ionic conductivity and facilitates the migration and penetration of monovalent ions such as Li. The work was further expanded [109] to investigate parameters that should be used to assess the performance and effectiveness of such HCDI processes. The first parameter discusses the salt adsorption capacity (SAC) of the process. This parameter is usually affected by (i) redox reactions between competing ions and the intercalating electrode, (ii) the specific surface area of the adsorbent affecting the spontaneity of the adsorption process, and (iii) the formation of solid electrolyte interface multilayers. The second parameter is the reproducibility of the HCDI process, which must be relatively high if it is to become an effective process. The last important parameter is the energy consumption of each step of the HCDI process.

The flow-electrode-based capacitive deionization (FCDI) process has long been studied and developed in the field of water desalination. It has gained tremendous attention as a low energy consumption process that provides high and continuous salt removal. Unlike conventional CDI that uses a fixed solid electrode, FCDI provides the advantage of eliminating the need for a rinsing process by using suspended electrode material that provides continuous electrostatic adsorption and desorption of desired ions [110]. Continuous extraction of Li from an aqueous solution using flow-electrode capacitive deionization was investigated by Ha and co-workers [111]. In this study, activated carbon anode and cathode slurries were continuously introduced and circulated (25 mL/min) through flow channels against a feed solution of LiCl flowing at a rate of 3 mL/min. Fig. 15 shows a schematic diagram of the process in two circulation modes. The continuous feed mode achieved multiple salt removal efficiencies and the batch feed mode operated with higher desalination capacities. The study showed that Li could be effectively collected from the saline feed at numerous concentrations. Here, the salt removal varied with the change of feed concentration and flow rate, and the process showed the highest salt removal efficiency of 91.7% when the feed concentration was the highest value of 100 mg/L. Also, the process showed an improvement in the salt removal rate when the feed flow rate was decreased from 9 to 3 mL/min.

Although the studies on CDI for lithium recovery are clear, they lack consistency in terms of their research focus and what functional parameters were tested. This discrepancy is crucial and should be addressed to maintain a continuing adequate development in this field. Table 1 provides a summary of the operating parameters and main results from the previously discussed research. Most of the research papers discussed are intensely focused on the development of AEM/CEM and electrode materials, but the desirable focus on the important process parameters for effective Li recovery is somewhat lacking. This inadequate research focus can be reversed by concentrating on developing improved operating modes and system architectures, as well as testing various Li source solutions. The feed solutions that have been tested were mostly single-component solutions of Li salts. In light of exploring new processes for effective and efficient Li recovery, testing with multi-ion feed solutions and real brine solutions such as salt lake brine and geothermal brine is highly needed. The acquisition of data for operation with such real waters is strongly advisable, since real feed waters contain abundant organic matter and hardness ions that may hinder the performance of the CDI process and cause scaling and fouling issues on its electrode surface. Hence, this area needs much evaluation. As can be seen in Table 1, varied source solution concentrations and flow rates have been tested (16–1457 ppm, 10–67 mL/min). However, there is little work that evaluates the effects of flowrate and residence time in the presence of trace amounts of Li that is important data for the development of such applications. Most CDI systems run at constant potentials ranging between 0.6 V to 3.5 V, but they still have a high specific capacitance, which is reflected in the good desorption efficiency of the process. Although reported efficiencies were good (see Table 2), they lack consistency with each other. Some were evaluated by their faradaic efficiencies, while others relied on desorption or salt removal efficiency. Since Li recovery with HCDI is highly dependent on the intercalating electrodes used, recovery ratios are reported in terms of milligrams of lithium recovered per gram of electrode material used. The highest specific recovery ratio reported reached 800 $mg_{Li}/g_{\text{ of electrode}}$ when a 16 ppm of lithium in a geothermal brine solution was used as the feed source in the process.

CDI is an emerging technology that has been a strongly innovative process for removing charged ionic species from aqueous solutions. Up to this point, however, research on MCDI and HCDI for Li recovery applications is very limited. This underrepresentation may be attributed to the undesirable loss of Li ions during the continuously occurring charging and discharging cycles, which hinders the efficiency of the CDI process in comparison to the other ELiCSs. Additionally, it is noted that CDI employs costly equipment compared to ED and ESIX. Therefore, future work should focus on the effects of feed solution composition, a better alternative to the electrode pairs, optimization of current density, and the potential for a given system. This will make HCDI a strong competitor in the search for the dominant Li recovery process.

2.2.3. *Electrodialysis (ED)*

Electrodialysis (ED) is an electrochemical membrane-based separation process, which depends on the electric potential gradient for the separation of ionic species in aqueous solutions [78,112]. Under the influence of potential difference between two electrodes, an electric field is generated that induces the passage of ions through the ion exchange membranes (IEM). Consequently, concentration and dilution of specific ions relative to the feed solution occur in the concentrate and dilute streams, respectively [72,113]. A typical ED system contains a stack of repeating units called cell pairs that contain a cation exchange membrane (CEM) and an anion exchange membrane (AEM) that separate alternating concentrate and dilute compartments. The system also has electrode compartments at both ends [78]. Recently, ED has been widely used in various industrial fields for selective separation of ions and displays low energy consumption due to not requiring a phase transition. This environmentally friendly technology has been commonly used in industrial wastewater treatment and desalination of seawater and brackish water. Types of ED can be classified according to the characteristics of their IEM. Selective electrodialysis (SED) uses IEM that are selective for monovalent ions; bipolar membrane electrodialysis (BMED) uses bipolar IEM and ion liquid membrane (ILM) uses liquid ion membranes. ED-based technologies have been utilized in hydrometallurgical processes to recover Li from brines, spodumene concentrate, and spent LIBs recovery solution [72,78]. Nevertheless, only a limited number of research papers have examined the use of ED-based technologies for the recovery of Li, as summarized in Table 2.

2.2.3.1. Selective electrodialysis. Selective electrodialysis (SED) is a new electro-membrane process that employs monovalent selective IEMs instead of the conventional IEMs [114–116]. SED has been employed to extract Li^+ from brine solution (high Mg^{2+}/Li^+ ratio) and seawater, due to its excellent permselectivity of monovalent and high retention of multivalent ions and a lower requirement for pretreatment [117]. Thus, SED is considered a promising technology for Li^+ separation and recovery from aqueous Li resources. In general, the monovalent anion exchange membranes (MAEMs) and monovalent cation exchange membranes (MCEM) are placed in the SED stack in an alternating manner [116]. In ED, when a potential difference is applied between the cathode and anode electrodes, it induces the anions to move to the anode side and the cations to the cathode side. In SED, the monovalent anions (e.g., Cl^-) and monovalent cations (e.g., Li^+, Na^+, and K^+) are transferred only through MAEMs and MCEM, respectively [114–116]. Divalent anions (e.g., SO_4^{2-}) and cations (e.g., Mg^{2+} and Ca^{2+}) are

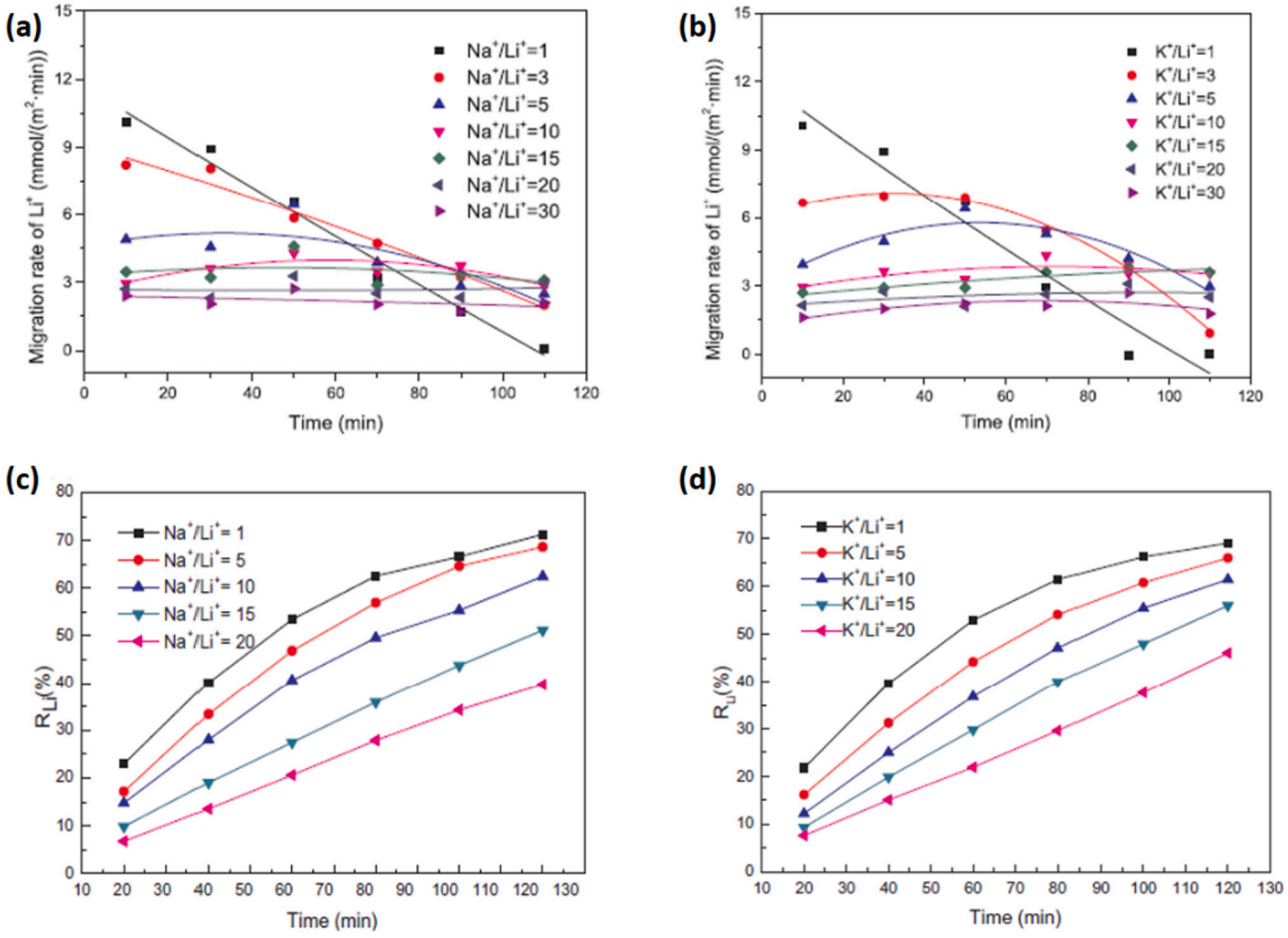

Fig. 16. The migration rate of Li (a) at a different mass ratio of Na^+/Li^+ and (b) at a different mass ratio of K^+/Li^+ [121]. The recovery percentage of Li (c) at a different mass ratio of Na^+/Li^+ and (d) at a different mass ratio of K^+/Li^+ [122].

rejected by MAEMs and MECM, respectively, as shown in Fig. 6(7) [118]. Consequently, the concentrations of monovalent ions increase in the concentrate chamber and decrease in the dilute chamber, while the concentrations of divalent ions remain constant in the dilute chamber [116,118]. Lastly, sodium carbonate (Na_2CO_3) is added to the flow of monovalent mixed ions, leaving the concentrate chamber and then heated to 80–90 °C in order to form a precipitate of lithium carbonate (Li_2CO_3) [64].

Parsa et al. [119] studied the application of SED for separating Li^+ and Na^+ from sodium-contaminated lithium bromide solution at different applied voltages and initial concentrations of Li^+. Increasing the applied voltage resulted in higher Li^+ recovery; however, it led to higher energy consumption. On the other hand, operating with a highly concentrated feed solution resulted in a negative impact on the recovery of Li^+ and increased the energy demand as well. The feasibility of applying SED for extracting Li from simulated brine with high Mg^{2+}/Li^+ has been investigated. Nie and co-workers [120] showed the technical capability of SED in this application and observed that the mass ratio of Mg^{2+}/Li^+ was significantly reduced from 150 to 8 and high recovery (95.3%) of Li^+ was achieved. The readiness of SED for the recovery of Li was tested through a preliminary study by using an artificial brine solution to evaluate and optimize the operating conditions that govern the performance of SED [121]. In this study, the effect of applied voltage, the mass ratio of Mg^{2+}/Li^+, pH, and linear velocity of feed solution were investigated. The results showed that at high-applied voltage, the separation coefficient, recovery of Li^+ and specific energy consumption were remarkably elevated. To minimize the energy requirement by SED, the optimum applied voltage was selected at 5 V. Moreover, the performance of SED was enhanced slightly when varying either pH or linear velocity at 5 V. Surprisingly, the separation coefficient rose to the maximum value of 51 at a mass ratio of 37 of Mg^{2+}/Li^+ and remained almost the same at mass ratios of 77 and 92, while the recovery of Li was improved at a high mass ratio of Mg^{2+}/Li^+. Correspondingly, the optimum Mg^{2+}/Li^+ mass ratio was selected to be 60. These results indicated that the mass ratio of M (e.g., Mg^{2+}, Ca^{2+}, Na^+ and K^+)/Li^+ in feed solution is a critical operating parameter, as it limits the Li^+ separation efficiency in the SED process.

A number of studies have intensively investigated how the characteristics of the feed solution affect the performance of SED in separating Li [122–124]. Nie [124] compared the selectivity of Li^+ by SED at a high mass ratio of Mg^{2+}/Li^+ and mass ratio of Na^+/Li^+. The results showed that higher selectivity of Li^+ was achieved when raising the mass ratio of Mg^{2+}/Li^+, while lower selectivity of Li^+ was exhibited at a higher mass ratio of Na^+/Li^+. This demonstrated a notable separation efficiency of monovalent ions toward divalent ions. Also, this finding proved that the competence in selectivity of Li^+ toward other monovalent cations. The effect of coexisting pairs of monovalent cations (Na^+, K^+) and divalent cations (Mg^{2+}, Ca^{2+}) on the migration rate and recovery percentage of Li were investigated by Chen and co-workers [122]. They found that the migration rate of Li sharply declined when the molar ratios of both Na^+/Li^+ and K^+/Li^+ were elevated from 1 to 3 and stabilized at higher ratios as shown in Fig. 16(a) and (b). At the same ranges of molar ratios, the percentages of Li recovered were gradually decreased as seen in Fig. 16 (c) and (d). The migration rate and recovery percentage of Li were improved when the mass ratio of both Mg^{2+}/Li^+ and Ca^{2+}/Li^+ rose from 1 to 3, which is consistent with previous studies [121]; however, they

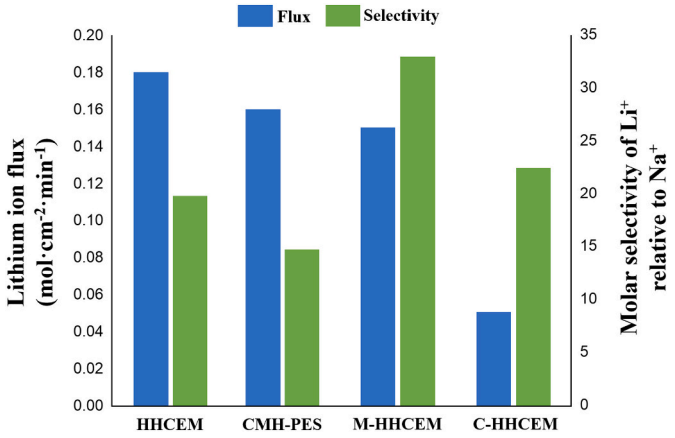

Fig. 17. A comparison of migration rate and molar selectivity of Li through four different cation exchange membrane (CEM); Home–made heterogeneous (HH-CEM), modified home-made heterogeneous (M-HHCEM), composite home–made heterogeneous (C-HHCEM), and commercial heterogeneous cation exchange membrane (CMH-PES) [125].

gradually dropped at high molar ratios. From here, Chen and co-workers related the effects of other cations on the migration rate of Li to their differences in radii size. The radii sizes of the monovalent cations (e.g., K^+ and Na^+) are close to that of Li^+ than are those for divalent cations. To further verify the separation of Li and magnesium, the effect of coexisting ions (K^+, Na^+, and SO_4^{2-}) was studied [123,124]. The results showed that high molar concentration ratios of monovalent ions to Li^+ lead to poor ion fractioning. This result was also related to radii size, where the effect of coexisting monovalent cations on the separation of Li at a high ratio of Mg/Li is in the sequence of $K^+ > Na^+$. On the other hand, the ion fractioning of Li and Mg was improved significantly with the insertion of HCO_3^- and SO_4^{2-} since Mg^+ forms $MgHCO_3^+$and $MgSO_4$.

Guo and co-workers [19] investigated the implementation of SED separating lithium chloride (LiCl) from concentrated seawater and salt lake brine over a range of applied voltages. Compatible with previous studies [119,121], high Li recovery (80%) was achieved when concentrated seawater was used as feed. However, at the maximum applied voltage tested, the recovery ratio decreased due to ion leakage phenomena. As a result, the high concentration of Li in the feed chamber became weak because of the high concentrations of Mg^{2+} and Ca^{2+}. Moreover, the mass ratio of Mg^{2+}/Li^+ was reduced from 16.07 to 5.62. For salt lake brine, SED was operated at a higher range of applied voltages, since it had a higher ionic strength and higher mass ratio of Mg/Li than the concentrated seawater. Notably, a substantial Li recovery ratio of 76.45% was obtained, and its specific energy consumption was about an order of magnitude lower than that for concentrated seawater. Accordantly, salt lake brine was selected to be more suitable for ion fractioning of Li and Cl, owing to lower energy requirement. Overall, most SED studies indicate that the selectivity of MCEM toward Li^+ in the presence of other monovalent cations is insufficient and needs further improvement in order to extract a considerable amount of Li from primary liquid resources of Li.

To enhance the selectivity of MCEM toward Li, Bajestani and co-workers [125] demonstrated a novel experimental work by fabricating a three homemade CEMs for recovery of Li^+ from a LiBr solution contaminated with Na^+. A basic homemade CEM was prepared (HH-CEM). Another membrane was developed by first modifying the surface of HH-CEM by inserting a spinal type of Li selective adsorbent on the surface of the membrane (M-HHCEM). A third membrane was formed by placing the same adsorbent material within its matrix (C-HHCEM). The performance of all fabricated membranes was assessed and verified compared to a commercial CEM (CMH-PES). The results revealed that all homemade membranes performed better in terms of the migration rate of Li and molar selectivity of Li than the commercial one. This is attributed to the type of material used in membrane fabrication, where HH-CEM is made of less heterogeneous materials than CMH-PES. As a result, Na^+ passed through the membrane more easily, hence there was a lower molar selectivity of Li in the commercial membrane. In addition, Fig. 17 shows that the highest Li^+ flux was achieved by HH-CEM; however, it exhibited a lower molar selectivity compared to M-HHCEM and C-HHCEM. This was attributed to the presence of Li–sieve adsorbents on the surface or within the membranes that improved the

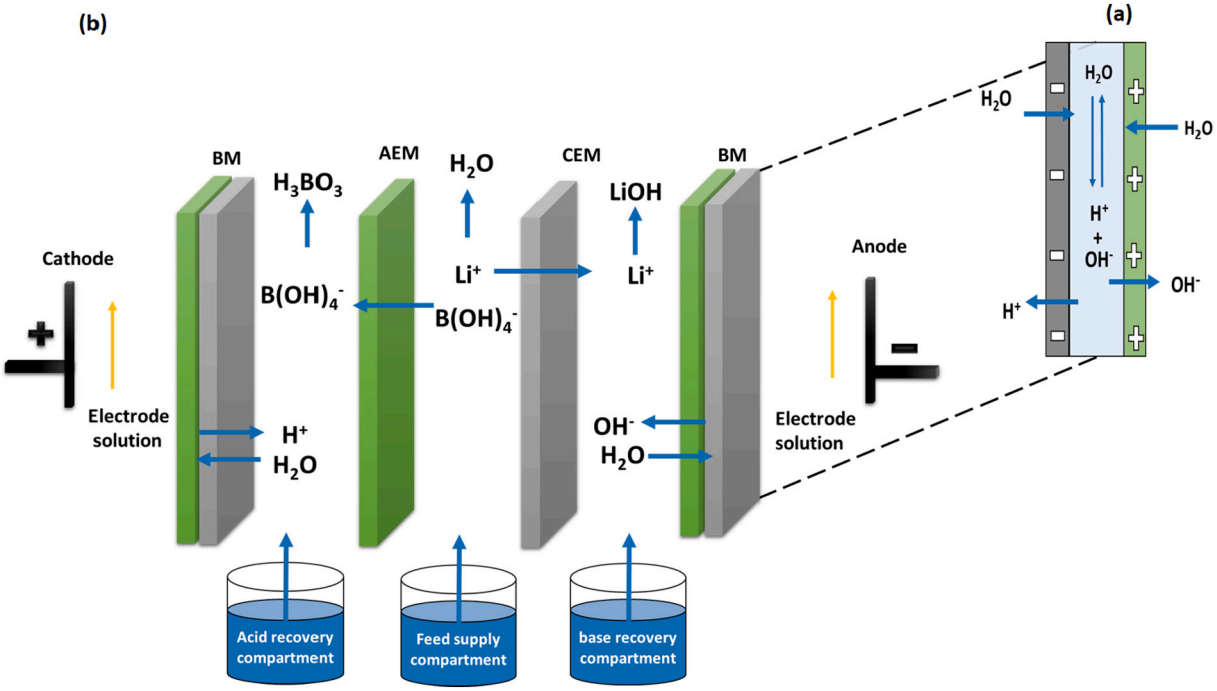

Fig. 18. (a) Structure of bipolar membrane, (b) schematic diagram of bipolar membrane electrodialysis (BMED) consisting of anion exchange membrane (AEM), cation exchange membrane (CEM), and bipolar membrane (BM) (modified from [126]).

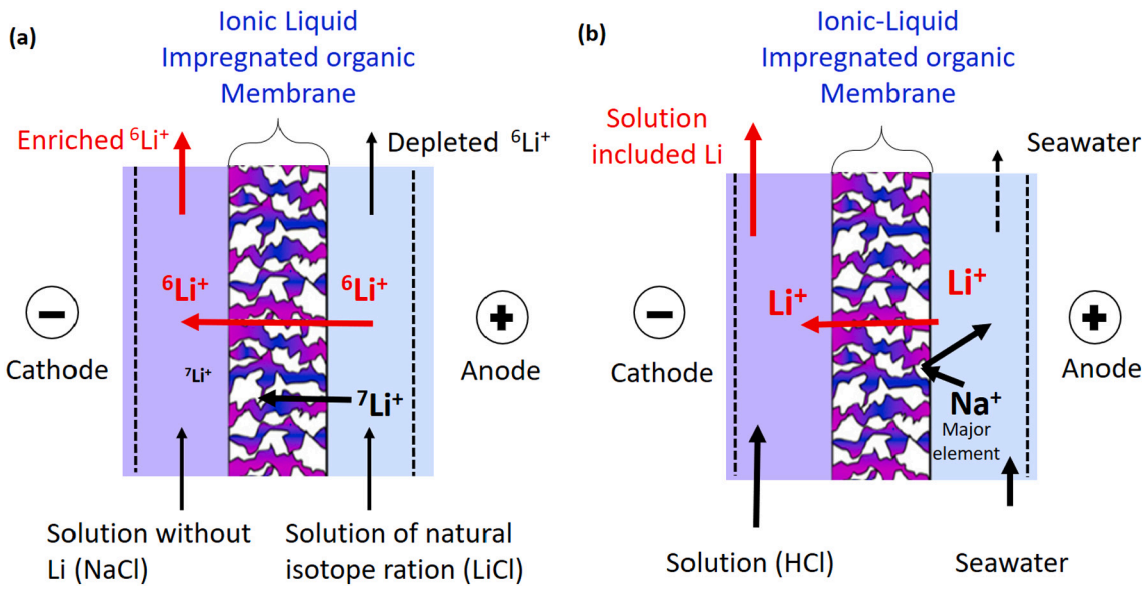

Fig. 19. Schematic diagram of an ionic liquid impregnated organic membrane combined with ED (IL-I-OM-ED). This system is composed of a cation exchange membrane, an anion exchange membrane, and an ionic liquid impregnated organic membrane embedded between them, which acts as a mobile medium for transported Li^+; (a) ^6Li enrichment from Li solution of natural isotope ratio [142] and (b) Li^+ recovery from seawater [144].

molar selectivity of Li^+. In addition, the highest molar selectivity was achieved when inserting the adsorbent material on the surface of membrane (M-HHCEM).

2.2.3.2. Bipolar membrane-based ED. The bipolar membrane electrodialysis (BMED) method is an integration of bipolar membrane (BM) with the IEM in the ED stack (Fig. 18). A BM is a type of IEM that consists of three layers: a cation-exchange layer, an anion-exchange layer and a hydrophilic interface layer, as shown in Fig. 18(a) [72,126,127]. When a direct current electric field is applied in a BMED, the water molecules present in the hydrophilic layer dissociate into hydrogen ions (H^+) and hydroxide ions (OH^-) [128]. The electric field also induces the negatively charged ions to be transferred toward anode through the AEM and the positively charged ions toward cathode through the CEM (Fig. 18 (b)). Simultaneously, the H^+ and OH^- from BM are combined with the anions and cations that pass through the AEM and CEM, respectively [128]. As a result, the acidic and basis solutions resulted from the BMED process are concentrated in acid and base recovery compartment, respectively. BMED is a promising technology with high efficiency that separates an aqueous solution into a basic stream containing its cations and an acidic stream containing its anions [72,129]. BMED can also be considered an environmentally benign and sustainable method because it eliminates the need for added chemicals [126]. Furthermore, BMED has an advantage compared to ED due to its high chemical and mechanical stability, low electrical resistance, low voltage drop, high current efficiency, high permselectivity, and long lifetime [127].

Iizuka and co-workers [130] investigated the implementation of a BMED process for the simultaneous separation and recovery of Li from a simulated spent LIBs solution (mixture of Li and cobalt (Co)) with the addition of chelating agent (EDTA). The results showed a high recovery of Li (about 99%) and that the concentration of Li^+ increased with increasing feed. They also observed that the amount of Li recovered was reduced when the feed solution becomes more alkaline (~pH 12). This work confirmed the capability of the BMED process with EDTA to recover Li from spent LIBs solution at moderate pH levels. Another interesting study evaluated the design of a Li^+ desorption rate using BMED for the recovery of Li from lithium manganese oxide (LMO) [131]. The effects of the number of BM sheets, applied voltage, pH level and flow rate on recovery of Li were studied. The highest desorption efficiency of Li^+ of 70% was removed from LMO at higher applied potential per BM sheet. The lowest flowrate was able to shorten the operating time by 30 min. Overall, the optimum performance of the module was observed when four BM sheets were used at a pH value of 4 or below, with applied potential of about 6 V per sheet and at minimum circulation flow rate.

The feasibility of BMED was further investigated for simultaneous recovery and separation of Li and boron (B) from the simulated geothermal brine solution. The effects of applied voltage and pH on process performance were studied by Bunani [132]. Consistent with previous studies [131,133], the separation efficiency of Li in the base chamber reached as high as 99% at high voltages (18 V). However, an adverse impact on the recovery ratio was observed at the maximum applied voltage, which was caused by ion leakage that takes place at high applied voltages.

Therefore, Bunani and co-workers selected an optimum applied voltage of 15 V based on minimizing ion leakage at 2.41% and 2.65% of Li and B in the acid and base compartments, respectively. In addition, the highest Li^+ recovery ratio of 99.5% was achieved at a moderately high pH in the feed solution. On the other hand, the Li separation efficiencies showed almost no change with pH and had an average value of 99.6%. The BMED was able to recover Li and B as LiOH and H_3BO_4, respectively. This work was extended to study the effect of initial feed concentration of co-existing monovalent ions (Na^+ and Cl^-) on the performance of the BMED [134]. At the different initial concentration of Na^+ and Cl^-, a negligible influence of the separation of the BMED was observed with respect to time. In addition, Bunani et al. reported that the separation efficiency of lithium and boron were greater than 90% at an applied voltage between 25 V and 30 V.

Further studies were conducted on BMED for simultaneous separation and recovery of Li and B from a solution of lithium tetraborate. İpekçi et al. [135] investigated the effect of concentration and type of acid and base solutions used in the acid and base recovery compartment at different applied voltages on the migration rate and recovery of Li. They found that when the initial concentrations of acid and base were increased at fixed applied voltage, the removal ratio of both Li and B were enhanced a certain extent, since high ion conductive medium induced more ions transfer. In addition, replacing NaOH and HCl with LiOH and H_3BO_3 at otherwise fixed operating conditions resulted in lower recoveries of Li and B. Such behavior is related to ion conductive medium that does not ionize to the extent that a strong acid would act

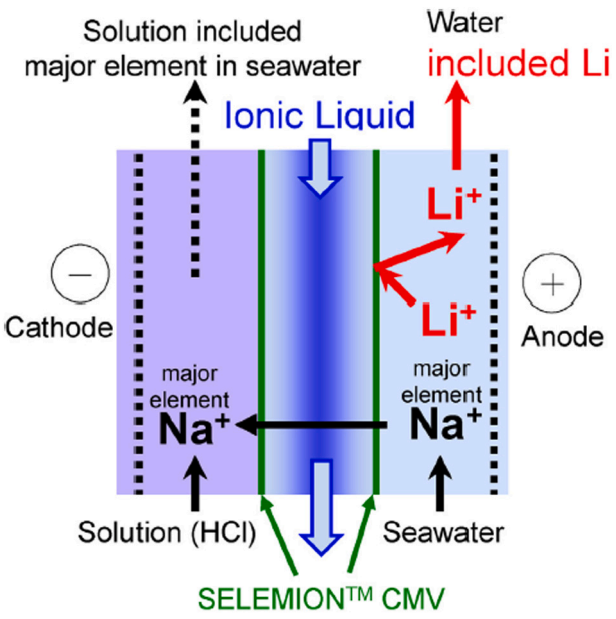

Fig. 20. Schematic diagram of an ionic liquid membrane (ILM-ED). This system is composed of two cation exchange membranes installed at both ends of the ILM. The Li^+ concentrates at the anode side and allows the permeation of all other cations toward the cathode side [145].

when a weak acid (e.g., H_3BO_3) is employed in the acid chamber. Nevertheless, at higher initial concentrations of H_3BO_3 and LiOH, the performance of the BMED system was improved. Such a finding verified that the recoveries of Li and B were significantly affected by the initial concentration of acid and base used in the BMED system. These results implied that the conductivity of acid and base solutions should fall between 0.3 and 0.5 mS/cm, regardless of the strength of the acid and base. In a similar manner, İpekçi et al. [136] conducted additional research to further verify the adaptability of BMED system. The influence of heterogeneous BM implementations at different operating conditions was examined. Heterogeneous BM is fabricated from more heterogeneous materials compared with homogenous BM. In agreement with their previous work [135], the separation efficiencies and recoveries of Li and B increased to a certain extent with increasing applied potential. Moreover, the results showed that the performance of the BMED was strongly influenced by flowrate of the feed solution. They found that a low feed flowrate allowed the membrane to come into contact with the feed solution longer, causing partial adsorption of Li^+ and BO_3^{3-} on the membrane surface. Furthermore, the replacement of HCl and NaOH with H_3BO_3 and LiOH in the acid and base feed showed a negligible effect on the recoveries of Li and B at the optimal operating parameters.

2.2.3.3. Ionic liquid membrane-ED. Ionic liquid membrane electrodialysis (ILMED) technology is a membrane-based separation process that consists of feed and permeate phases separated by an ionic liquid (IL) [137]. ILs are ionic compounds that are liquids at room temperature and they have attractive properties such as high thermal stability, non-flammability, and negligible vapor pressure [137,138]. Moreover, ILs can be utilized to select specific cations and anions due to their physicochemical properties [139]. In the past few years, ionic liquid membranes (ILMs) have gained great attention in the separation of mixtures of organic compounds as well as mixtures of gases and metals [139–141].

Recently, the demand for lithium-6 (^6Li) has increased since it is a major component material used in the production of tritium, which is

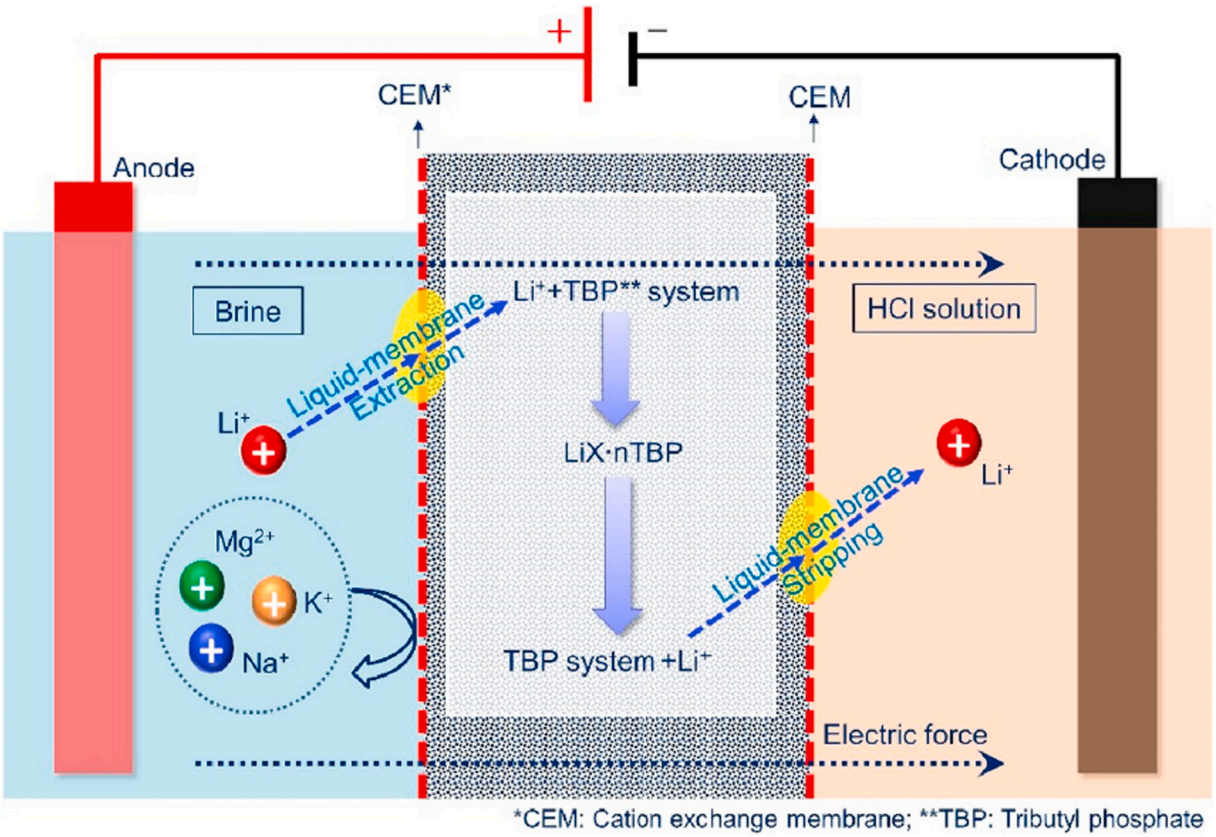

Fig. 21. Schematic diagram of the sandwiched liquid membrane electrodialysis (ILM-ED). This system is composed of two cation exchange membranes and a liquid membrane-embedded between them, which act as a carrier to enhance electro-migration of ions [18].

Table 3
Performance matrices of ED, ESIX and CDI.

Parameters Method	ED			ESIX	CDI
	SED	BMED	ILMED		
Concentration of Li in the feed (mg/L)	104–34,705 mg/L	245–333 mg/L	0.34 mg/L	0.063 mM to 1 M	2.3 mM to 0.21 M
Time required for quantitate extraction of the Li	360–120 min	120–20 min	720 min	25 min to 18 h	30 min to 3 days
Applied voltage	5–20 V	15–35 V	2–3 V	(−0.25)–3.5 V	0.6–3.5 V
Electrode used	***Working:*** Pt coated Ti, Ni mesh, Ti ***Counter:*** Pt coated Ti, AC	***Working:*** Pt coated Ti, Ag/AgCl, Ti ***Counter:*** Pt coated Ti, stainless steel, Ag/AgCl, Ti	***Working:*** Pt coated Ti, Ni, Ti ***Counter:*** Pt coated Ti, AC RuO_2-coated Ti	***Working:*** MnO_2, LMO, modified LMO, $LiFePO_4$ ***Counter:*** Pt/Ag/Zn/NiHCF/Ppy/BDD	***Working:*** AC, PVDF coated AC, AC slurry, LMO, modified LMO, LMTO. ***Counter:*** AC, AC slurry
Membrane used	***CEM***[a]***:*** Homogeneous polystyrene, CIMS, CSO, FKS-PET-130, CJCM, CMIX. ***AEM***[b]***:*** Homogeneous polystyrene, ACSASA, FAS-PET-130, CJAM	***CEM:*** Heterogeneous Polyethylene, CMIX, MA-40 ***AEM:*** Heterogeneous Polyethylene, Neosepta, AMX, MK-40 ***BM***[c]***:*** Neosepta-BP-1a, BM-3	***CEM:*** CAS, CMV, CSO ***ILM:*** PP13-TFSI, [C_4mim][$FeCl_4$], [C_4mim][TFSI], [C_2mim][TFSI], (TMPA–TFSI)	n.a.	***CEM:*** MCEM (CIMS). ***AEM:*** Conventional AEM, PVDF-EDA based AEM, Poly(vinyl chloride)/ethylene diamine AEM
Operation mode	Batch	Continuous	Continuous	Batch	Batch
Recovery (Li^+)	68%–80%	60%–98%	n.m.	2–37.6 mg/g	2.4–800 mg/g
SEC (kWh/kmol)	5–2400 0.01–40.5[d]	3–19	110–130	1.4–18.5	1.3–160.7
References	[18,19,119–125,132,134–136,144–146,148]			[17,54–56,64,69,73,76,80–86,88,90–95,99]	[99,101,103–105,107–109,111]

[a] CEM: cation exchange membrane.
[b] AEM: anion exchange membrane.
[c] BM: bipolar membrane.
[d] Specific energy consumption (kWh/$m^3$of Li).

used as fuel in fusion reactors. However, the natural sources of ^{6}Li are limited. Therefore, a novel Li isotope separator method using ionic liquid impregnated organic membranes (IL-I-OM) integrated with ED was developed by Hoshino and Terai, as illustrated in Fig. 19(a) [142]. The results showed that Li isotopes were separated and concentrated by ED, because the IL-I-OM allows the permeation of only Li^+ and the rates of permeation of different Li isotopes differ based on characteristics of the IL-I-OM. To improve the durability of IL-I-OM and increase the separation efficiency of ^{6}Li, the effects of membrane thickness (1 mm, 2 mm, and 3 mm) and a protection cover on the integrity of the IL-I-OM were investigated [143]. They found that the durability of IL-I-OM was improved by an overcoat of nafion 324, since it limited the overflow of ionic liquid. Moreover, the separation coefficient of ^{6}Li in the ED process was improved when using a highly porous organic membrane of 3 mm thickness. Hoshino [144] proposed a new approach that verified the applicability of using IL-I-OM to extract Li^+ from seawater, and a schematic of the process is shown in Fig. 19(b). He found that the concentration of Li^+ in the cathode side increases up to 5.94% at minimum applied voltage, showing that the IL-I-OM has high selectivity for Li^+ relative to coexisting ions. Consistent with his previous work [142,143], the outflow of the ionic liquid was prevented and the recovery of Li increased up to 22.2% when both sides of the impregnated membranes were covered with nafion 324.

Hoshino and co-workers conducted another study on applying the ionic liquid membrane electrodialysis (ILMED) method to the recovery of Li^+ from SW at an electric potential of 2-3 V [145]. In this study, the outflow of IL was prevented by installing two CEMs on both ends of the IL, as illustrated in Fig. 20. The selected commercial CEM is permeable to all cations (e.g., Na^+, K^+, Ca^{2+}, Mg^{2+}) expect for Li^+. The results showed that the divalent coexisting ions were separated and concentrated at the cathode side with the help of IL-I-OM, while all Li^+ remained at the anode side. This led to an increase in the separation efficiency to a maximum value of 63% [145].

Currently, the application of ILMED for Li recovery has gained great interest. Liu et al. [18] developed a new ILMED to be selective for Li to recover it from simulated brine solution with a high mass ratio of Mg/Li. The ILMED consists of a liquid membrane between two CEMs, as illustrated in Fig. 21. The ILM increased the electro-migration of Li^+ and resulted in a significant drop of Mg/Li ratio in the brine from 50 to 0.5 at a current density of 4.375 A·m^{-2} after 12 h of operating time. In addition, lower specific energy consumption of 16 Wh/g of Li was achieved by the ILMED system compared to a typical ED. Another study on the ILMED method for recovering Li from salt lake brines was conducted by Zhao et al, and they studied the effects of electric potential and temperature. [146]. In agreement with Liu et al. [18], a remarkable reduction of Mg/Li ratio in the brine from 100 to less than 2 was observed with minimum specific energy consumption of 0.13 kWh/mol at the optimal applied voltage of 3 V and temperature of 20 °C. These experimental results verified that ILMED is a promising method because of its high selectivity for Li and efficient energy consumption when treating a brine solution that contains several ions.

Most of the research conducted on ED and ED-based processes for separation and recovery of Li has focused on studying the influence of applied voltages and the characteristics of feed solutions in bench-scale experiments. The highest Li recovery of 90.5% with a minimum specific energy consumption of 0.0045 kWh/mol was achieved by a SED process treating a simulated brine solution. Moreover, a number of studies on SED processes have shown that the degree of Li^+ selectively is limited by the presence of monovalent cations (e.g., Na^+ and K^+). However, there are many novel approaches to improving the selectivity of Li in SED

Table 4
ED, ESIX and CDI processes in a nutshell.

Method		Mechanism	Source of lithium	Technical maturity	Advantage	Disadvantage	Reference
ED	SED	Electro-membrane based	- Simulated brine solution - Simulated spent LIBs - Salt lake brine	Bench-scale	- Eco-friendly. - High separation efficiency and recovery of Li	- Recovery unit after SED - Scaling	[18,19,119–125,132,134–136,144–146,148]
	BMED		- Simulated pre-treated geothermal brine - Simulated spent LIBs	Bench/ Pilot scale	- High permselectivity and long lifetime of bipolar membrane - No chemical additive - Production of pure acid and base (LiOH)	- Pre-treatment of feed solution.	
	ILM-ED		- Salt lake brine - Seawater	Bench-scale	- High selectivity of ion liquid membrane toward Li^+	- Scalability	
ESIX		Battery based	- Simulated salar de atacama, uyuni and olaroz brine - Natural brine - Li salt solutions-with and without $MgCl_2$	Bench/ Pilot scale	- Can support source solution of complex nature - Does not require skilled labor to operate the process - Easy upscaling with film-based electrodes - No membranes involved, no scaling and fouling issues requiring of membrane replacement - Li extraction time is reduced from 1 to 2 years to less than 24 h	- Upscaling requires large space to switch between source and recovery solution tanks	[17,54–56,64,69,73,76,80–86,88,90–95,99]
CDI		Membrane enhanced battery based	- Lithium based single or binary solutions - Geothermal brine	Bench-scale	- A simple process, gives means for electrode and membrane fabrication/ testing - Require application of low voltages (between 0.6 and 3.5 V)	- Prone to Li ions loss during charging and discharging cycles - Can undergo scaling and fouling issues, require replacement of membranes - Scalability is hard with the need for large intercalation electrodes	[99,101,103–105,107–109,111]

processes. The studies on BMED have demonstrated the feasibility of producing a pure Li salt solution (e.g., LiOH) from a boron-lithium mixed stream at considerable specific energy consumption. Nonetheless, the feed solution is needed to be treated in order to produce a pure LiOH product and to prevent membrane scaling. Unlike BMED, SED needs a basic solution (e.g., Na_2CO_3) to be added to the concentrate chamber in order to obtain a high-grade lithium salt (e.g., Li_2CO_3) and improve the purity of the recovered Li. An integrated SED-BMED system was developed to extract lithium from simulated salt lake brine and produce LiOH [147]. Such a system eliminated the need for a recovery unit after the SED process and prior to the BMED process. In addition, studies on ILMED and LM-I-O-ED processes have shown that they have a superior selectivity for Li^+ over other cations. Moreover, these studies revealed the feasibility of extracting lithium from primary liquid resources with efficient energy utilization. To the best of our knowledge, the vast majority of research conducted on ED-based technologies for Li recovery have been at bench-scale, and most of them were conducted using a simulated brine solution. Moreover, the effect of membrane fouling and scaling have not been addressed, though the separation and recovery of Li depend on IEMs in ED-based processes. From a practical perspective, future work needs to be directed toward developing improved membranes that have greater Li selectively and reduced membrane scaling. Additionally, economic analysis of the processes should be conducted to evaluate their potential to be operated at a large scale.

2.3. Technology readiness levels of processes

The ED, ESIX and CDI processes are compared with performance analysis matrices as shown in Table 3 in order to evaluate their technology readiness levels (TRL). In general, SED and BMED have been studied at higher Li salt solutions (˃100 mg/L), while ILMED and ESIX have been applied to trace Li solutions (0.4 mg/L). From a practical point of view, salt lake brines contain Li ≥100 ppm, while seawater has a low Li concentration of 0.17 ppm. Therefore, ED demands further experimenting with seawater or concentrated seawater as a source solution. ED requires higher applied voltages than ESIX and CDI, which makes ED relatively energy-intensive. The majority of cathode materials tested for ED are based on Pt, Ti, Ag, and Ni. Usually, anode materials are of similar origin, except for graphite which has been used in some. CDI mainly depends on capacitive-type AC-based electrodes, while ESIX showed better performance with modified LMO electrodes as cathodes. However, the time required for the extraction of a quantitative amount of Li by ED is 20 min to 6 h, while ESIX can take up to 18 h and CDI takes up to 3 days. Recovery of Li in ED cannot be directly compared with that in ESIX and CDI since recovery in ED is the relative amount of Li transferred to the concentrate relative to that initially in the dilute chamber. Li recovery was in similar ranges for ESIX and CDI (2–30 mg/g), except for one study where the authors found outstanding Li recovery with very low SEC and an extremely high Li recovery of 800 mg/g. Analysis of performance matrices allows us to summarize the performance of the three processes, as given in Table 4. Accordingly, only BMED and ESIX have been studied from the bench scale through to the

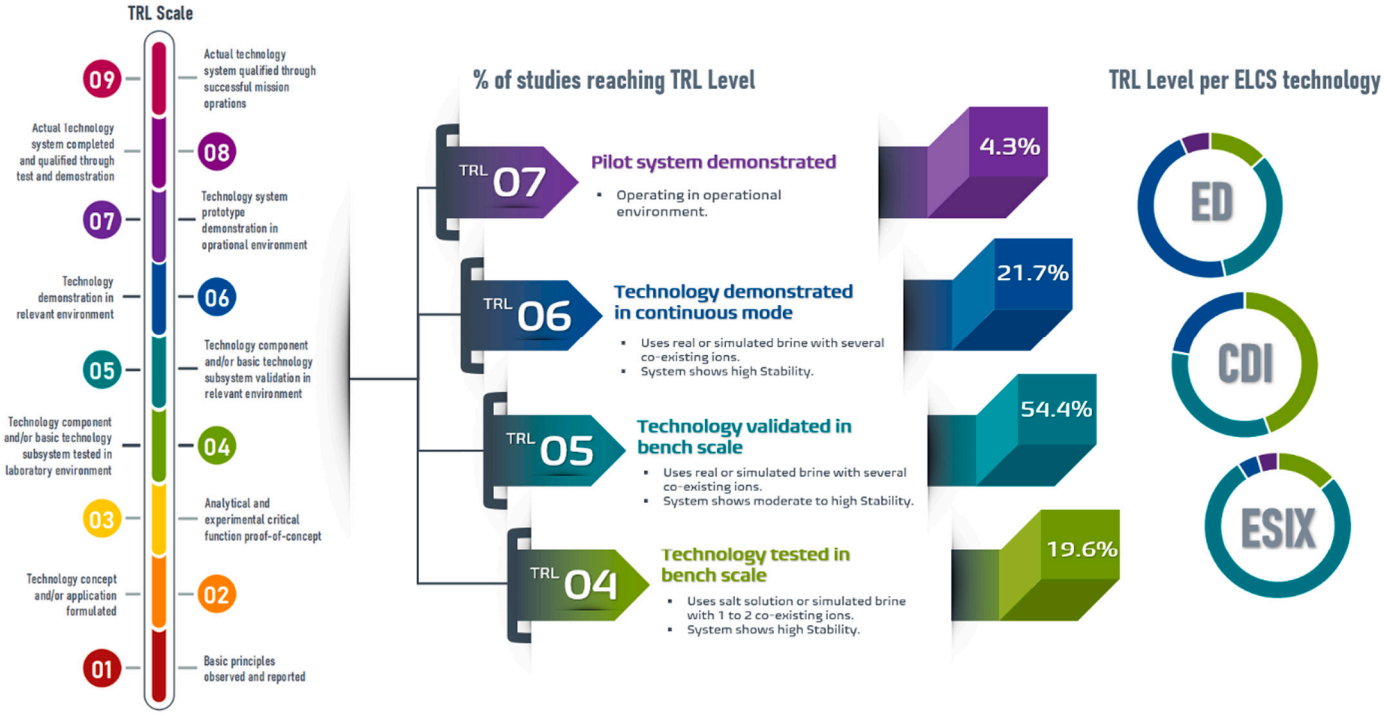

Fig. 22. (Left) Standard technology readiness scale [149]; (Right) technology readiness levels of ED, CDI and ESIX processes discussed in Sections 2.2.1, 2.2.2 & 2.2.3 clustered together [17–19,54–56,64,69,73,76,80–86,88,90–95,99,101,103–105,107–109,111,119–125,132,134–136,144–146,148].

pilot scale.

The TRL chart provides a quick view of how easy it will be to convert a process into a commercial, industrial process. Here, we classified ELiCSs based on the system scale (lab/bench/pilot), flow conditions (batch/continuous), and Li source (mono salt/brine/seawater). All ELiCSs were found to be at TRL 4 or above, as depicted in Fig. 22. To date, only a small fraction of the processes studied (4.3%) have demonstrated functioning systems at the pilot-scale, which should motivate the scientific community to do more work on EliCSs at the pilot-scale. Appropriate validation of the processes at the pilot scale will enable the cost-effective utilization of liquid Li resources, paving the way for the production of commercially available forms of Li economically and quickly. Nevertheless, a higher proportion (54.4%) of studies have validated processes at the bench scale, including studies that evaluated the stability of the electrodes and IEMs in cycling experiments that utilized different types of brine solutions as feed instead of single component Li salt solution. Another, 21.7% of studies demonstrated high stability of the system in continuous operation mode. These processes at TRL 5, 6, and 7 can be upscaled and implemented to achieve TRL 8 through continuous research on process improvement and testing the systems in real industrial environments.

Industrial implementation incurs the capital cost for infrastructure and equipment, operational costs, and maintenance costs. Capital cost is related to the process; for instance, CDI requires the highest capital investment compared to ED and ESIX. Furthermore, the CDI process's desorption efficiency is only at a satisfactory level, which is unsuitable for upscaling. This shortcoming is reflected in the TRL rating with respect to the industrial process, where most CDI processes are in TRL 4 and 5, while only 22.2% of CDI processes are in TRL 6 with no system reaching TRL 7. On the other hand, 46.7% of the ED systems studied are in TRL 6, and the others (6.7%) are in TRL 7. The improved performance of the ED at larger scales could be shown up because the technology has been studied over a longer period than CDI, since CDI is considered a new approach for Li recovery. ESIX is the most versatile technique that is easy to set up and operate, but most of the processes reported to date are in TRL 5 (72%), TRL 6 (5%), and TRL 7 (5%). With regards to ESIX, systems that have been studied are generally batch processes with switchable feed and recovery solutions. Switching between tanks requires a larger surface area of the tanks, which has a serious impact on the capital cost. On the other hand, flushing the feed to refill the recovery solution consumes high volumes of scarce fresh water. Addressing these issues will enable easy transfer of the bench and pilot-scale technologies to real commercial environments.

3. Perspective and outlook

Increased demand for Li promotes the rapid transition of lab-scale research processes to full-scale, functioning industrial processes. Electrochemical processes are playing a pivotal role in driving force for ion separation processes toward industrialization. However, the lack of uniformity in parameters used to evaluate process performance between various studies limits meaningful comparison of alternative processes. Specific energy consumption and purity of the recovered Li are dominant factors for performance evaluation.

SEC has a direct impact on the operational cost of the ELiCSs. Fig. 23 shows that ESIX has SEC in the range of 1.4 to 18.7 kWh/kmol, which is lower than that for CDI and ED. Bench-scale testing of CDI was performed mainly with LiCl and LiOH salt solutions. In the limited studies of CDI using simulated brine or geothermal brine as the feed, SEC was higher than 100 kWh/kmol. SED has higher energy consumption than BMED and ILMED, but the SEC of ED-based processes cannot be directly compared to those of CDI and ESIX. However, the SEC for ED is around a few kWh/kmol or kWh/m^3, so the energy demand for ED processes seems to be between ESIX and CDI processes. The ambiguity in units is a problem that should motivate the ELiCSs research community to report process performance parameters in a standard form that allows meaningful comparisons among the systems.

In brine processing, the Mg/Li ratio plays a significant role due to the similar ionic radii of Mg^{2+} and Li^{+}. Fig. 24 summarizes how ED, CDI, and ESIX systems perform with brines of different Mg/Li, as demonstrated by SEC and RR. All of the studies reported so far on CDI have focused on feed solutions with an Mg/Li ratio of less than 10. Fig. 24(a)

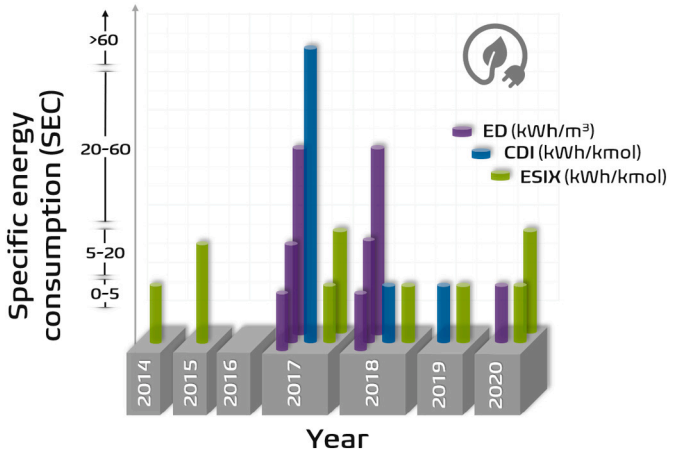

(caption on next column)

Fig. 23. Energy consumption of ELiCSs over the years. Data obtained from

indicates that regardless of the Mg/Li ratio in the feed, ESIX consumed less than 5 kWh/kmol in 80% of the occurrences, and no system exceeds the SEC of 20 kWh/kmol. The industry makes tradeoffs among the following parameters: time, energy, and production output (quality and quantity) to achieve a balance between the cost and benefits of the production. Thus, the lower SEC with higher RR is preferred. The quality of the product is measured by its purity, and the purity of products produced by ESIX was above 95%, except for pilot-scale demonstrations. As already discussed, pilot-scale systems must address the inherent process performance issues related to scale-up. CDI offers a high level of recovery with values over 80 mg/g for source solutions below the Mg/Li ratio of 10 (Fig. 24(b)). ESIX has been tested and validated for handling high Mg brines (Mg/Li > 80) and produced up to 80 mg of Li per gram of the working electrode. Industry prefers the latter scenario because natural salt lake brines/seawater/spent LIBs all contain coexisting ions and successful processes operating with these feeds must be designed to have higher recovery and purity.

From the perspective of several studies on the SEC, favorable energy consumption for optimized future process is found to be below 55 kWh/kmol or less. Developing full-scale applications, however, is not an easy task and requires massive capital input and infrastructure. Therefore, validation of these SEC numbers by more studies is required. With regards to ESIX processes, a capacitive type, carbon-based counter electrodes and modified NiHCF-based electrodes offer greater promise for improved efficiency and utilization of real brines. Despite their low SEC, no ESIX process provides more than 80% of Li recovery with moderately high or high Mg-containing brine. Hence, it is important to find new electrode combinations and process parameters that can further increase Li recovery with high Mg brines. The majority of ED processes have dealt with brines containing Li in the presence of B. It is timely to test the ED process with an exclusive focus on system parameters and IEM performance to offer lower SEC along with higher RRs. On the other hand, CDI is heavily in need of testing recovery using simulated or real salt lake brine because most of the work has been done with a solution containing a single Li salt.

4. Conclusion

This study combines and critically reviews and discusses most of the state-of-the-art electrochemical lithium capturing systems (ELiCSs) and provides future perspectives on their development. Three broad classifications of ELiCSs were identified: electrodialysis (ED) as an electromembrane-based process, capacitive deionization (CDI) as a membrane enhanced battery-based process, and electrochemically switchable ion exchange (ESIX) as a battery-based process. Brief conclusions from this review are as follows:

- In ED-based processes, applied voltage guides the ions toward the respective electrodes and IEMs collect Li^+ and other monovalent ions in the middle compartment/(s). Therefore, the electrodes used in ED

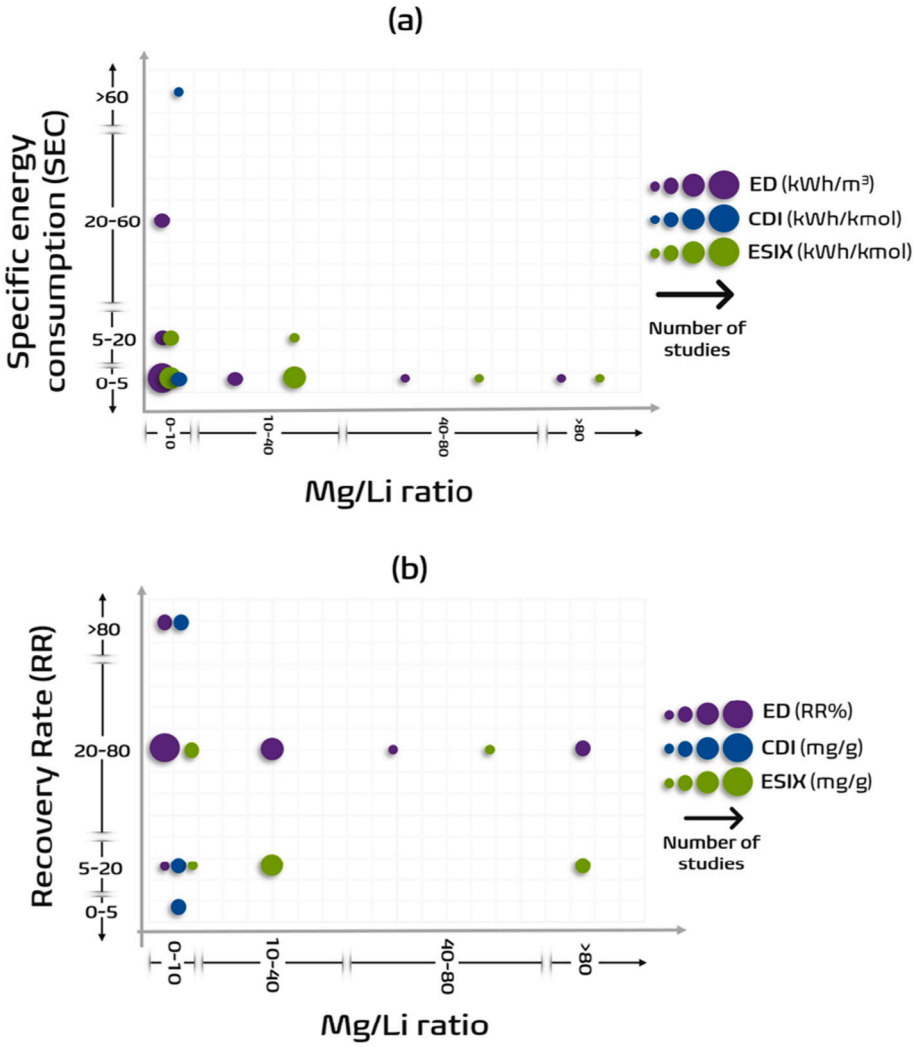

Fig. 24. Illustration of the relationship between magnesium to lithium feed ratio, (a) specific energy consumption (SEC), and (b) recovery ratio (RR) of Li. Summary is based on the data from [17–19,54–56,64,69,73,76,80–86,88,90–95,99,101,103–105,107–109,111,119–125,132,134–136,144–146,148].

are general with no particular affinity for Li^+, which results in higher applied cell voltages. The ED-based processes studied so far for Li recovery have mostly focused on demonstrating a practical approach to evaluating the operating variables that describe Li's separation and recovery from an aqueous solution. Among the ED-based processes, SED and BMED are the most appropriate methods for high recovery of Li^+ at low SEC.

- Studies involving ESIX technology for Li recovery considered extracting Li from other liquid Li resources instead of from solutions of individual Li salts. The $Li_{(1-x)}Mn_2O_4/LiMn_2O_4$ system reported the highest Li recovery rate. Activated carbon counter electrodes provide shorter cycles with high Li concentrations in the source solution, compared to Pt and Ag counter electrodes. However, the use of NiHCF counter electrode allows the brine to be a recovery solution.
- CDI is a membrane-enhanced battery-based process that takes advantage of the selectivity of the intercalation electrodes along with the ion transport regulation of the IEMs to attain good Li ion recovery. CDI is a well-established technology that has proven its reliability as a promising electrochemical ion-separation technology. CDI is an advancement of ESIX since it utilizes intercalating electrodes in combination with IEMs. However, its use for selective Li recovery is still very limited and 95% of studies show that its SEC and RR are similar to those of ESIX. This demands further study so that process and operating parameters can be optimized.
- Most ELiCSs have been evaluated at the bench scale, with some of them studied at pilot-scale using continuous processes. Most CDI processes used as ELiCSs have been tested or verified only at the laboratory, bench-scale, while ED and ESIX are better-established technologies for Li recovery.
- Future ELiCSs-related research needs to focus on experiments using natural Li liquid resources and optimized process parameters. This will provide results that can be used in an economic analysis that can provide an overview of ELiCSs' required capital costs, which can be used to evaluate the potential for scalability and pilot expansion.

Declaration of competing interest

The authors declare that they have no known competing financial interests or personal relationships that could have appeared to influence the work reported in this paper.

Acknowledgements

This publication was made possible by NPRP grant # [NPRP12S-0227-190166] from the Qatar National Research Fund (a member of Qatar Foundation). The findings achieved are solely the responsibility of

the authors. Open Access funding provided by the Qatar National Library.

References

[1] G. Liu, Z. Zhao, A. Ghahreman, Novel approaches for lithium extraction from salt-lake brines: a review, Hydrometallurgy 187 (2019) 81–100.
[2] E.N. Wilson, Exploring new energy frontiers with petroleum geoscience talent and technology, in: AAPG Pacific Section Convention, 2019.
[3] R. Borah, F.R. Hughson, J. Johnston, T. Nann, On battery materials and methods, Mater. Today 6 (2020) 100046.
[4] C. Research, Ten years of the cnesa enegry storage industry white paper, in, China Energy Storage Allliance (CNESA), http://en.cnesa.org/, 2019.
[5] Y. Zhang, Y. Hu, L. Wang, W. Sun, Systematic review of lithium extraction from salt-lake brines via precipitation approaches, Miner. Eng. 139 (2019) 105868.
[6] C. Liu, J. Lin, H. Cao, Y. Zhang, Z. Sun, Recycling of spent lithium-ion batteries in view of lithium recovery: a critical review, J. Clean. Prod. 228 (2019) 801–813.
[7] X. Zhao, Y. Jiao, P. Xue, M. Feng, Y. Wang, Z. Sha, Efficient lithium extraction from brine using a three-dimensional nanostructured hybrid inorganic-gel framework electrode, ACS Sustain. Chem. Eng. 8 (2020) 4827–4837.
[8] S. Yang, F. Zhang, H. Ding, P. He, H. Zhou, Lithium metal extraction from seawater, Joule 2 (2018) 1648–1651.
[9] X. Zhao, G. Li, M. Feng, Y. Wang, Semi-continuous electrochemical extraction of lithium from brine using CF-NMMO/AC asymmetric hybrid capacitors, Electrochim. Acta 331 (2020) 135285.
[10] P. Ralon, M. Taylor, A. Ilas, H. Diaz-Bone, K. Kairies, Electricity Storage and Renewables: Costs and Markets to 2030, International Renewable Energy Agency, Abu Dhabi, UAE, 2017.
[11] U.S.G. Survey, Mineral commodity summaries 2020, in: Mineral Commodity Summaries, Reston, VA, 2020, p. 204.
[12] F. Meng, J. McNeice, S.S. Zadeh, A. Ghahreman, Review of lithium production and recovery from minerals, brines, and lithium-ion batteries, Miner. Process. Extr. Metall. Rev. (2019) 1–19.
[13] D. Jimenez, Lithium market outlook, in: 2nd Lithium Forum 2018, SVP Iodine, Lithium and Industrial Chemicals, Santiago , Chile, 2018, pp. 35.
[14] L. Li, V.G. Deshmane, M.P. Paranthaman, R.R. Bhave, B.A. Moyer, S. Harrison, Lithium recovery from aqueous resources and batteries: A brief review, Johnson Matthey Tech. 62 (2018).
[15] X. Li, Y. Mo, W. Qing, S. Shao, C.Y. Tang, J. Li, Membrane-based technologies for lithium recovery from water lithium resources: a review, J. Membr. Sci. 591 (2019) 117317.
[16] V. Flexer, C.F. Baspineiro, C.I. Galli, Lithium recovery from brines: a vital raw material for green energies with a potential environmental impact in its mining and processing, Sci. Total Environ. 639 (2018) 1188–1204.
[17] H. Joo, S. Kim, S. Kim, M. Choi, S.-H. Kim, J. Yoon, Pilot-scale demonstration of an electrochemical system for lithium recovery from the desalination concentrate, Environ. Sci.: Water Res. 6 (2020) 290–295.
[18] G. Liu, Z. Zhao, L. He, Highly selective lithium recovery from high Mg/Li ratio brines, Desalination 474 (2020) 114185.
[19] Z.-Y. Guo, Z.-Y. Ji, Q.-B. Chen, J. Liu, Y.-Y. Zhao, F. Li, Z.-Y. Liu, J.-S. Yuan, Prefractionation of licl from concentrated seawater/salt lake brines by electrodialysis with monovalent selective ion exchange membranes, J. Clean. Prod. 193 (2018) 338–350.
[20] A. Battistel, M.S. Palagonia, D. Brogioli, F. La Mantia, R. Trócoli, Electrochemical methods for lithium recovery: a comprehensive and critical review, Adv. Mater. 1905440 (2020).
[21] T. Shiga, H. Kondo, Y. Kato, K. Fukumoto, Y. Hase, Mediator catalyst for lithium fluoride decomposition for lithium recovery, ACS Sustain. Chem. Eng. 8 (2020) 2260–2266.
[22] L.I. Barbosa, G. Valente, R.P. Orosco, J.A. Gonzalez, Lithium extraction from β-spodumene through chlorination with chlorine gas, Miner. Eng. 56 (2014) 29–34.
[23] J. Lee, Extraction of lithium from lepidolite using mixed grinding with sodium sulfide followed by water leaching, Minerals 5 (2015) 737–743.
[24] D.E. Garrett, Handbook of Lithium and Natural Calcium Chloride, Elsevier, 2004.
[25] L. Gong, W. Ouyang, Z. Li, J. Han, Direct numerical simulation of continuous lithium extraction from high Mg^{2+}/Li^{+} ratio brines using microfluidic channels with ion concentration polarization, J. Membr. Sci. 556 (2018) 34–41.
[26] X. Wen, P. Ma, C. Zhu, Q. He, X. Deng, Preliminary study on recovering lithium chloride from lithium-containing waters by nanofiltration, Sep. Purif. Technol. 49 (2006) 230–236.
[27] Y. Gang, S. Hong, L. Wenqiang, X. Weihong, X. Nanping, Investigation of Mg^{2+}/Li^{+} separation by nanofiltration, Chin. J. Chem. Eng. 19 (2011) 586–591.
[28] S.-Y. Sun, L.-J. Cai, X.-Y. Nie, X. Song, J.-G. Yu, Separation of magnesium and lithium from brine using a desal nanofiltration membrane, J. Water Process. Eng. 7 (2015) 210–217.
[29] Q. Bi, Z. Zhang, C. Zhao, Z. Tao, Study on the recovery of lithium from high Mg^{2+}/Li^{+} ratio brine by nanofiltration, Water Sci. Technol. 70 (2014) 1690–1694.
[30] A. Somrani, A. Hamzaoui, M. Pontie, Study on lithium separation from salt lake brines by nanofiltration (NF) and low pressure reverse osmosis (LPRO), Desalination 317 (2013) 184–192.
[31] S. Piletsky, T. Panasyuk, E. Piletskaya, I.A. Nicholls, M. Ulbricht, Receptor and transport properties of imprinted polymer membranes–a review, J. Membr. Sci. 157 (1999) 263–278.
[32] J. Cui, Z. Zhou, S. Liu, Y. Zhang, L. Yan, Q. Zhang, S. Zhou, Y. Yan, C. Li, Synthesis of cauliflower-like ion imprinted polymers for selective adsorption and separation of lithium ion, New J. Chem. 42 (2018) 14502–14509.
[33] X. Luo, B. Guo, J. Luo, F. Deng, S. Zhang, S. Luo, J. Crittenden, Recovery of lithium from wastewater using development of li ion-imprinted polymers, ACS Sustain. Chem. Eng. 3 (2015) 460–467.
[34] Q. Feng, Y. Miyai, H. Kanoh, K. Ooi, Lithium (1+) extraction/insertion with spinel-type lithium manganese oxides. Characterization of redox-type and ion-exchange-type sites, Langmuir 8 (1992) 1861–1867.
[35] D. Sun, M. Meng, Y. Yin, Y. Zhu, H. Li, Y. Yan, Highly selective, regenerated ion-sieve microfiltration porous membrane for targeted separation of Li^{+}, J. Porous. Mater. 23 (2016) 1411–1419.
[36] G. Zhu, P. Wang, P. Qi, C. Gao, Adsorption and desorption properties of Li^{+} on PVC-$H_{1.6}Mn_{1.6}O_4$ lithium ion-sieve membrane, Chem. Eng. J. 235 (2014) 340–348.
[37] B.K. Pramanik, K. Thangavadivel, L. Shu, V. Jegatheesan, A critical review of membrane crystallization for the purification of water and recovery of minerals, Rev. Environ. Sci. Biotechnol. 15 (2016) 411–439.
[38] V.G. Gude, Energy storage for desalination processes powered by renewable energy and waste heat sources, Appl. Energy 137 (2015) 877–898.
[39] F. Macedonio, E. Curcio, E. Drioli, Integrated membrane systems for seawater desalination: energetic and exergetic analysis, economic evaluation, experimental study, Desalination 203 (2007) 260–276.
[40] C.A. Quist-Jensen, F. Macedonio, E. Drioli, Integrated membrane desalination systems with membrane crystallization units for resource recovery: a new approach for mining from the sea, Crystals 6 (2016) 36.
[41] A. Razmjou, M. Asadnia, E. Hosseini, A.H. Korayem, V. Chen, Design principles of ion selective nanostructured membranes for the extraction of lithium ions, Nat. Commun. 10 (2019) 1–15.
[42] A. Galama, M. Saakes, H. Bruning, H. Rijnaarts, J. Post, Seawater predesalination with electrodialysis, Desalination 342 (2014) 61–69.
[43] S.-i. Jeon, H.-r. Park, J.-g. Yeo, S. Yang, C.H. Cho, M.H. Han, D.K. Kim, Desalination via a new membrane capacitive deionization process utilizing flow-electrodes, Energy Environ. Sci. 6 (2013) 1471–1475.
[44] M.A. Ashraf, J. Wang, B. Wu, P. Cui, B. Xu, X. Li, Enhancement in Li^{+}/Mg^{2+} separation from salt lake brine with PDA–PEI composite nanofiltration membrane, J. Appl. Polym. Sci. 49549 (2020).
[45] P. Xu, J. Hong, X. Qian, Z. Xu, H. Xia, Q.-Q. Ni, "Bridge" graphene oxide modified positive charged nanofiltration thin membrane with high efficiency for Mg^{2+}/Li^{+} separation, Desalination 488 (2020) 114522.
[46] H. Wu, Y. Lin, W. Feng, T. Liu, L. Wang, H. Yao, X. Wang, A novel nanofiltration membrane with [MimAP][Tf2N] ionic liquid for utilization of lithium from brines with high Mg^{2+}/Li^{+} ratio, J. Membr. Sci. 117997 (2020).
[47] G. Zante, M. Boltoeva, A. Masmoudi, R. Barillon, D. Trebouet, Highly selective transport of lithium across a supported liquid membrane, J. Fluor. Chem. 236 (2020) 109593.
[48] C. Yu, J. Lu, J. Dai, Z. Dong, X. Lin, W. Xing, Y. Wu, Z. Ma, Bio-inspired fabrication of ester-functionalized imprinted composite membrane for rapid and high-efficient recovery of lithium ion from seawater, J. Colloid Interface Sci. 572 (2020) 340–353.
[49] Y. Lu, D. Sun, Y. Lu, Y. Yan, B. Hu, Zwitterion imprinted composite membranes with obvious antifouling character for selective separation of li ions, Korean J. Chem. Eng. 37 (2020) 707–715.
[50] S. Roobavannan, S. Vigneswaran, G. Naidu, Enhancing the performance of membrane distillation and ion-exchange manganese oxide for recovery of water and lithium from seawater, Chem. Eng. J. 125386 (2020).
[51] F. Xue, X. Zhang, Y. Niu, C. Yi, S. Ju, W. Xing, Preparation and evaluation of α-Al_2O_3 supported lithium ion sieve membranes for Li^{+} extraction, Chin. J. Chem. Eng. 28 (2020) 2312–2318.
[52] B. Swain, Recovery and recycling of lithium: a review, Sep. Purif. Technol. 172 (2017) 388–403.
[53] H. Yoon, J. Lee, S. Kim, J. Yoon, Review of concepts and applications of electrochemical ion separation (EIONS) process, Sep. Purif. Technol. 215 (2019) 190–207.
[54] J. Lee, S.-H. Yu, C. Kim, Y.-E. Sung, J. Yoon, Highly selective lithium recovery from brine using a λ-MnO_2–Ag battery, Phys. Chem. Chem. Phys. 15 (2013) 7690–7695.
[55] R. Trócoli, A. Battistel, F.L. Mantia, Selectivity of a lithium-recovery process based on $LiFePO_4$, Chem. Eur. J. 20 (2014) 9888–9891.
[56] R. Trócoli, C. Erinmwingbovo, F. La Mantia, Optimized lithium recovery from brines by using an electrochemical ion-pumping process based on λ-MnO_2 and nickel hexacyanoferrate, ChemElectroChem 4 (2017) 143–149.
[57] Z. Wang, Y. Feng, X. Hao, W. Huang, X. Feng, A novel potential-responsive ion exchange film system for heavy metal removal, J. Mater. Chem. 2 (2014) 10263–10272.
[58] X. Du, H. Zhang, X. Hao, G. Guan, A. Abudula, Facile preparation of ion-imprinted composite film for selective electrochemical removal of nickel (II) ions, ACS Appl. Mater. Interfaces 6 (2014) 9543–9549.
[59] M.A. Lilga, R.J. Orth, J. Sukamto, S. Haight, D. Schwartz, Metal ion separations using electrically switched ion exchange, Sep. Purif. Technol. 11 (1997) 147–158.
[60] K.M. Jeerage, D.T. Schwartz, Characterization of cathodically deposited nickel hexacyanoferrate for electrochemically switched ion exchange, Sep. Sci. Technol. 35 (2000) 2375–2392.
[61] P. Srimuk, X. Su, J. Yoon, D. Aurbach, V. Presser, Charge-transfer materials for electrochemical water desalination, ion separation and the recovery of elements, Nat. Rev. Mater. (2020) 1–22.

[62] A. Soffer, M. Folman, The electrical double layer of high surface porous carbon electrode, J. Electroanal. Chem. Interfacial Electrochem. 38 (1972) 25–43.
[63] E.J. Calvo, Electrochemical methods for sustainable recovery of lithium from natural brines and battery recycling, Curr. Opin. Electrochem. 15 (2019) 102–108.
[64] M. Pasta, C.D. Wessells, Y. Cui, F. La Mantia, A desalination battery, Nano Lett. 12 (2012) 839–843.
[65] F. La Mantia, M. Pasta, H.D. Deshazer, B.E. Logan, Y. Cui, Batteries for efficient energy extraction from a water salinity difference, Nano Lett. 11 (2011) 1810–1813.
[66] D.P. Dubal, O. Ayyad, V. Ruiz, P. Gomez-Romero, Hybrid energy storage: the merging of battery and supercapacitor chemistries, Chem. Soc. Rev. 44 (2015) 1777–1790.
[67] J.-S. Kim, Y.-H. Lee, S. Choi, J. Shin, H.-C. Dinh, J.W. Choi, An electrochemical cell for selective lithium capture from seawater, Environ. Sci. Technol. 49 (2015) 9415–9422.
[68] X. Zhao, H. Yang, Y. Wang, Z. Sha, Review on the electrochemical extraction of lithium from seawater/brine, J. Electroanal. Chem. 850 (2019) 113389.
[69] S. Kim, J. Lee, J.S. Kang, K. Jo, S. Kim, Y.-E. Sung, J. Yoon, Lithium recovery from brine using a λ-MnO_2/activated carbon hybrid supercapacitor system, Chemosphere 125 (2015) 50–56.
[70] X. Zhao, M. Feng, Y. Jiao, Y. Zhang, Y. Wang, Z. Sha, Lithium extraction from brine in an ionic selective desalination battery, Desalination 481 (2020) 114360.
[71] M. Bryjak, A. Siekierka, J. Kujawski, K. Smolinska-Kempisty, W. Kujawski, Capacitive deionization for selective extraction of lithium from aqueous solutions, J. Memb. Separ. Tech. 4 (2015) 110.
[72] S. Gmar, A. Chagnes, Recent advances on electrodialysis for the recovery of lithium from primary and secondary resources, Hydrometallurgy 189 (2019) 105124.
[73] R. Trócoli, A. Battistel, F. La Mantia, Nickel hexacyanoferrate as suitable alternative to Ag for electrochemical lithium recovery, ChemSusChem 8 (2015) 2514–2519.
[74] Y. Kim, W.S. Walker, D.F. Lawler, Competitive separation of di-vs. Mono-valent cations in electrodialysis: Effects of the boundary layer properties, Water Res. 46 (2012) 2042–2056.
[75] C.P. Lawagon, G.M. Nisola, R.A.I. Cuevas, R.E.C. Torrejos, H. Kim, S.-P. Lee, W.-J. Chung, $Li_{1-x}Ni_{0.5}Mn_{1.5}O_4$/Ag for electrochemical lithium recovery from brine and its optimized performance via response surface methodology, Sep. Purif. Technol. 212 (2019) 416–426.
[76] M.-Y. Zhao, Z.-Y. Ji, Y.-G. Zhang, Z.-Y. Guo, Y.-Y. Zhao, J. Liu, J.-S. Yuan, Study on lithium extraction from brines based on $LiMn_2O_4$/$Li_{1-x}Mn_2O_4$ by electrochemical method, Electrochim. Acta 252 (2017) 350–361.
[77] H. Strathmann, Electrodialysis, a mature technology with a multitude of new applications, Desalination 264 (2010) 268–288.
[78] A. Campione, L. Gurreri, M. Ciofalo, G. Micale, A. Tamburini, A. Cipollina, Electrodialysis for water desalination: a critical assessment of recent developments on process fundamentals, models and applications, Desalination 434 (2018) 121–160.
[79] H. Strathmann, Ion-exchange Membrane Separation Processes, Elsevier, 2004.
[80] H. Kanoh, K. Ooi, Y. Miyai, S. Katoh, Selective electroinsertion of lithium ions into a platinum/. Lambda.-manganese dioxide electrode in the aqueous phase, Langmuir 7 (1991) 1841–1842.
[81] H. Kanoh, K. Ooi, Y. Miyai, S. Katoh, Electrochemical recovery of lithium ions in the aqueous phase, Sep. Sci. Technol. 28 (1993) 643–651.
[82] S. Kim, H. Joo, T. Moon, S.-H. Kim, J. Yoon, Rapid and selective lithium recovery from desalination brine using an electrochemical system, Environ Sci Process Impacts 21 (2019) 667–676.
[83] X. Xu, Y. Zhou, Z. Feng, N.U. Kahn, Z.U. Haq Khan, Y. Tang, Y. Sun, P. Wan, Y. Chen, M. Fan, A self-supported λ-MnO_2 film electrode used for electrochemical lithium recovery from brines, ChemPlusChem 83 (2018) 521–528.
[84] D.F. Liu, S.Y. Sun, J.G. Yu, Electrochemical and adsorption behaviour of Li^+, Na^+, K^+, Ca^{2+}, and Mg^{2+} in $LiMn_2O_4$/λ-MnO_2 structures, Can. J. Chem. Eng. 97 (2019) 1589–1595.
[85] M. Velický, K.Y. Tam, R.A. Dryfe, On the stability of the silver/silver sulfate reference electrode, Anal. Methods 4 (2012) 1207–1211.
[86] P. Biesheuvel, A. Van der Wal, Membrane capacitive deionization, J. Membr. Sci. 346 (2010) 256–262.
[87] C.D. Wessells, S.V. Peddada, R.A. Huggins, Y. Cui, Nickel hexacyanoferrate nanoparticle electrodes for aqueous sodium and potassium ion batteries, Nano Lett. 11 (2011) 5421–5425.
[88] S. Kim, J. Kim, S. Kim, J. Lee, J. Yoon, Electrochemical lithium recovery and organic pollutant removal from industrial wastewater of a battery recycling plant, Environ. Sci. Water Res. 4 (2018) 175–182.
[89] D.-F. Liu, S.-Y. Sun, J.-G. Yu, A new high-efficiency process for Li^+ recovery from solutions based on $LiMn_2O_4$/λ-MnO_2 materials, Chem. Eng. J. 377 (2019) 119825.
[90] F. Marchini, D. Rubi, M. del Pozo, F.J. Williams, E.J. Calvo, Surface chemistry and lithium-ion exchange in $LiMn_2O_4$ for the electrochemical selective extraction of licl from natural salt lake brines, J. Phys. Chem. 120 (2016) 15875–15883.
[91] M.S. Palagonia, D. Brogioli, F. La Mantia, Lithium recovery from diluted brine by means of electrochemical ion exchange in a flow-through-electrodes cell, Desalination 475 (2020) 114192.
[92] M.S. Palagonia, D. Brogioli, F. La Mantia, Influence of hydrodynamics on the lithium recovery efficiency in an electrochemical ion pumping separation process, J. Electrochem. Soc. 164 (2017), E586.
[93] M.S. Palagonia, D. Brogioli, F. La Mantia, Effect of current density and mass loading on the performance of a flow-through electrodes cell for lithium recovery, J. Electrochem. Soc. 166 (2019), E286.
[94] S. Kim, J. Lee, S. Kim, S. Kim, J. Yoon, Electrochemical lithium recovery with a $LiMn_2O_4$–zinc battery system using zinc as a negative electrode, Energy Technol. 6 (2018) 340–344.
[95] N. Xie, Y. Li, Y. Lu, J. Gong, X. Hu, Electrochemically controlled reversible lithium capture and release enabled by $LiMn_2O_4$ nanorods, ChemElectroChem 7 (2020) 105–111.
[96] J. Choi, P. Dorji, H.K. Shon, S. Hong, Applications of capacitive deionization: desalination, softening, selective removal, and energy efficiency, Desalination 449 (2019) 118–130.
[97] Y. Oren, Capacitive deionization (CDI) for desalination and water treatment—past, present and future (a review), Desalination 228 (2008) 10–29.
[98] M. Suss, S. Porada, X. Sun, P. Biesheuvel, J. Yoon, V. Presser, Water desalination via capacitive deionization: what is it and what can we expect from it? Energy Environ. Sci. 8 (2015) 2296–2319.
[99] W. Shi, X. Liu, C. Ye, X. Cao, C. Gao, J. Shen, Efficient lithium extraction by membrane capacitive deionization incorporated with monovalent selective cation exchange membrane, Sep. Purif. Technol. 210 (2019) 885–890.
[100] A. Siekierka, M. Bryjak, Hybrid capacitive deionization with anion-exchange membranes for lithium extraction, in: E3S Web of Conferences, EDP Sciences, 2017, pp. 00157.
[101] A. Siekierka, M. Bryjak, Novel anion exchange membrane for concentration of lithium salt in hybrid capacitive deionization, Desalination 452 (2019) 279–289.
[102] S. Porada, R. Zhao, A. Van Der Wal, V. Presser, P. Biesheuvel, Review on the science and technology of water desalination by capacitive deionization, Prog. Mater. Sci. 58 (2013) 1388–1442.
[103] D.-H. Lee, T. Ryu, J. Shin, J.C. Ryu, K.-S. Chung, Y.H. Kim, Selective lithium recovery from aqueous solution using a modified membrane capacitive deionization system, Hydrometallurgy 173 (2017) 283–288.
[104] T. Ryu, J.C. Ryu, J. Shin, D.H. Lee, Y.H. Kim, K.-S. Chung, Recovery of lithium by an electrostatic field-assisted desorption process, Ind. Eng. Chem. Res. 52 (2013) 13738–13742.
[105] T. Ryu, D.-H. Lee, J.C. Ryu, J. Shin, K.-S. Chung, Y.H. Kim, Lithium recovery system using electrostatic field assistance, Hydrometallurgy 151 (2015) 78–83.
[106] C. Rakousky, U. Reimer, K. Wippermann, S. Kuhri, M. Carmo, W. Lueke, D. Stolten, Polymer electrolyte membrane water electrolysis: restraining degradation in the presence of fluctuating power, J. Power Sources 342 (2017) 38–47.
[107] A. Siekierka, Lithium iron manganese oxide as an adsorbent for capturing lithium ions in hybrid capacitive deionization with different electrical modes, Sep. Purif. Technol. 236 (2020) 116234.
[108] A. Siekierka, B. Tomaszewska, M. Bryjak, Lithium capturing from geothermal water by hybrid capacitive deionization, Desalination 436 (2018) 8–14.
[109] A. Siekierkaa, E. Kmiecikb, B. Tomaszewskab, K. Wątorb, M. Bryjaka, The evaluation of the effectiveness of lithium separation by hybrid capacitive deionization from geothermal water with the uncertainty measurement application, Desalin. Water Treat. 128 (2018) 259–264.
[110] C. Zhang, D. He, J. Ma, W. Tang, T.D. Waite, Comparison of faradaic reactions in flow-through and flow-by capacitive deionization (CDI) systems, Electrochim. Acta 299 (2019) 727–735.
[111] Y. Ha, H.B. Jung, H. Lim, P.S. Jo, H. Yoon, C.-Y. Yoo, T.K. Pham, W. Ahn, Y. Cho, Continuous lithium extraction from aqueous solution using flow-electrode capacitive deionization, Energies 12 (2019) 2913.
[112] L.J. Banasiak, T.W. Kruttschnitt, A.I. Schafer, Desalination using electrodialysis as a function of voltage and salt concentration, Desalination 205 (2007) 38–46.
[113] M. Sadrzadeh, T. Mohammadi, Sea water desalination using electrodialysis, Desalination 221 (2008) 440–447.
[114] Y. Zhang, S. Paepen, L. Pinoy, B. Meesschaert, B. Van der Bruggen, Selectrodialysis: fractionation of divalent ions from monovalent ions in a novel electrodialysis stack, Sep. Purif. Technol. 88 (2012) 191–201.
[115] M. Reig, X. Vecino, C. Valderrama, O. Gibert, J. Cortina, Application of selectrodialysis for the removal of As from metallurgical process waters: recovery of Cu and Zn, Sep. Purif. Technol. 195 (2018) 404–412.
[116] J. Lambert, M. Avila-Rodriguez, G. Durand, M. Rakib, Separation of sodium ions from trivalent chromium by electrodialysis using monovalent cation selective membranes, J. Membr. Sci. 280 (2006) 219–225.
[117] K. Walha, R.B. Amar, L. Firdaous, F. Quéméneur, P. Jaouen, Brackish groundwater treatment by nanofiltration, reverse osmosis and electrodialysis in Tunisia: performance and cost comparison, Desalination 207 (2007) 95–106.
[118] H. Selvaraj, P. Aravind, M. Sundaram, Four compartment mono selective electrodialysis for separation of sodium formate from industry wastewater, Chem. Eng. J. 333 (2018) 162–169.
[119] N. Parsa, A. Moheb, A. Mehrabani-Zeinabad, M.A. Masigol, Recovery of lithium ions from sodium-contaminated lithium bromide solution by using electrodialysis process, Chem. Eng. Res. Des. 98 (2015) 81–88.
[120] X.-Y. Nie, S.-Y. Sun, Z. Sun, X. Song, J.-G. Yu, Ion-fractionation of lithium ions from magnesium ions by electrodialysis using monovalent selective ion-exchange membranes, Desalination 403 (2017) 128–135.
[121] Z.-y. Ji, Q.-b. Chen, J.-s. Yuan, J. Liu, Y.-y. Zhao, W.-x. Feng, Preliminary study on recovering lithium from high Mg^{2+}/Li^+ ratio brines by electrodialysis, Sep. Purif. Technol. 172 (2017) 168–177.
[122] Q.-B. Chen, Z.-Y. Ji, J. Liu, Y.-Y. Zhao, S.-Z. Wang, J.-S. Yuan, Development of recovering lithium from brines by selective-electrodialysis: effect of coexisting cations on the migration of lithium, J. Membr. Sci. 548 (2018) 408–420.

[123] P.-Y. Ji, Z.-Y. Ji, Q.-B. Chen, J. Liu, Y.-Y. Zhao, S.-Z. Wang, F. Li, J.-S. Yuan, Effect of coexisting ions on recovering lithium from high Mg^{2+}/Li^{+} ratio brines by selective-electrodialysis, Sep. Purif. Technol. 207 (2018) 1–11.
[124] X.-Y. Nie, S.-Y. Sun, X. Song, J.-G. Yu, Further investigation into lithium recovery from salt lake brines with different feed characteristics by electrodialysis, J. Membr. Sci. 530 (2017) 185–191.
[125] M.B. Bajestani, A. Moheb, M. Dinari, Preparation of lithium ion-selective cation exchange membrane for lithium recovery from sodium contaminated lithium bromide solution by electrodialysis process, Desalination 486 (2020) 114476.
[126] Y. Li, S. Shi, H. Cao, X. Wu, Z. Zhao, L. Wang, Bipolar membrane electrodialysis for generation of hydrochloric acid and ammonia from simulated ammonium chloride wastewater, Water Res. 89 (2016) 201–209.
[127] C. Huang, T. Xu, Electrodialysis with bipolar membranes for sustainable development, Environ. Sci. Technol. 40 (2006) 5233–5243.
[128] K. Mani, Electrodialysis water splitting technology, J. Membr. Sci. 58 (1991) 117–138.
[129] L. Bazinet, F. Lamarche, D. Ippersiel, Bipolar-membrane electrodialysis: applications of electrodialysis in the food industry, Trends Food Sci. Technol. 9 (1998) 107–113.
[130] A. Iizuka, Y. Yamashita, H. Nagasawa, A. Yamasaki, Y. Yanagisawa, Separation of lithium and cobalt from waste lithium-ion batteries via bipolar membrane electrodialysis coupled with chelation, Sep. Purif. Technol. 113 (2013) 33–41.
[131] C.W. Hwang, M.H. Jeong, Y.J. Kim, W.K. Son, K.S. Kang, C.S. Lee, T.S. Hwang, Process design for lithium recovery using bipolar membrane electrodialysis system, Sep. Purif. Technol. 166 (2016) 34–40.
[132] S. Bunani, M. Arda, N. Kabay, K. Yoshizuka, S. Nishihama, Effect of process conditions on recovery of lithium and boron from water using bipolar membrane electrodialysis (BMED), Desalination 416 (2017) 10–15.
[133] C. Jiang, Y. Wang, Q. Wang, H. Feng, T. Xu, Production of lithium hydroxide from lake brines through electro–electrodialysis with bipolar membranes (EEDBM), Ind. Eng. Chem. Res. 53 (2014) 6103–6112.
[134] S. Bunani, K. Yoshizuka, S. Nishihama, M. Arda, N. Kabay, Application of bipolar membrane electrodialysis (BMED) for simultaneous separation and recovery of boron and lithium from aqueous solutions, Desalination 424 (2017) 37–44.
[135] D. İpekçi, E. Altıok, S. Bunani, K. Yoshizuka, S. Nishihama, M. Arda, N. Kabay, Effect of acid-base solutions used in acid-base compartments for simultaneous recovery of lithium and boron from aqueous solution using bipolar membrane electrodialysis (BMED), Desalination 448 (2018) 69–75.
[136] D. İpekçi, N. Kabay, S. Bunani, E. Altıok, M. Arda, K. Yoshizuka, S. Nishihama, Application of heterogeneous ion exchange membranes for simultaneous separation and recovery of lithium and boron from aqueous solution with bipolar membrane electrodialysis (EDBM), Desalination 479 (2020) 114313.
[137] K.R. Seddon, A. Stark, M.-J. Torres, Influence of chloride, water, and organic solvents on the physical properties of ionic liquids, Pure Appl. Chem. 72 (2000) 2275–2287.
[138] K.R. Seddon, A. Stark, M.-J. Torres, Viscosity and Density of 1-alkyl-3-methylimidazolium Ionic Liquids, ACS Publications, 2002.
[139] X. Yang, A. Fane, K. Soldenhoff, Comparison of liquid membrane processes for metal separations: permeability, stability, and selectivity, Ind. Eng. Chem. Res. 42 (2003) 392–403.
[140] M.-A. Néouze, J. Le Bideau, P. Gaveau, S. Bellayer, A. Vioux, Ionogels, new materials arising from the confinement of ionic liquids within silica-derived networks, Chem. Mater. 18 (2006) 3931–3936.
[141] J.G. Huddleston, H.D. Willauer, R.P. Swatloski, A.E. Visser, R.D. Rogers, Room temperature ionic liquids as novel media for 'clean'liquid–liquid extraction, Chem. Commun. (1998) 1765–1766.
[142] T. Hoshino, T. Terai, Basic technology for 6li enrichment using an ionic-liquid impregnated organic membrane, J. Nucl. Mater. 417 (2011) 696–699.
[143] T. Hoshino, T. Terai, High-efficiency technology for lithium isotope separation using an ionic-liquid impregnated organic membrane, Fusion Eng. Des. 86 (2011) 2168–2171.
[144] T. Hoshino, Preliminary studies of lithium recovery technology from seawater by electrodialysis using ionic liquid membrane, Desalination 317 (2013) 11–16.
[145] T. Hoshino, Development of technology for recovering lithium from seawater by electrodialysis using ionic liquid membrane, Fusion Eng. Des. 88 (2013) 2956–2959.
[146] Z. Zhao, G. Liu, H. Jia, L. He, Sandwiched liquid-membrane electrodialysis: Lithium selective recovery from salt lake brines with high Mg/Li ratio, J. Membr. Sci. 596 (2020) 117685.
[147] Y. Qiu, L. Yao, C. Tang, Y. Zhao, J. Zhu, J. Shen, Integration of selectrodialysis and selectrodialysis with bipolar membrane to salt lake treatment for the production of lithium hydroxide, Desalination 465 (2019) 1–12.
[148] Y. Zhou, H. Yan, X. Wang, L. Wu, Y. Wang, T. Xu, Electrodialytic concentrating lithium salt from primary resource, Desalination 425 (2018) 30–36.
[149] C.P. Graettinger, S. Garcia-Miller, J.M. Siviy, R.J. Schenk, P.J. Van Syckle, Using the Technology Readiness Levels Scale to Support Technology Management in the DoD's ATD/STO Environments (a Findings and Recommendations Report Conducted for Army Cecom), 2002.